2006

IGE PRODUCTION REGULATION VIA CD23 STALK ENGAGEMENT AND CELL CYCLE STIMULATION

Timothy Hays Caven
Virginia Commonwealth University

IGE PRODUCTION REGULATION VIA CD23 STALK ENGAGEMENT AND CELL CYCLE STIMULATION

A dissertation in partial fulfillment of the requirements for the degree of Doctor of Philosophy at the Medical College of Virginia, Virginia Commonwealth University

By

Timothy Hays Caven

B.S. University of New England, Maine 1996

Director: Daniel H. Conrad, Ph.D.
Professor
Department of Microbiology and Immunology

Virginia Commonwealth University
Richmond, VA
May, 2006

Acknowledgements

The list is long to whom I owe a great debt of gratitude for bringing me to this road less traveled…seeking an advancement of knowledge for the sake of one's fellow man. It is with great pleasure that I acknowledge the contributions of my Mom and Dad, Bob and Judy Caven who, though both firm and kind, have shaped me into the man that I have become today. They have provided me with the tools for life that shape one's heart and soul that God has given to all.

Secondly, I would like to thank my mentor Dr. Daniel Conrad through lo' these many years for providing me with the tools necessary to get through the rigors of a working lab. He has not only shaped my understanding of the science and intricacies that abound in the world of research, but he has also provided me with the tools to operate the machines that are required to do one's work, namely the computer. If it were not for endless hours of filing, re-booting, formatting, downloading, installing, and re-installing, I would not have made even my first graphical representation of data, never mind the more difficult interpretation of stated data. It is with a great sense of appreciation that I recall our discussions on the inner workings of "what is and what might be".

Also to my committee members: Dr. Deborah Lebman, who has pioneered the advancement on interleukin-4 and immunoglobulin A; Dr. Christopher Kepley, who has contributed to the understanding of the inflammatory mediator cells, the basophil and the mast cell; Dr. John Ryan, who has provided an enthusiastic and positive outlook while deciphering mechanisms involving the differentiation of the mast cell; and Dr. Darrell Peterson, who has provided me with useful discussions pertaining to protein generation and purification; a much appreciated thank you.

And to my friends and loved ones, thank you for providing me with the ability to share in your lives as we travel this journey.

TABLE OF CONTENTS

Materials and Methods

Results

List of Tables

List of Figures

LIST OF ABBREVIATIONS

-/-	homozygous deletion of a gene (knockout (KO) mouse)
a.a	amino acid
Ab	antibody
ADAM	A Disintegrin And Metalloprotease
Ag	antigen
AID	Activation-Induced Cytidine Deaminase
AP-1	Activator Protein 1
APE-1/Ref1	Apurinic/aPyrimidinic Endonuclease 1/Redox factor 1
ATF2	Activating Transcription Factor 2
B1E3	Rat anti-mouse IgE antibody
β_2-AR	beta-2 Adrenergic Receptor
BACH2	BTB and CNC homology 1, basic leucine-zipper transcription factor 2
BAD	BCL2-antagonist of cell death
BCAP	B-cell receptor-associated protein
BCL6	B-cell CLL/lymphoma 6
BCR	B-cell Receptor
BLIMP-1	B lymphocyte-induced Maturation Protein 1

BLNK	B-cell linker
BMP-7	Bone Morphogenetic Protein (osteogenic protein 1)
CBP	p300/CREB-Binding Protein
CCP	Clathrin-Coated Pit
CD40LT	CD40 Ligand Trimer
c-Jun	helps to form AP-1 (transcription factor)
c-Met	cell surface receptor with tyrosine kinase activity
Csk	c-src tyrosine kinase
CSR	Class Switch Recombination
DAG	Diacylglycerol
DNA	deoxyribonucleic acid
EGF	epidermal growth factor
ELISA	Enzyme-Linked ImmunoSorbant Assay
ELISpot	Enzyme-linked Immunospot Assay
EMSA	electrophoretic mobility shift assay
ErbB	receptor tyrosine kinase
ERK	Extracellular Regulated Kinase
FACS	Fluorescence Activated Cell Sorting
FAK	PTK2 protein tyrosine kinase 2 (Focal Adhesin Kinase)
FBS	fetal bovine serum
FcεRI	high affinity IgE receptor
FcεRII	low affinity IgE receptor

FcγRIIb	low affinity IgG receptor; only IgG receptor on mouse B cells
FDC	Follicular Dendritic Cell
FGF-R1	Fibroblast Growth Factor Receptor 1
FITC	fluoroscein isothyocyanate
GAG	Glycosaminoglycan
GC	Germinal Center
GLT	Germline Transcript
GPI	glycosyl-phosphatidylinositol
^{3}H	Tritium
HA	Hyaluronic Acid
huCD23	human CD23
HRP	Horseradish Peroxidase
ICD	Intracellular Domain
IFNα or IFNβ	Interferon alpha or beta
Ig	Immunoglobulin
IL-1, 4, 6, 8, 10, 12	Interleukins-1, 4, 6, 8, 10, 12
IL-4R	Interleukin-4 Receptor
IP_3	inositol 1,4,5-trisphosphate
IRAK	interleukin-1 receptor-associated kinase
IRE1?	endoplasmic reticulum (ER) to nucleus signalling 1
IRF3	interferon regulatory factor 3
IRF4	interferon regulatory factor 4

IRG	immunoresponsive gene
IRS	Insulin Receptor Substrate
ITAM	Immunoreceptor Tyrosine-based Activation Motif
ITIM	Immunoreceptor Tyrosine-based Inhibitory Motif
JAK	Janus Kinase
JNK	c-Jun NH2-terminal Kinase
kDa	kiloDalton
LZ-CD23	Leucine zipper-CD23
LPS	Lipopolysaccharide
mAb	Monoclonal Antibody
MAPK	Mitogen-Activated Protein Kinase
mCD23	mouse CD23 (or membrane CD23)
MEK	mitogen-activated protein kinase kinase
mIG	membrane (surface) Ig
MMP	Matrix Metalloprotease
mRNA	Messenger RNA (ribonucleic acid)
MTI-MMP	matrix metallopeptidase 14
MyD88	Myeloid Differentiation Factor 88
NFAT	Nuclear Factor of Activated T Cells
NFκB	Nuclear Factor kappa B
N-linked	Asparagine-linked
OBF1	octamer-binding transcription factor (OCT)-binding factor 1

O-linked	serine or threonine-linked
PAMPs	Pathogen-Associated Molecular Patterns
PAX5 (BSAP)	paired box gene 5 (B-cell lineage specific activator)
PBL	peripheral blood lymphocytes
PBS	phosphate buffered saline
PCR	Polymerase Chain Reaction
PI-3 KINASE (PI3K)	phosphatidylinositol 3-kinase
PIP_2	Phosphatidylinositol (4,5)-bisphosphate
PIP_3	Phosphatidylinositol (3,4,5)-trisphosphate
PLCγ	phospholipase C gamma
PTB	Phosphotyrosine binding
PTK	Protein Tyrosine Kinase
Rac	ras-related C3 botulinum toxin substrate (rho family, small GTP binding protein)
RANTES	chemokine (C-C motif) ligand 5 (CCL5)
RT-PCR	Reverse transcriptase polymerase chain reaction
Rho	member of the Ras GTPase family
sCD23	soluble CD23
TCR	T-cell Receptor
T_H2	T helper cell, type 2
TF	Transcription Factor
TGFβ	Transforming Growth Factor beta

TGFβR1	Transforming Growth Factor beta Receptor I
TI	T cell Independent
Xbp-1	X-box binding protein-1

Abstract

IGE PRODUCTION REGULATION VIA CD23 STALK

ENGAGEMENT AND CELL CYCLE STIMULATION

By Timothy Hays Caven

A dissertation in partial fulfillment of the requirements for the degree of Doctor of Philosophy at the Medical College of Virginia, Virginia Commonwealth University

Virginia Commonwealth University, May, 2006

Director: Daniel H. Conrad, Ph.D. Professor, Department of Microbiology and Immunology

CD23, the low affinity receptor for IgE, is expressed mainly on B cells and has been shown to regulate IgE production. Previously, recombinant mouse and human CD23 were constructed with a trimerizing isoleucine zipper motif attached in frame to the N-terminus of the entire extracellular CD23 (*lz*-ECCD23). The goal was to examine the role of the necessity of the CD23 stalk for binding IgE. Using PCR-based mutagenesis to delete the majority of the stalk, binding to IgE was lost. Further studies examined the effect of *lz*-ECCD23 in preventing IgE from binding FcεRI and therefore acting as a therapeutic agent. It was determined that the *lz*-ECCD23 construct was capable of doing

this, albeit most effectively at 4ºC rather than at physiological temperature. In addition, antibodies to the stalk region of CD23 were developed and assessed for their capacity to modulate IgE. Rabbit anti-CD23 stalk (RAS) antibodies were found to inhibit IgE production in IL-4/antiCD40 stimulated B cells. The inhibition observed was dependent on the Fc portion of the antibody, implicating a role for FcγRIIb, an inhibitory receptor, in the IgE reduction. It was also shown that the addition of anti-stalk antibodies caused significant release of soluble CD23 (sCD23). Finally, I show that optimal IgE production was cell density dependent and was achieved through the addition of IL-21 and/or IL-10 to IL-4/antiCD40 stimulated B cells. While IgE production is inversely proportional to plated cell densities, it is directly correlated to increased cellular division, as determined by CFSE staining, and to increased cellular differentiation, as determined by FACS analysis. This work is the first demonstration that human IgE production is dependent on cell density, that IL-21 affects all isotypes tested, and that maximal Ig production is found at lower cell densities, correlating with increased cell division. I also show for the first time that the increase in IgE observed after IL-10 addition to IL-4 and anti-CD40 stimulated cells correlates with increased cellular division. When IL-10 and IL-21 were added together, there was a synergistic increase in IgE, but interestingly, no further cell division was seen, suggesting an increase in differentiation

INTRODUCTION

I. Allergic Disease and IgE

IgE plays an important role in allergic disease. Evolutionarily, it is thought to be the most recent of the five isotypes (IgM, IgG, IgA, IgE and IgD) expressed in humans. The primary role of IgE is in protecting against parasitic infections, which have been largely eliminated from industrialized societies. What is left in the Western world are innocuous particles such as pollen and dust, which have become the primary triggers for the IgE response. Approximately twenty percent of the world's population suffers from allergic disease, with the incidence in the Western world increasing two to three fold in the last forty years [1]. Societial advancements are potentially exacerbating the problem. On the one hand, we have removed the intended target of IgE, yet on the other, we have created novel targets such as aromatic hydrocarbons, the by-products of our American character, the automobile. Both these phenomena further enhance IgE-mediated histamine release to otherwise asympotomatic stimuli [2]. The symptoms of IgE mediated allergy, also known as type I hypersensitivity, can be expressed as merely minor irritants, such as red,swollen,itchy eyes or coughing, or as more serious life threatening conditions, such as systemic anaphylactic shock. Anaphylactic shock can result in death by edema and severe hypotension.

Because of its impact on society, the quest to solve the riddle behind and the role of the IgE equation has become increasingly important. This journey took a great leap forward in 1921 when Prausnitz and Kutstner [3] demonstrated that a factor in the serum of the blood of an allergic individual when transferred to a non-allergic individual was the "reagin" responsible for the allergic response. It took another forty five years before the Ishizaka lab finally identified "reagin "as the fifth isotype in 1967 [4]. Once identified, it became apparent why this antibody was able to remain elusive for so many years after the first antibodies were identified. That reason is due to the serum concentration levels being several orders of magnitude lower than that of the most commonly found antibody in the body, IgG. The serum concentration of IgE ranges from 50-300 nanograms per milliliter (ng/ml), whereas the concentration of IgG is ~10 milligrams per milliliter (mg/ml), nearly 100,000 times more prevalent. The significant advances that have been achieved in the IgE field and its role in normal function and disease can largely be attributed to the discovery of two patients that developed IgE-producing myelomas. These two patients' IgE were named after their initials, ND [5] and PS [6]. PS is one of the IgE that is used in this current body of work.

The molecule IgE.

The IgE molecule is noticeably larger than the other immunoglobulin (Ig) molecules, measuring ~180 daltons [7] compared to 150 daltons for IgG. Like other Igs, IgE is a glycoprotein, but it contains considerably greater carbohydrates (~12%) [8]. The full molecule is made up of 4 subunits, two light chains, either kappa (κ) or lambda (λ), and

two heavy chains, epsilon (ε), that define the molecular class. The IgE heavy chain has four constant domains (Cε1-Cε4) and one variable domain. One heavy chain is bound to one light chain, with the light chain binding near the amino terminus. The two heavy chains are then bound to each other, giving the classic immunoglobulin shape seen in the Ig family. At the amino terminus is the Fc portion, the 'fraction' of the molecule that is 'crystalizable'. With IgE, this Fc is highly glycosylated and only recently crystallized [9;10]. The Fc portion of the molecule is responsible for the ability of IgE to confer sensitivity to an effector cell such as a mast cell or a basophil. There are two main regions that are found on an immunoglobulin molecule. The first is the variable region, which is comprised of the V_H and V_L domains, is found at the amino terminus and mediates antigen binding and specificity. Since there are two arms, there are two variable regions. The remainder of the molecule consists of the constant region, the other main domain, which is comprised of four (Cε1- Cε4) Ig domains, of which the last three, (Cε2- Cε4) make up the Fc. Crystallography has suggested that the molecule can exist in two conformations, with different Fc domain states, either open or closed: open when unbound to its high affinity receptor, FcεRI, found on mast cells or basophils, or closed when bound asymmetrically [11]. These differing flexibility conformations are purported to allow ideal binding of IgE to either of its two receptors, FcεRI or FcεRII. Although the two receptors for IgE share a common ligand, they are not related. The two receptors are found on a variety of cell types from the haematopoetic lineage. While both receptors appear on a wide range of hematopoetic cells, the high affinity receptor is primarily restricted to mast cells and basophils, whereas, the low affinity

receptor is found on both B and T lymphocytes, macrophages, platelets, eosinophils, and basophils.

II. The high affinity receptor for IgE, FcεRI

Three years after Ishizaka identified "reagin"as IgE, he and his team discovered that radiolabeled IgE preferentially bound to basophils when administered to human leukocytes [12]. As extensive washing was performed, it was not surprising that the first of the two receptors found was the high affinity receptor. Subsequent studies demonstrated that "such armed" mast cells or basophils had the IgE cross-linked with antigen, initiating inflammatory mediator release. The affinity of the FcεRI for IgE has been shown to be in the range of 10^{10} to 10^{12} M^{-1} [13] [14] and this is the highest affinity of all the Fc receptors. The exceptionally high binding affinity of the IgE to the mast cell receptor has been shown to play a part in the long retention of the IgE on the cell surface, as an unbound receptor will more readily be recycled. The receptor on dendritic cells has also been shown to be involved in antigen processing [15;16].

The FcεRI is made up of several subunits and can be found in two forms, depending on which cell type it is found. There is an alpha (α) subunit, a beta (β) subunit and a gamma (γ) subunit. If the cell types are the classic mediators of inflammation, the mast cell or the basophil, the isoform of the receptor is $\alpha\beta\gamma\gamma$, or $\alpha\beta\gamma_2$ [17] and has been found on both mouse and man. However, on monocytes [18], eosinophils [19], dendritic cells [15] and Langerhan cells [20], the beta isoform is absent and the subunit structure is $\alpha\gamma_2$. Since the beta subunit is required for receptor

expression in rodents, the $\alpha\gamma_2$ isoform has only been found in man. The alpha subunit is the binding domain of the Fc portion of the IgE molecule. As the beta and gamma chains are minimally surface exposed, the beta subunit is responsible for amplifying the cell activation signals which initiate via the gamma chains. These signals cause the mast cell or basophil to degranulate and release preformed histamine and other mediators of inflammation, the cause of type I hypersensitivity. Later, lipid mediators and cytokines are produced causing aptly named late phase allergic reactions.

III. The low affinity IgE receptor, FcεRII

The method employed in the discovery of the high affinity receptor by Ishizaka would have made it impossible to find receptors that were of low affinity due to the numerous washings that were performed. However, several years later in 1972, it was noticed that patients with lymphoproliferative disease and X-linked agammaglobulinemia had IgE complexes on the surface of their lymphocytes. It was thought at first to be due to potential contamination from IgE coated basophils. It took another three years, but Lawrence *et al.* were able to demonstrate that IgE binds to other cells than mast cells and basophils, and that they bind to receptors that are uniquely different from the high affinity receptor FcεRI [21]. They demonstrated that human myeloma IgE complexed with rabbit anti-human $F(ab')_2$ bound to human lymphocytes [21]. This IgE receptor being found on lymphocytes, monocytes, macrophages, and eosinophils was termed the low affinity receptor for IgE, FcεRII. Subsequently, the B cell activation antigen, CD23, was found to be identical with the FcεRII, and will be

hereafter referred to as CD23. CD23 is found on many cell types, and as mentioned earlier, was first identified on the B lymphocyte. CD23 has two known isoforms, CD23a and CD23b. The form that is constitutively expressed on B cells is CD23a and it is thought to play a role in endocytosis of IgE-coated particles through a dependence on a cytoplasmic tyrosine amino acid residue.

The CD23b isoform is upregulated in the presence of the cytokine interleukin-4 (IL-4) and is expressed by B cells as well as other cells, such as T cells, Langerhans cells, monocytes, macrophages, eosinophils [22], and platelets [23]. CD23b mediates the phagocytosis of IgE complexes, a process dependent on cytoplasmic asparagines and proline residues. CD23b has been shown to be present *in situ* in human intestine and cultured epithelial cells [24]. The two CD23 isoforms were discovered by Yokota et al. [25] and differ in the first six amino acids of the amino terminus found on the intracellular portion of the molecule. In addition to normal, healthy cellular expression, over expression of CD23 is a hallmark of B cell chronic lymphocytic leukemia (B-CLL).

CD23 expression has been shown to increase in the presence of IL-4. In B-CLL it has been shown that the binding site for Notch2 protein has been identified in the CD23a promoter. Notch2 is a member of the family involved in encoding transmembrane receptors involved in differentiation, proliferation, and apoptosis. In mice it has also been shown that CD40 ligation will also up regulate CD23 expression. Additionally in mice it has been shown that INF-γ will down regulate the molecule at least on the B cell [26].

The structure of CD23 is generally defined as a type II transmembrane protein. It is unique among other Fc receptors in that is has no immunoglobulin-like domains and is therefore not part of the immunoglobulin superfamily. It has a calcium dependent lectin domain (C-type) at the carboxy terminus which is found outside the cell. It belongs to the superfamily that includes several adhesion molecules and carbohydrate recognition receptors. In fact, there have been observations that CD23 can interact with other complexes, such as CD21/CD19 (complement receptor (CR) 2), CD11b/CD18 (CR3), CD11c/CD18 (CR4) and vitronectin, thus supporting a role for CD23 as an adhesion molecule in addition to its role in IgE regulation. The extracellular lectin domain is separated from the cell membrane by a stalk region that consists of a repeating heptad sequence of hydrophobic amino acids as seen in **Figure 1**. Three monomers are found together on the cell surface as a trimer, bound together as an α-helical coiled coil, forming what looks like a trimeric zipper. The lectin heads from two of the CD23 monomers are involved in the binding of one IgE molecule (**Figure 2**). As mentioned earlier, CD23 is a C-type lectin and requires Ca^{++} for not only binding but also has Ca^{++} ions lodged in the structure of the lectin head, which are necessary for proper structural integrity and folding. It is for these reasons that during renaturation of recombinant CD23, as well as binding to IgE, that Ca^{++} must be present. The existence of CD23 on the cell surface has been reported to exist in an equilibrium in monomer, dimer, as well as trimer.

The targeting of the cleavage points on CD23 is of interest to us, as it has been previously demonstrated that $CD23^{-/-}$ mice have increased IgE expression, suggesting a

role for CD23 in the synthesis of IgE. The initial cleavage of the CD23 stalk generates the largest fragment of 37kDa. This fragment is studied in my experiments analyzing the effects of antibodies targeting that area. These fragments have been reported to be involved in the generation of B cells into plasma cells by preventing the cells from undergoing apoptosis.

Two signals are required for the generation of IgE, IL-4 and antiCD40. However, it has been shown that if suboptimal concentrations of these two stimuli are used, the addition of sCD23 can stimulate IgE synthesis, and it has been argued that this may be due to increased cellular proliferation.

Figure 1. Schematic representation of human CD23. The lectin domain is located at the carboxy terminus and contains several cystein residues (shown in red). The stalk portion is made up of multiple heptad repeats.

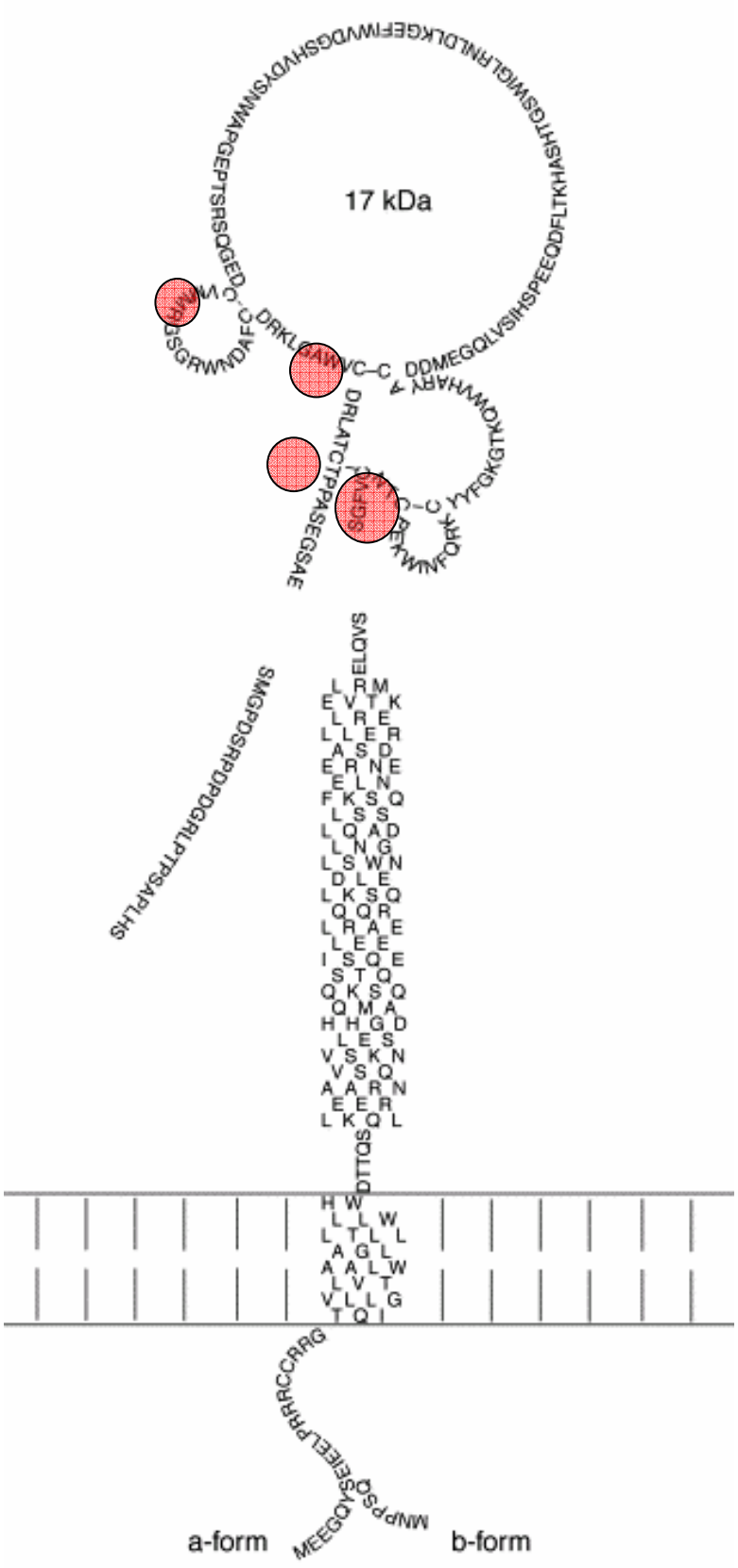

Head

Neck

Stalk

Transmembrane

Cytoplasmic Domain

Figure 2. Schematic representation of the FcεRII in trimeric form. The stalk forms an alpha-helical coiled-coil keeping the lectin heads in close proximity to one another, allowing binding of two lectin heads to one IgE molecule.

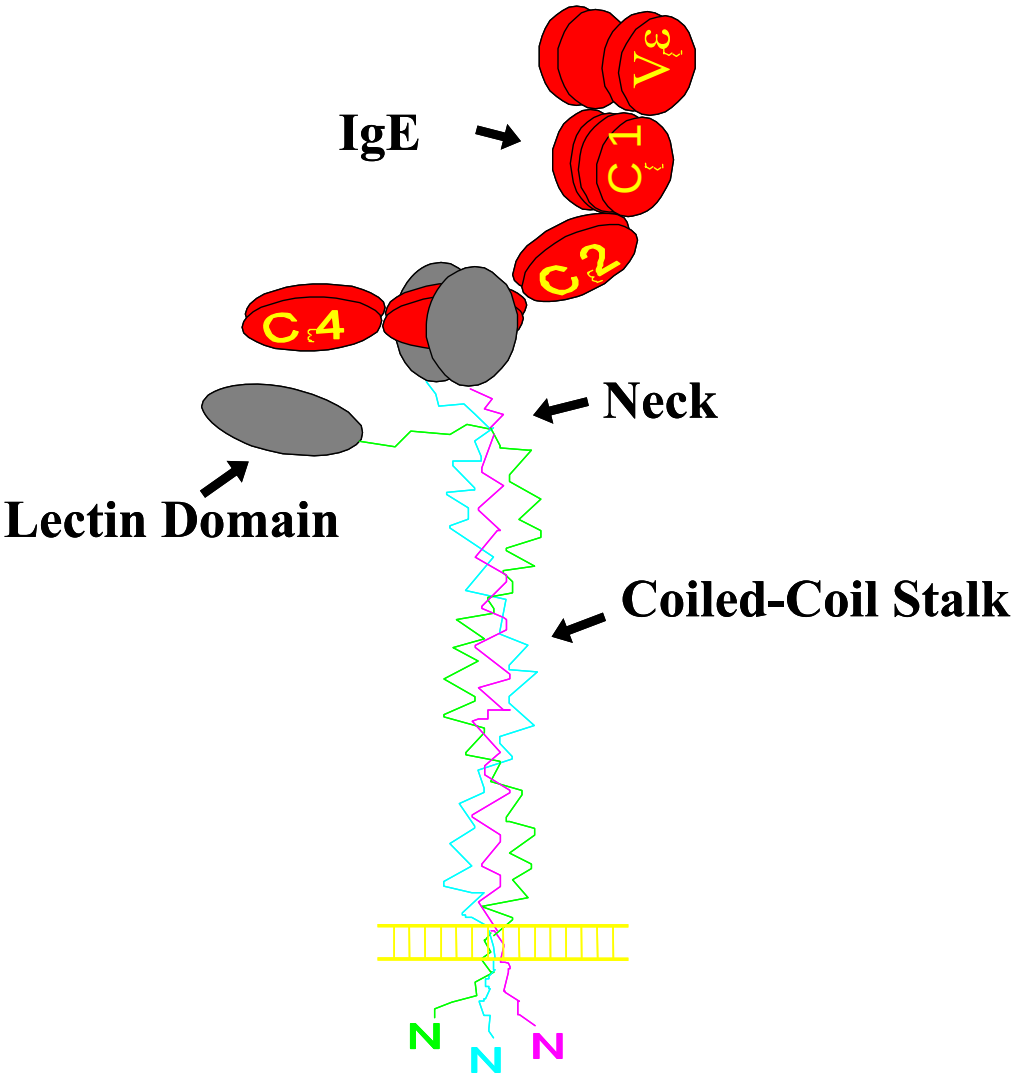
IgE
Cε3
Cε1
Cε2
Cε4
Neck
Lectin Domain
Coiled-Coil Stalk
N
N
N

IV. IgE Regulation: For isotype switching to IgE to occur, antigen-activated IgM+ IgD+ B cells are thought to require two signals [27]; the first of these signals is provided by either IL-4 or IL-13. IL-4 was initially shown to be involved in isotype switching to IgE to occur [28], by activating mouse B cells with rIL-4 treated with LPS [29]. Confirmation of this importance is seen in that IL-4 knock out mice are largely unable to synthesize IgE [30]. In humans, IL-13, which has approximately 30% homology to IL-4, also induces IgE. IL-4 and IL-13 [31;32] use a two chain receptor that is highly homologous and indeed, IL-13 can use either its own unique IL-13Rα or share the same IL-4Rα. However, IL-13 uses a unique second chain that is closely related to the common γ chain shared by a plethora of other cytokines. Both IL-4 and IL-13 triggering result in phosphorylation of STAT6, which then is translocated to the nucleus and interacts with the promoter regions of Cε (as well as Cγ4). The second signal by CD40L is expressed on activated T cells [33]. The primary transcription factor activated by CD40 signaling is NFκB. Class switch recombination occurs within tandem repeats called switch regions (S) that are found upstream of the constant region for the heavy chain (CH). Upon receiving the IL-4 signal, germline RNA transcripts are made and in the case of IgE are termed Iε. The exact role for these transcripts remains controversial, but the end result is the placement of the variable domain next to the IgE constant region; mRNA splicing then leads to the mature IgE heavy chain mRNA [32]. There are several cytokines that are known to inhibit the production of IgE and IgG4. Some of those include TGF-β [34], INF-α [35], and INF-γ [36]. While others have been shown to stimulate the production of IgE, such as IL-2 [37], IL-5 [38] IL-6 [39], IL-7,

[40] IL-9 [41] and IL-10, as well as some chemokines [42] and histamine [43]. In addition, there have been other B cell accessory molecules such as CD21, CD54 (ICAM-1), CD58 (LFA-1) [44-46] as well as CD44 and CD86 (B7-2) [47] that have been shown capable of regulating IgE production. So as can be seen the regulatory mechanisms regarding IgE synthesis production and homeostatic inhibition indicate the delicate balance that is required to keep this very powerful antibody in tight control.

IL-4 and IL-13 can induce the generation of IgE RNA transcripts [30] [48] and provide the first signal, and CD40L being the second signal for class switching. A newly discovered cytokine IL-21 has been recently shown to greatly enhance the production of IL-4 and anti-CD40 stimulated cells in humans [32]. The promoter region in the exon mentioned earlier has a binding site for STAT6, thereby explaining the IL-4 and IL-13 responsive element [49]. STAT proteins are found in the cytoplasm and are activated after tyrosine phosphorylation. After phosphorylation they translocate into the nucleus and activate gene transcription through binding of STAT binding sequences. Both IL-4 and IL-13 have been shown to induce STAT6. Interestingly IL-21 signals through STAT 1, STAT3 and/or STAT5 according to various reports [50;51] but not all report similar results [52] .

IL-21 is a newly discovered cytokine that was identified by its ability to induce proliferation in Ba/F3 cells transfected with the IL-21 receptor [53]. The IL-21 receptor (IL-21R) was first discovered by using a series of genomic studies by Ozaki in 2000 [54] and Parrish-Novak [53] independent from each other. At the time it was called an orphan receptor as it had no known ligand to which it bound. However, after cloning

into the BaF3 line and treating the newly dubbed BaF3/IL-21R with conditioned media from over one hundred primary and immortalized cells, it was discovered that the supernatants from PMA/ionomycin-activated human peripheral $CD3^+$ cells induced proliferation in the BaF3/IL-21R. cDNA from these activated T cells were then transfected into baby hamster kidney (BHK) cells and the supernatants were retested on the BaF3/IL-21R cells. After being satisfied that the cells were truly positive for the activating protein by neutralization with IL-21R, the plasmids, from the BHK clones producing the peptide, were sequenced. The resulting cytokine was designated IL-21. Initially it was determined that the tissue distribution of IL-21R is found mainly in the lymphoid tissues of the spleen, thymus, lymph node, and peripheral blood leukocytes. Specific cell types where IL-21R are found include resting B cells, activated PBMC, and in some of the cell lines of B, T, and NK origin. It has also been detected in human bone marrow and has been found on fresh peripheral NK cells. Ozaki *et al.* [55] found elevated levels of IgE in IL-$21R^{-/-}$ mice [56], indicating that IL-21 could be involved in IgE isotype switching. This was further shown in mice in that IL-21 injection inhibited IgE [55]. Interestingly, it was also shown that IgG_1 (analogous to IgG_4 in humans) also went down in IL-$21R^{-/-}$ mice, thus suggesting that IL-21 may be differentially regulate two antibodies that are thought to be generated through the same mechanisms. This differential regulation was shown to be such when Suto *et al.* administered IL-21 throughout the course of LPS and IL-4 treatment to mice, and the results showed a decrease in IgE and an increase in IgG_1 [57]. In humans a polymorphism in the IL-21R gene locus has been associated with high serum IgE [58].

IL-21 is a member of the four-helix bundle cytokine family that is clearly associated with the IL-2 family of cytokines that uses the common gamma chain (γ_c) receptor subunit for signal transduction. Other members of the γ_c family are IL-4, IL-7, IL-9, and IL-15 [59]. These cytokine family members are of particular interest because all of their actions are inactivated in the cases of X-linked severe combined immunodeficiency (XSCID) which is deficient in the γ_c [60] as well as in the Janus activated kinase 3 (JAK3)-deficient SCID, as JAK3 associates with the γ_c. [61]. IL-21 is most homologous to the human IL-15 cytokine, sharing about 25% a.a. identity [53], although it has also reported to have homology to IL-2 as well. The cytokine is produced as mentioned previosuly by $CD3^+$ T cells, specifically $CD4^+$. Additionally, it has been shown during this project in 2004 by Ozaki, that IL-21 can induce expression of B-lymphocyte-induced maturation protein 1 (BLIMP-1) [62] which is a transcription factor known to be a master regulator of plasma cell maturation [63]. Furthermore, IL-21 has been shown to induce Bcl-6. What adds to the complexity is that it is known that BLIMP-1 and Bcl-6 repress the gene transcription of one another [63;64].

IL-10 is a lymphokine that is produced by numerous cell types including activated T cells, mast cells, and macrophages. *In vitro*, IL-10 added to IL-4/anti-CD40 treated cells has been shown to enhance IgE production in B cells and PBMC [65] [66]. However in other cases, such as IL-4 treated PBMC IL-10 has been shown to inhibit IgE production [67], as well as inhibiting IgE production from purified B cells treated with IL-4 and soluble CD154 (CD40L) [68]. Like the IgE studies in mice that indicate

that under certain circumstances there can be differential regulation of protective IgG_4 and IgE this also seems to hold true in the human system as well.

In vitro studies using human cells have been problematic due to the small amount of IgE produced, usually close to the limits of detection. *In vitro* IgE production, while somewhat variable, is in the picogram per milliliter to nanogram per milliliter range, requiring highly sensitive ELISAs for detection. This also complicates experiments which seek to examine agents which inhibit IgE production. Generation of an *in vitro* model in which larger amounts of IgE are produced would greatly assist future studies looking at ways to control IgE synthesis.

Murine studies by several investigators have demonstrated that IgE production, rather than being proportional to B cell concentration, is optimal at very low cell concentrations, in the range of $5x10^2$-$5x10^3$ cells/well [69;70]. Studies by Hodgkin *et al.* have demonstrated that specific classes of antibody require multiple B cell divisions before isotype switching can occur, providing a potential explanation for the cell density effect. In the mouse *in vitro* system, a minimum of three divisions are required before IgG is observed whereas five divisions are required for IgE [71;72]. This may be explained by the observation that mouse B cells display sequential switching first from IgM to IgG_1 and then to IgE [73;74]. Recently, it has been shown that the cell division relationship persists in the human *in vitro* model, at least for IgG [75;76]. However, demonstration of a similar phenomenon for human IgE has been hindered by the low level of IgE that is produced *in vitro*.

In vitro IgE synthesis levels in the murine system easily reach μg/ml levels suggesting that additional stimuli may be needed for optimal IgE production in the human system. Given its relationship to B cell proliferation, a logical candidate would be IL-21 [53]. In view of this finding, I examined human and mouse IL-21 for its ability to enhance IgE production *in vitro*. While this work was in progress, a report was published demonstrating that human IL-21 plus IL-4/anti-CD40 could induce class switching to IgG_1 and IgG_3, as well as enhance IgE production [48]. A second publication reported that IL-13 and IL-21 added to IL-4/anti-CD40 stimulated cells increased both proliferation and IgE [32]. However, these studies only examined a single concentration of cells in culture; thus, the dependence of cell division on IL-21 mediated IgE production was not tested. The IL-13 paper examined B cells purified from PBMC but had no cell division reports. In this thesis, I examined both human and mouse IgE production as a function of cell concentration in the presence of combinations of IL-4/anti-CD40 and IL-21. IL-21 stimulation of naïve human tonsilar B cells resulted in increased production of IgE, total IgG, and IgM in a cell density dependent manner. While mouse IL-21 did enhance B cell proliferation, IgE production was reduced by the inclusion of IL-21 at high cell densities. However, at lower cell densities, IL-21 modestly enhanced IgE production. Finally, while IL-10 addition caused an increase in IgE production, increases in cell division were modest. Addition of both IL-10 and 21 gave a synergistic increase in IgE but no further increase in cell division.

V. Research Objective

1. To compare the role of the human CD23stalk to that of the murine model I will construct a stalk deletion mutant and study its role in binding IgE. As mentioned earlier, previous studies had indicated that over-expression of CD23 in mice resulted in the inhibition of IgE [77;78] [69]in both the *in vivo* and *in vitro* models. This led to the investigation of whether a soluble CD23 chimera could be used as a way to modulate IgE production by competing with the FcεRI found on mast and basophil cells. Such a chimera was designed to have a leucine zipper motif attached in frame to the amino terminus and was shown to have similar binding to membrane bound CD23 [79]. It was hypothesized that the membrane was integral to the binding of IgE; and that even though the stalk region is not purported to bind IgE, it assists in the alignment necessary for proper binding of two of the lectin heads to IgE. Therefore a murine chimera CD23 was made and the role of the stalk in binding IgE was investigated [80].

2. Investigate the role of the stalk on surface expressed CD23 on human cells on IgE production by generating a variety of antiCD23stalk antibodies of rabbit, rat, and mouse, through studies of binding and temperature analysis. Work had been done in our lab demonstrating that the membrane CD23 stalk could be targeted by rat monoclonal antibodies and IgE synthesis could be modulated. I sought to determine the role of the anti-stalk/stalk in modulating IgE synthesis. I hypothesize that certain epitopes of the stalk of CD23 may be able to either enhance IgE synthesis or inhibit IgE

synthesis dependent on the stabilizing capacity of the antibody to prevent cleavage of the CD23 trimer, keeping the CD23 molecule on the surface of the cell longer, and potentially sending a signal via its putative ITIM motif.

3. Maximize human *in vitro* IgE production by examining the effects of additional IL-21 and/or IL-10 on CD40 stimulated B cells, and determine the role of cellular division, and cell density on IgE production in the human system. IgE production in B cells has been shown to be dependent on cell density in mice [70]. Because there are increasing demands in research today to find correlations between the classic models of investigation, the mouse and the human, I wished to explore the effects of cell density and IgE production in human cells. Also it has been shown that in the mouse model, when stimulated with IL-21, the production of IgE is inhibited. In the human, the opposite is true. I sought to explain the inhibition and enhancement of IgE seen in human and mouse, as a function of cell density, as it had been determined that the production of IgE under normal conditions of a single cell density is not linear but bi-phasic. In addition, because it had been reported that there were some conditions were IL-10 increased IgE production but decreased IgG_4 production depending on the stimuli, I sought to find if IgE production was dependent on cell density And finally if the additional stimuli of IL-21 would enhance or inhibit the IL-10 effects.

Materials and Methods

Animals, antibodies, reagents and cytokines: 6-8 wk old BALB/c mice were obtained from National Cancer Institute (Frederick, MD) and housed in an accredited animal facility. All animal studies were performed according to an approved IACUC protocol. Baculovirus supernatant containing recombinant murine IL-4 was a gift from Dr. William Paul (National Institutes of Health, Bethesda, MD). Recombinant murine IL-5, recombinant murine interleukin-21, human IL-4 and huIL-21R-Fc chimera were purchased from R&D Systems (Minneapolis, MN). Recombinant CD40 ligand trimer (CD40LT) and mouse IgG_1 anti-CD40LT clone M15 [81] were obtained from Amgen (Seattle, WA). Mouse anti-human IgD-FITC and anti-human IgE-HRP were obtained from Becton-Dickenson Biosciences (San Diego, CA) or Dako Cytomation, Inc. (Ft Collins, CO), respectively. Mouse anti-human CD40 clone G28-5 (American Type Culture Collection, (ATCC), Manassas, VA) was purified from ascites by salt fractionation and FPLC using MEP-Hypercel chromatography (Ciphergen, Fremont, CA). Purified mAb (99%) was eluted with acetate buffer, pH4.9, and dialyzed against PBS prior to use in culture. IL-10 (Sigma) was brought to a working concentration of 12.5μg/mL. Human IgE standards were purified from JW8 IgE myeloma cells (ATTC), grown in Integra CeLLine 1000 flasks (IBS Integra Biosciences, Switzerland). Collected supernatants were dialyzed three times against PBS and purified by FPLC using MEP-Hypercel. IgE elutes at pH 5.5 and was further purified (98%) by gel filtration. Goat anti-human Ig, goat anti-human and anti-mouse IgM (AP and unlabeled), goat anti-mouse IgG_1-Unlabeled, goat anti-mouse IgG_1-AP and mouse anti-

human IgM-HRP were obtained from Southern Biotechnologies (Birmingham, Alabama). Goat anti-human IgG-Fc-AP, human polyclonal IgG, and human IgM were obtained from Sigma. Production of biotinylated rat anti-mouse IgE mAb R1E4 and B1E3 has been previously described [69]. [^{3}H]-Thymidine (50Ci/mMole) was purchased from NEN, Boston, MA.

Expression of Recombinant Proteins in Prokaryotic Cells: Transformed BL21 cells were grown in Luria Broth (LB) with the selective antibiotics added of either 50μg/ml ampicillin or 30μg/ml kanamycin to ensure that only those bacteria that had been successfully transformed with the plasmid. M9 media was prepared by mixing 200 mls of 5x M9 salts (2 grams NaCl, 27.3 grams of Na_2HPO_4, 12 grams of KH_2PO_4, and 4 grams of NH_4Cl and brought to a final volume of 800 mls), 1 ml of 0.1 M $MgSO_4$, 1 ml of 0.1 M $CaCl_2$, and 725 mls dH_2O. Additives were then added to provide nutrition consisting of 25 mls of 20% CAA (casein, acid hydrosylate), 50 mls of 20% glucose, ad 1 ml of 10 mg/ml thiamine) to the cooled M9 media. One liter of the media that had been added with 10mls of the transformed bacteria, which had been grown overnight, was placed in a rotating, 37˚C shaker allowing for oxygenation until the concentration of the bacteria reached the appropriate concentration determined by optical density on a spectrophotometer of 600, OD_{600}. Upon the arrival at the beginning of log phase growth IPTG was added, stopping bacterial division but allowing continued protein expression for another 6 hours. After this time the bacterial cells were collected by centrifugation and either stored as a pellet in a -70˚C freezer, or subjected to protein purification.

The protocol of Bohmann and Tjian [82] was followed with some slight modifications. After the cells were thawed the pellet was resuspended in 72 mls of cold solution (25% sucrose, 100mM KCl, 2mM DTT, 2mM PMSF, and 10mM Tris, and pH 7.9). Then a second solution (100mM EDTA, 4mg/ml lysozyme, and 300 mM Tris, pH 7.9) was added add incubated for another 10 minutes on ice allowing for digestion of the bacterial wall. After this time 90 mls of the third solution (1M LiCl, 20mM EDTA, and 0.5% Triton X-100) was added and the mixture was kept on ice and sonicated at a 60% cycle and output control setting of 6 using a Branson Sonifier (VWR Scientific, West Chester, PA) for 5 minutes, or until there were no remaining brown bacterial pellet particles visible. The pellet containing the proteins in inclusion bodies was collected and resuspended in 200 mls of the fourth solution (0.1mM EDTA, 0.5mM LiCL, 1 mM DTT, 1 mM PMSF, 0.5% Triton X-100, and 10 mM Tris, pH 7.9). The mixture was sonicated once again and again pelleted. The inclusion bodies were washed in the fifth solution (0.1mM EDTA, 0.5mM LiCL, 1 mM DTT, 1 mM PMSF, 2% Triton X-100, and 10 mM Tris, pH 7.9) and again in a sixth solution (same at fifth but with only 0.5% Triton X-100) with again a final sonication and centrifugation. The final pellet was either frozen at -20˚C for later use or used directly by being dissolved in 5 mls 6M GnHCl, 20% sucrose, and 10mM DTT at room temperature for an hour. After this time the solution was filtered through a 0.45µm Acrodisc syringe filter (Gelma Sciences, Ann Arbour, MI). Aliquots ~2ml in volume were loaded on to a Sephycryl-200 gel filtration column (Pharmacia) and purified using an FPLC (Pharmacia) with 6M GnHCl as the running buffer. The fractions that came off the column that had an OD_{280}

were the protein fractions. These were then pooled and concentrated down using a PM10 or YM10 ultra-filtration membrane (Millipore, Bedford, MA) in an Amicon stirred cell protein concentrator (Millipore). The now fully denatured protein was brought to a concentration of 10mg/ml.

To renature the protein, a protocol modified from Taylor was utilized [83]. A strong reducing agent, DTT, was added to one ml of the GnHCl solubilized inclusion bodies. The final DTT concentration was 10mM and there should be 10mg of protein. This incubated for one hour at room temperature and was then brought to 10 mls with the addition of the refolding buffer (6M GnHCl, 0.1 M oxidized/reduced glutathione pair, 0.5M Tris, at pH 8.6) and incubated for another 24 hours at 4˚C. The solution was then diluted another 1:100 in the second refolding buffer with significantly reduced GnHCl (1M) in the presence of 1mM $CaCl_2$, 3mM L-cysteine, and 100mM Tris pH 8.6. This was kept in the cold room (4˚C), and continually stirred for another 36 hours. The solution was again concentrated using the Amicon unit and reduced in volume to ~10mls. The concentrated protein solution was dialyzed against 1L of HBS/Ca^{++} (2mM $CaCl_2$, 150 mM NaCl, 20mM HEPES, pH 7.4) overnight in a 12-14 KDa molecular weight cut-off Spectra-Por 4 dialyzing tubing (Spectrum Laboratories, Rancho Domingues, CA). After dialysis, the solution was centrifuged, filtered through a 0.45µm Acrodisc syringe filter. The protein concentration was determined was by spectrophotometer OD_{280} where a solution with 1mg/ml had an extinction coefficient of 1.66.

HumanCD23stalk$^{48-153}$ generation and purification. I needed to have large amounts of human CD23stalk$^{48-153}$ for a variety of reasons. One was that significant quantities would be needed for animal injection for rabbit, rat, and mouse antibody production. Another would be for the ELISAs that would determine specificity of any possible antibody that might bind the stalk. I was also looking to coat an Affigel-15 to purify one of the rabbit antistalk antibody pools. As a hyperimmunized rabbit, such as the rabbits that I was working with, produced only a maximum of 10-20% specific IgG, I thought that is would be best to have a purified antibody that was only binding the stalk. I started with growing up the *E.Coli* BL21-huCD23stalk$^{48-153}$ overnight in 100 mls media with 100μg/ml ampicillin. A total of 4L of Luria Broth (LB), with 100μg/ml ampicillin, with 25mls of each being added to a single L of LB was prepared. To determine the best time for adding IPTG, absorbance was taken at each hour and at A_{600}=0.4 1mM IPTG was added. After 4 hours the cells were spun down and the pellet resuspended in 200mls buffer A (25mM Tris (pH7.5), 1mM EDTA, 1mM DTT, and 0.01% Triton X-100). The cells were homogenized as to disrupt the cells. Following a freeze thaw cycle, the insoluble material was pelleted by centrifugation for 30 minutes. A Q-fast flow 16cm XK20 column was equilibrated with 0.1M NaCl in buffer A. Half of the supernatant was loaded at 2.5ml/min and the human CD23stalk was eluted with 600 ml gradient of 0.1 NaCl to 1.0M NaCl in buffer A. Human CD23stalk$^{48-153}$ was found in the column wash and low salt fractions. This was repeated a second time to ensure the removal of bacterial DNA and protein contamination. The volume was concentrated on an Amicon concentrator using a YM3 membrane. As the

concentration of CD23stalk increased the material precipitated. 6M GnHCl in 0.1M Tris pH 7.5 was added and the stalk redissolved. The purified huCD23stalk was purified by gel filtration on a Sephacry S-200 HR 100cm column with 6M GnHCl and 0.1MTris. Fractions containing the stalk were identified by SDS-PAGE. These were pooled and diluted with 4 volumes of 0.1M NaCl, 25mM Tris (pH 7.5) and 1mM EDTA. This was concentrated on a YM 3000 membrane. Samples were diluted and concentrated one more time to remove residual guanidine hydrochloride.

Rabbit anti-huCD23stalk$^{48\text{-}153}$ Antibody production. Human CD23stalk$^{48\text{-}153}$ was injected into mice by Strategic BioSolutions (Newark,DE). When I received the serum, it was glass wool filtered and then centrifuged. The total volume was determined and the antibody fraction was purified by 40% ammonium sulfate precipitation. The solution is allowed to sit overnight at 4ºC and is then centrifuged. The precipitate is brought up to a working volume 10:1 in a dialyzing buffer (0.02M Na_2HPO4, 0.02 M NaH_2PO4, and 0.05 M NaCl) and dialyzed overnight changing the buffer three times. The dialyzed sample is filtered and is further purified by Protein G purification. A column is filled with Protein G (Amersham Phamacia) and equilibrated with running buffer (0.02M Na_2HPO4, 0.02M NaH_2PO4, and 0.02M NaCl and 0.05% NaN_3) The sample was continuously recycled over the column and kept at a pump speed of 1 ml/mim. The column was washed with running buffer for 2 hours and eluted with 0.2M glycine pH2.5, 1M Tris, 0.5M NaCl. The solution containing the rabbit antibody was

concentrated down using an Amicon concentrator to ~10mg/ml and then finally dialyzed in HEPES/ $CaCL_2$ overnight.

Rat anti-humanCD23stalk$^{48-153}$ monoclonal antibody production. Monoclonal antibodies were first made by taking purified human CD23stalk$^{48-153}$ and injecting 100µg of antigen in 150µl of complete Freund's adjuvant (CFA) into the dermis of the rat. A second and third injection 3 weeks apart, were injected into the rat both subcutaneously and intramuscularly keeping the total to 150µg for each occasion in incomplete Freund's adjuvant (IFA). A fourth injection one week after the third was given with 50µg of stalk in IFA. Three days before the animal is to be sacrificed the final injection was given intraperitoneally in PBS with a final 100µg of stalk. PBS is chosen as the vehicle of delivery as this will allow a very rapid dispersement unlike the slow release of antigen when delivered in CFA. Intravenous delivery would be preferred as the route to get the antigen to the spleen the fastest, but in terms of time and ease, the IP route was decided on as the preferential route of delivery.

Rats were bled after the third delivery to ensure that the antigen was being responded to and that antibodies were being produced. To determine the presence of antibody in the blood specific to the stalk, the blood was plated on ELISA. Once it had been determined that the mice were producing antigen specific antibodies the rats were sacrificed and the spleen was harvested washed and centrifuged. Spleen cells were mixed 3:1 to IR983F myeloma cells (spleen cells:myeloma cells). The rat splenic cells were fused to the myeloma cells using polyethylene glycol (PEG). Stepwise removal of

PEG by slowly adding media ended the fusion process. The fused spleen/myeloma cells were then plated at several concentrations of 300k cells/well, 100k cells/well and 30k cells/well in complete culture media containing HAT and 10% hybridoma cloning factor. After ~4 days the media was refreshed and this was repeated every three days until colonies began to become visible around day 21. Aliquots of supernatant were taken from well that had only one visible colony and content of rat anti-humanCD23stalk antibodies was determined by ELISA. The antibodies that tested positive were grown up and injected IP into either LouM rats or nude mice that had been primed with Pristane (Sigma) with 1.0 or 0.5mls, respectively. Ascites were collected by abdominal puncture. Antibody content was collected by 40% ammonium sulfate precipitation and purified by a combination of ion exchange and gel filtration or by Protein G affinity chromatography. The isotype of each antibody was determined by a rat isotyping kit from BD BioSciences.

In addition to rat anti-human CD23stalk antibodies that were generated, I also made several **mouse monoclonal antibodies** as well. The differences being merely a lower amount of stalk given to the animal (50μg), the mouse myeloma line used for fusion was p3x63-AG8.653, and of course mouse isotyping kits from BioSciences were used.

^{125}I-IgE binding analysis. Increasing concentrations of chimeric CD23 proteins were added to constant concentrations (usually 100 ng) of ^{125}I-mIgE or -huIgE and the reactions were incubated on ice for 30 min. Then, 1×10^6 FcεRI$^+$ RBL-2H3 cells (with

huIgE, RBL transfected with human FcεRIa were used) were added, and the incubation continued at 4°C for an additional 60 min. At the end of the incubation, a phthalate oil cushion centrifugation procedure was employed to separate free from cell-bound ^{125}I-IgE. The cell-bound radioactivity of each reaction was determined in duplicate on an LKB-Wallac CliniGamma-1272 automatic gamma counter (LKB-Wallac, Perkin Elmer Life Sciences, Gaithersburg, MD). Specific binding of samples was calculated by subtracting background controls incubated with 100-fold excess of cold mIgE and compared to controls without any inhibitor added. The percentage inhibition [in counts per minute (c.p.m.)] was calculated as follows: % Inhibition = [(c.p.m.experimental – c.p.m. 100-fold excess of unlabeled IgE) ÷ (c.p.m. control with no inhibitor- c.p.m. 100-fold excess of unlabeled IgE)]x 100.

^{125}I-IgE binding inhibition with anti-CD23stalk antibodies. This study employed techniques very similar to that of the chimeric CD23 binding studies, except CD23^{+} 8866 cells were used. 1x10^{6} of 8866 cells were kept at either 4ºC or 37ºC, and incubated with increasing concentrations of mouse anti-CD23stalk antibodies for one hour at appropriate temperature. After one hour cells were washed and 100ng/ml of ^{125}I-huIgE was added and incubated for another hour, again at either 4^{oC} or 37^{oC}.At the end of the incubation, a phthalate oil cushion centrifugation procedure was employed to separate free from cell-bound ^{125}I-IgE. The cell-bound radioactivity of each reaction was determined in duplicate on the gamma counter. Specific binding of samples was calculated by subtracting background controls incubated with 100-fold excess of cold

IgE and compared to controls without any antibody added. The percentage inhibition [in counts per minute (c.p.m.)] was calculated as follows: % Inhibition = [(c.p.m.experimental –c.p.m. 100-fold excess of unlabeled IgE) ÷ (c.p.m. control with no inhibitor- c.p.m. 100-fold excess of unlabeled IgE)] x 100.

Surface Plasmon Resonance Analysis: Surface plasmon resonance was performed using a BIAcoreT-100 instrument (BIAcore, Piscataway, NJ). A carboxymethyl dextran-based CM5 biosensor chip was utilized for the immobilization of the anti-*lz* antibody M15 (Amgen) according to manufacturers' instructions [84]. Flow cell two, the experimental cell, was activated by the addition of 50µl NHS and EDC (equal volumes, premixed just prior to addition) at a flow rate of 5µl/min. Immediately thereafter, 10µg/ml M15 was passed over flow cell two at 5µl/ml for 10 minutes. This then provided a covalently bound anti-lzCD23 antibody to the chip. Unreacted groups of dextran that had no M15 bound to them were quenched with 1M ethanolamine (pH 8.0). The control cell, cell one, was activated and quenched as the experimental flow cell two with no M15 added to provide background control. 10µg/ml lz-$C23^{45\text{-}321}$ full length stalk and lectin-head was then added to the M15 anti-*lz* and allowed to bind at a flow rate of 5µl/ml for 10 minutes. Following successful binding of the *lz*-CD23 molecule, the anti-CD23stalk antibody, mouse #18 was added and allowed to bind. Following the binding of the anti-CD23stalk antibody, a second anti-CD23stalk antibody was added. Additional binding was determined by the additional response. To return the chip back to a base of M15 for additional studies, glycine-HCl (pH 2.0)

was added. The BIAEVALUATION 3.0 software was used for the analysis of the interaction kinetics.

Human IL-21 preparation: $4x10^7$ T cells were obtained by MACS purification of disrupted human tonsils and stimulated overnight with PMA (10ng/mL) and ionomycin (2μM). RNA was isolated with Trizol (Invitrogen, Carlsbad, CA) and RT-PCR was performed with GTGTCCAACTGCAAG (anti-sense) and GTCTAGCTCTACTGTTGG (sense) primers (Applied Biosystems, Foster City, CA). The IL-21 cDNA was cloned into pCR2.1 (Invitrogen, CA) and confirmed by sequencing. For expression, the cDNA was inserted into pEF4MycHisA (Invitrogen) using BamH1 and Not1 and used to transfect HEK293T cells (ATCC), using Fugene6 (Roche Diagnostics Corp., Indianapolis, IN) according to manufacture's directions. Transfected cells were cultured for 72 hours and supernatants were collected and pooled. Supernatants were dialyzed against PBS and kept at -70°C prior to use.

Human B cell purification Human B cells were purified from PBMC or tonsils. PBMC were obtained from Virginia Blood Services as a buffy coat preparation and leukocytes were purified by differential density centrifugation over Ficoll 1077; for some experiments, tonsilar B cells were further purified as described below. Whole tonsil biopsies were qualified as an approved exemption under Internal Review Board regulations as discarded anonymous tissue. In some experiments $CD19^+$ B cells were purified from PBMC. In others IgD^+ tonsilar B cells were isolated as follows. Tonsil disruption was accomplished using a Cellector Tissue Sieve (VWR International, West

Chester, PA) using two wire screens, mesh sizes 0.14 mm and 0.0381 mm, respectively. PBMC or disrupted tonsils were diluted 1:2 in RPMI, layered over Ficoll Hypaque (Amersham Biosciences, Piscataway, NJ), centrifuged at 200g for 20 minutes at 4°C, and washed twice with 1% FBS/PBS. The cells were then stained for 10 minutes at 4°C with mouse anti human IgD-FITC (isotype I) (Pharmingen). After 2 washes, the cells were incubated for 10 minutes at 4°C with anti-FITC microbeads (Miltenyi Biotech), washed and re-suspended in PBS containing 1% BSA and 2mM EDTA. Cells were then placed over a MACS LS separation column with the magnetically retained cells being the IgD^+ fraction. There are studies that have shown that heavy cross-linking of the B cell receptor can influence IgE production [85] but the MACS uses monoclonal antibodies which would only have minimal cross-linking. In addition I also used the MACS naïve B cell kit and had similar IgE and proliferation results (data not shown), but preferred the yield using the IgD^+ selection method. For the PBMC purification, $CD19^+$ staining was followed by the anti-FITC-microbeads. After removal of the magnet, the retained cells were collected then centrifuged and then resuspended in B cell media (RPMI 1640 containing 10% FCS, glutamine, 10μg/mL insulin, 35μg/mL transferrin and antibiotics). FACS analysis with anti-CD19 indicated B cell purities were above 95% using this protocol. B cells were cultured in 96 well culture plates at the indicated cell densities for 96 hours with last 16 hours pulsed with [^{3}H]-thymidine) or 12-14 days for antibody production, respectively.

Mouse B cell preparation. Resting B cells were purified as previously described [69]. Briefly, B cells were isolated from Balb/c spleens and enriched by complement lysis of T cells and further purified using by Percoll gradient centrifugation. Resting B cells were collected from the 66-70% Percoll layer, washed and placed in culture. To examine the effect of mIL-21 on cell proliferation and IgE production, B cells were plated from $0.1x10^3$-$50x10^3$ cells/well in 96 well culture plates in the presence of IL-4, IL-5, CD40LT, M15 (standard activation cocktail) and with or without 25ng/mL mIL-21 in mouse B cell media (RPMI 1640 containing 10% FCS, 50 μM 2-ME, 1 mM pyruvate and 1x non-essential amino acids) [69] for 3 or 8 days. Standard activation cocktail contained 0.1 μg/mL CD40LT, 5ng/mL IL-5, and 10,000U/mL mouse IL-4, and 0.1μg/mL M15. IL-21 volumes were added as indicated in 50μL aliquots. Proliferation was measured on day three by [^{3}H]-thymidine incorporation (1μCi/well) during the last 8 hours of culture and antibody secretion was determined by ELISA after 8 days of culture. Stimulations were conducted in triplicate.

ELISA protocols. Determination of soluble human **CD23** levels was performed by coating a 96-well ELISA plate with 3μg/ml Rabbit anti huCD23 lectin-head in 50μL borate buffered saline (BBS) for one hour at 4ºC and blocked one hour with 2%FBS/PBS at 4ºC. Supernatants were added and diluted accordingly and incubated for one hour. After washing, biotinylated mouse anti-humanCD23lectinhead (bio-IDEC 152 (IDEC San Diego, CA)) was added in block for one hour at 37ºC. Then followed anti-biotin HRP 1:5000 in block at one hour. Finally 50μL TMB solution was added

and stopped with 0.18M H_2SO4 and color was read at 450nm Determination of human IgE levels utilized the monoclonal anti-human IgE antibodies, clones 4.15 and 7.12 mouse anti-human IgE (HB 235 and 236 from ATCC) as capture antibodies [86], which were plated in combination at 5μg/mL in 0.05M borate buffered saline (BBS), pH 8.5. Samples and standards were detected using rabbit anti-human IgE-HRP diluted in PBS/2% FBS. Human IgE standards and samples were serially diluted 1:2 in RPMI media containing 10% FBS. The lower limit of linear detection was consistently ~5ng/mL. Total human IgG was detected by coating plates with 3μg/mL goat anti-human antibody (H+L) in borate buffered saline (BBS). Capture antibodies were goat anti-human IgG-Fc-AP, diluted in Tris buffer/0.5% goat serum. Standard curves were generated from polyclonal human IgG. The human IgM ELISA utilized goat anti-human IgM (Sigma) as capture at 5μg/mL for coating and samples and standards were detected using mouse anti-human IgM-HRP. Standard curve was generated using polyclonal human IgM. Mouse IgE, IgG_1 and IgM production was measured by ELISA as described previously [69]. Briefly, mouse IgE ELISA utilized rat anti-mouse IgE mab B1E3 and R1E4 [87], while IgG_1 and IgM utilized goat polyclonal reagents from Southern Biotech. Color was generated by addition of AP substrates (S0942-Sigma) or HRP substrates (51-2607KC and 51-2606KC BD Pharmingen). Plates were read on a Molecular Devices SpectraMax 250 ELISA plate reader at either 405 nm for alkaline phosphatase (AP), or 450 nm for horseradish peroxidase (HRP) detection, respectively. ELISA plates for determining IL-21 content in supernatants were plated with 1μg/mL rabbit anti-human IL-21 (aa 121-135) in BBS (QED, San Diego, CA). Plates were

blocked and a standard curve of commercially available IL-21 (BioSource, Camarillo, CA) was generated. Supernatant dilutions were plated and compared to Standard curve. IL-21 was detected using chicken anti-human IL-21 at 1:200 (Genway, San Diego, CA). Color was generated by incubating rabbit anti-chicken IgY HRP conjugate 1:1000 Upstate, Lake Placid, NY). IL-21 containing supernatants were determined to contain 2.5ng IL-21 per μL supernatant (data not shown). In most experiments, 10 μL of supernatant were used resulting in the equivalence of 25ng/mL IL-21.

Analysis of cell division numbers: CFSE staining: Carboxyfluorescein diacetate succinimidyl ester (CFSE) (Molecular Probes Eugene, OR) was prepared according to the manufacturer's recommendations. Resting B cells were washed and resuspended at 10^7cells/mL with PBS with 0.1% BSA. CFSE was then added to final concentration of 0.5-5μM (1μM for mouse studies) and incubated in the dark at 37°C for 10 minutes. Cells were then washed twice and re-suspended in B cell media. Human CFSE labeled cells were plated at either $1x10^3$ cells/well, $1x10^4$ cells/well or $1x10^5$ cells/well in a 96 well plate and cultured for 8 days with 10ng/mL IL-4 alone, 1000ng/mL anti-CD40, or IL-4 and anti-CD40 in the presence or absence of IL-21. Cells were harvested and then analyzed by flow cytometry using a FC500 (Beckman-Coulter, Miami, FL). Murine CFSE labeled cells were plated at either $5x10^3$ cells/well or $1x10^5$ cells/well in a 96 well plate and cultured for 4 days with IL-4 alone or IL-4, IL-5, CD40LT and M15 with or without 25ng/mL IL-21. The percentages of cells in each cell division were determined

by setting sequential gates one-half intensity starting with the highest intensity peak, which represents undivided cells.

ELISPOT Determination: Cells were purified and treated as previously mentioned for IgD^+ tonsilar conditions. At either day 8 or 11, respectively, cells from each density (plated in triplicate) were collected, pooled, and washed six times to remove any IgE that might be present in the supernatant. Cells were then brought up to original volumes and plated neat or with increasing dilutions in Complete media in either IL-4/antiCD40 +/- IL-21 on pre-coated anti-human IgE (monoclonal antibody 4.15 at 5µg/ml in 50µl PBS) Millipore sterile 96-well plates with Immobilon-P PVDF membranes (#S2EM0 04M 99) overnight in 37˚C,5% CO2. After 16 hours plates were washed 10 times in 0.5% Tween/PBS to remove cells and any unbound IgE. The wells then had AP-anti IgE (BD Pharmingen #555859) added in 50 µl aliquots in complete media at 1:1000 and incubated for one hour at 37˚C. After one hour, plates were washed and 50µl substrate was added. Substrate consisted of AMP Substrate (15mg $MgCl_2$-$6H_20$, 10 µl Triton X-405, 25mg NaN_3, 9.6mls AMP (2-amino-2-methyl-1-propanol) in 100mls dH_2O at pH 10.5.) and 1mg BCIP (5-bromo-4-chloro-3-indoyl) was dissolved in 1ml AMP substrate and filtered. 50µl substrate per well was used. Plates incubated for 1 hour at 37˚C until blue spots appeared. Plates were read and analyzed on a CTL 2.01 ELISPOT reader (Cellular Technology Limited Cleveland OH).

Data analysis: Data are summarized as mean ± Standard Deviation (SD). The statistical analysis of the results was performed by the paired student *t* test. A p value of <0.05 was considered significant.

Results

Expression of *lz*-CD23 stalk mutants in *E.Coli*. Previous work in this lab initiated the work on the murine CD23 mutant stalk mutants. Beavil *et al*. had observed that there were a series of amino acid sequence repeats in the stalk portion of the molecule. These repeats were thought to form an alpha-helical coiled coil based on other similar proteins related in the C-lectin binding family. The question was therefore raised as to whether there was any functionality to the stalk regarding binding to the IgE molecule. Given that the observation was made that the high affinity binding required multiple CD23 interaction, or oligimerization, the role of the stalk in CD23 function was examined. To ensure that the heptad repeats would remain intact and that the molecule itself would not lose the natural interaction with its other self members allowing for oligimerization, PCR primers were chosen to preserve this heptad repeat pattern (**Figure 3**). The proteins were expressed in BL21 bacteria, and after the addition of IPTG to stop growth but allow continued protein synthesis, aliquots were collected at each subsequent hour to determine optimal protein content. From hour 3, significant protein is observed by 10% SDS-PAGE gel analysis, with maximal presence seen by hours 5 and 6. After each one liter bacterial growth of protein ~200mg of inclusion body proteins were recovered. After the renaturation process the presence of contamination was virtually nil. When purifying full length *lz*-CD23, the protein was further purified on a column using an affinity chromatography method using human IgE (PS) coupled to Affigel-10 and was used to further purify the renatured protein. Renatured protein as well as the Affigel

column was equilibrated with HBSS buffer (pH 7.4) and contained 2mM Ca^{++}, a requirement as the CD23 is dependent on Ca^{++} for binding to IgE as it belongs to the C-type lectin family. The effluent of unbound CD23 is recycled over the column at a flow rate of ~2 ml/min. After a number of cycles, the bound CD23 is removed by elution using HBSS buffer containing 50mM EDTA to remove the Ca^{++} enabling binding ions from the solution. Eluates were dialyzed against HBSS/ Ca^{++}. ELISA precoated with IgE was used to determine binding capacity.

***lz*-CD23$^{148-321}$ Stalk Mutant loses the ability to inhibit IgE from Binding to FcεRIα.** In concert with others in this lab who were working on the mouse CD23 stalk involvement, I compared intact and mutated CD23 versions on whether the stalk could influence binding of IgE to the high affinity receptor. Increasing concentrations of chimeric CD23 proteins were added to constant concentrations of ^{125}I-mIgE or -huIgE and the reactions were incubated on ice for 30 min. Then, 1×10^6 FcεRI$^+$ RBL-2H3 cells (with huIgE, RBL transfected with human FcεRIa were used) were added, and the incubation continued at 4° for an additional 60 min. At the end of the incubation, a phthalate oil cushion centrifugation procedure was employed to separate free from cell-bound ^{125}I-IgE. As can be seen from **Figure 4**, both the mouse mutant (**A**) and the human mutant (**B**) (open symbols) were unable to prevent binding to FcεRI$^+$. Both the mouse and human intact full length *lz*-CD23 were able to completely inhibit IgE from binding by ~100x excess of CD23 over IgE (A) and ~20x excess (B) respectively.

F**igure 3. Schematic representation of human CD23 stalk mutants. (A)** cDNA of a human dhimeric CD23 construct, lz-ECCD23, composed of a N-terminal isoleucine zipper (lz) attached inframe to the entire extracellular domain. **(B)** A PCR strategy was utilized to construct lzECCD23 mutants with increasing deletion of the stalk portion. The mutant in B is one that was constructed and studied. **(C)** Designs of further CD23stalk mutants.

A.

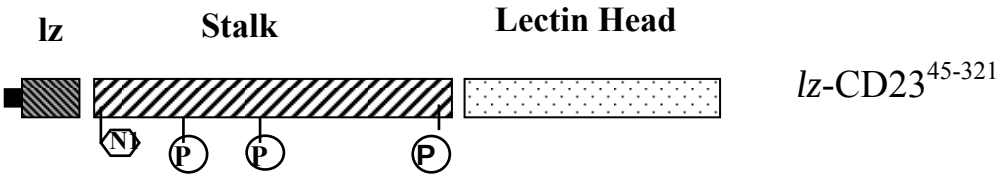

lz-CD23$^{45\text{-}321}$

B.

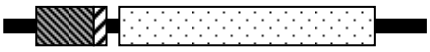

lz-CD23$^{148\text{-}321}$

C.

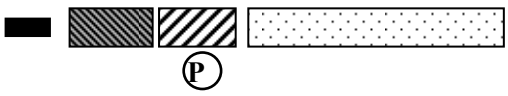

lz-CD23$^{-130\text{-}321}$

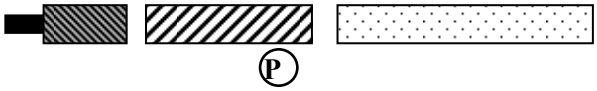

lz-CD23$^{-116\text{-}321}$

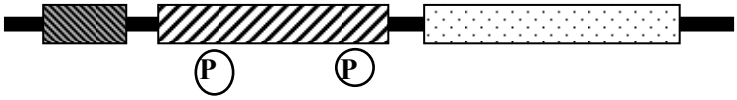

lz-CD23$^{-88\text{-}321}$

***lz*-CD23$^{148\text{-}321}$ Stalk Mutant loses the ability to inhibit IgE from Binding to FcεRII.** From the results seen from the inhibition studies with the high affinity RBL-FcεRI^{+}, I sought to determine if the results would differ due to the fact that the low affinity receptor for IgE is several orders of magnitude weaker than FcεRI^{+}. The experimental design was similar to that of the high affinity study except that 8866 cells were used, which consitutively express high levels of FcεRII. Increasing concentrations of chimeric CD23 proteins were added to constant concentrations of ^{125}I-mIgE or -huIgE and the reactions were incubated on ice for 30 min. Then, 1×10^{6} FcεRII^{+} 8866 cells were added, and the incubation continued at 4°C for an additional 60 min. At the end of the incubation, a phthalate oil cushion centrifugation procedure was employed to separate free from cell-bound ^{125}I-IgE. As can be seen from **Figure 5**, the IgE that had been preincubated with intact *lz*-CD23 (heavy dash) reaches total inhibition by ~2μg of CD23 added together with 100ng/ml IgE. However, the two mutants *lz*-CD23$^{148\text{-}321}$ (dotted) and (solid line) (with a single amino acid point mutation) were unable to prevent IgE from binding across the range of CD23 concentrations tested.

Figure 4. Inhibition of IgE binding to the FcεRI by *lz*-CD23 mutants. Capacity of murine and human *lz*-CD23 constructs to inhibit ^{125}I-labelled immunoglobulin E (IgE) binding to FcεRI^{+} RBL-2H3 cells. A 100-ng concentration of (**A**) ^{125}I-mouse IgE or (**B**) ^{125}I-human IgE was added to increasing amounts of the corresponding purified murine or human *lz*-CD23 stalk-deletion mutant constructs. After a 30-min incubation, the reaction mixtures were added to FcεRI^{+} RBL-2H3 cells (**A**) or huFcεRI^{+} RBL cells (**B**) in a 1-hr binding assay. Error bars represent 1 SE of triplicate measurements. IgE binding chimeric constructs of full stalk length *lz*-CD23$^{86-331}$ (•), and stalk shortened mutants *lz*-CD23$^{139-331}$ (■), *lz*-CD23$^{157-331}$ (○), *lz*-CD23$^{164-331}$ (□), and *lz*-CD23$^{171-331}$ (△) are shown. The inset shows the percentage inhibition for *lz*-CD23$^{86-331}$ (•) and *lz*-CD23$^{139-331}$ (○) incubated for longer periods to control for the possibility that binding was not being influenced by short incubation times. (**B**) Increasing amounts of full length *lz*-huCD23$^{45-321}$ (•) or the stalk-deletion mutant *lz*-huCD23$^{148-321}$ (○). The values shown represent the average of an experiment performed in duplicate.

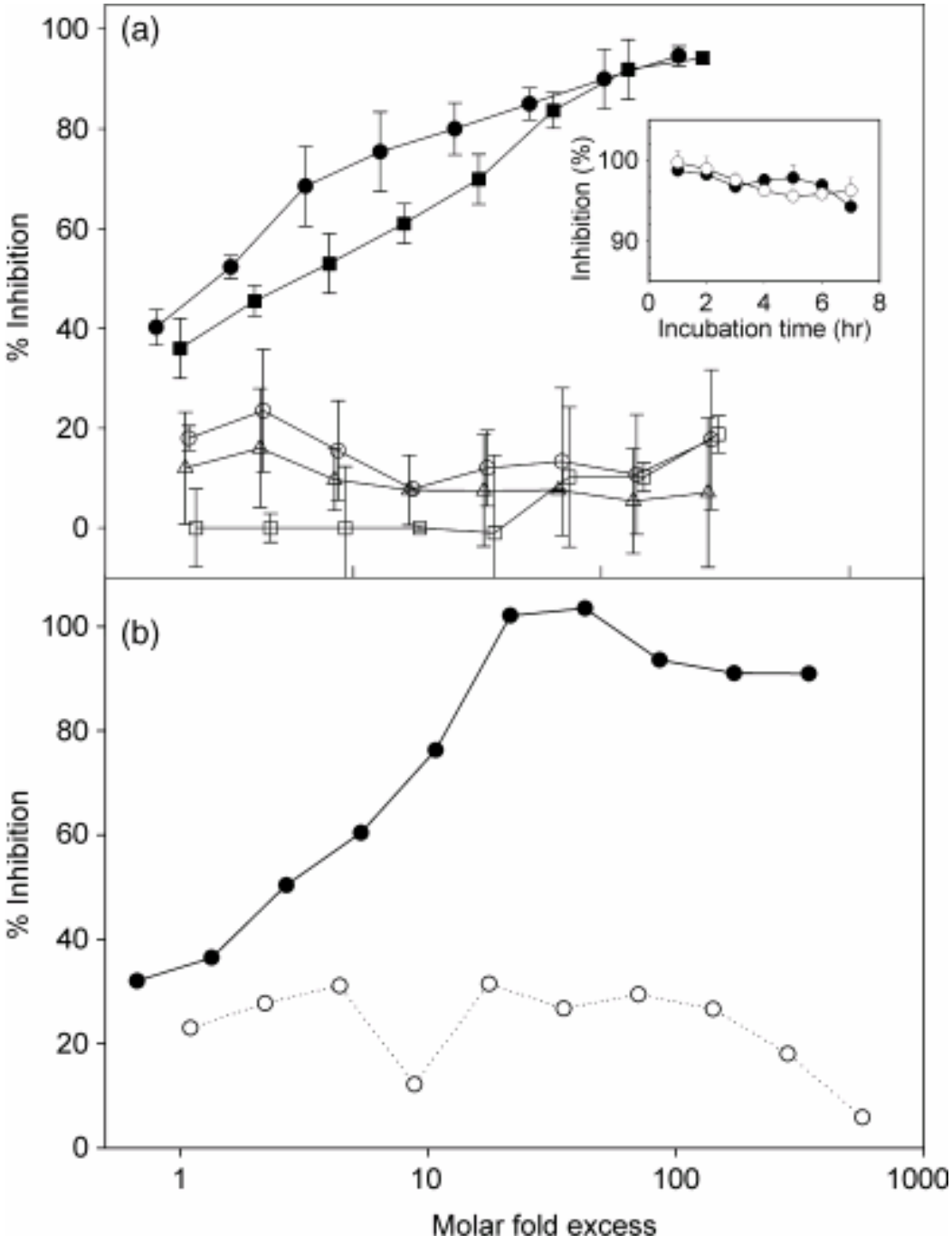
(a)
% Inhibition
100
80
60
40
20
0
Inhibition (%)
100
90
0
2
4
6
8
Incubation time (hr)
(b)
% Inhibition
100
80
60
40
20
0
1
10
100
1000
Molar fold excess

Binding Inhibition of IgE prebound to CD23 is Temperature Dependent on binding to the high affinity receptor FcεRI^{+}. Studies done in concert with these human studies in this lab demonstrated that there is a temperature dependency on the ability of IgE to bind to CD23. At that time it was sought to determine if there was a possible method to prevent binding of IgE to the high affinity receptor on mast cells, thus preventing sensitization. It was demonstrated that there is a preferential binding of IgE to CD23 at the lower temperatures analyzed (~4˚C-20˚C) and less so at physiological temperatures. I sought to determine if there were also temperature preferences with IgE binding to the high affinity receptor as well. Mouse *lz*-CD23$^{139–331}$ (**Figure 6A**) or *lz*-huCD23$^{45–321}$ (**Figure 6B**) were incubated with 100 ng of ^{125}I-labeled mouse or human IgE, respectively, at the temperatures indicated. After 30 min, RBL-2H3 **(Figure 6A**) or RBL-2H3 expressing human FcεRI (**Figure 6B**) were added. After another 1hr incubation, cell-bound radioactivity was determined, and the inhibitory effect was determined. In both mouse and human the preferential temperature for IgE to bind to FcεRI is physiological at 37˚C as seen by the loss of inhibitory ability of the *lz*-CD23. At 4˚C, the *lz*-CD23 chimera of both the mouse and human retains the IgE bound to itself at maximal inhibition.

Figure 5. Inhibition of IgE binding to the FcεRII by *lz*-CD23 mutants. This experiment is similar to that seen in Figure 4, except that RPMI-8866 cells were used rather than the RBL-FcεRIα^{+}. As can be seen the CD23$^{45\text{-}321}$ (------) completely inhibits binding of human IgE to the corresponding FcεRII, while *lz*-huCD23$^{148\text{-}321}$ (……..) was ineffective. Also included is another stalk mutant of *lz*-huCD23$^{148\text{-}321}$ (solid line), but due to an amino acid mutation, this was not used further out of concern of loss of heptad repeat. Increasing concentrations of chimeric CD23 proteins were added to constant concentrations (usually 100 ng) of ^{125}I-mIgE or -huIgE and the reactions were incubated on ice for 30 min. Then, 1×10^{6} FcεRI^{+} RBL-2H3 cells (with huIgE, RBL transfected with human FcεRIa were used) were added, and the incubation continued at 4° for an additional 60 min. At the end of the incubation, a phthalate oil cushion centrifugation procedure was employed to separate free from cell-bound ^{125}I-IgE. The cell-bound radioactivity of each reaction was determined in duplicate. Specific binding of samples was calculated by subtracting background controls incubated with 100-fold excess of cold mIgE and compared to controls without any inhibitor added.

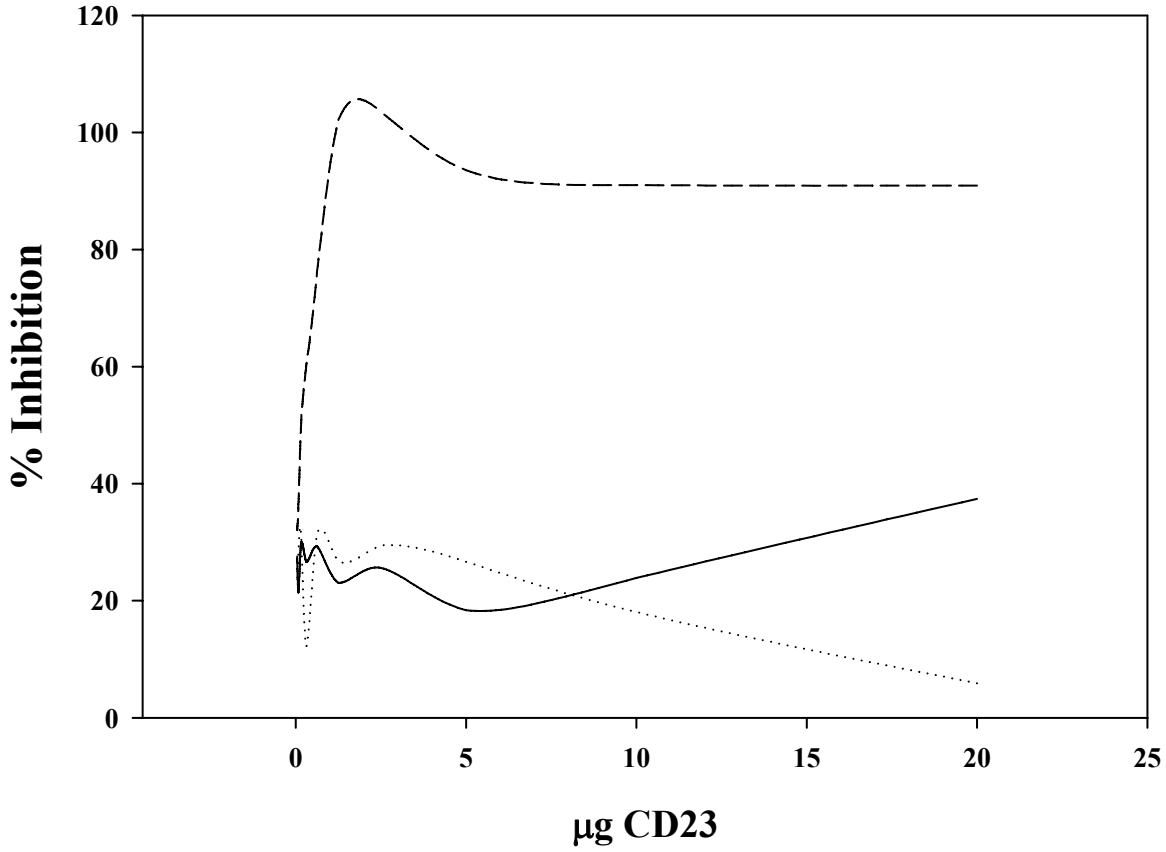
120
100
80
60
40
20
0
% Inhibition
0
5
10
15
20
25
µg CD23

Figure 6. Dose dependence of *lz*-CD23-mediated inhibition of IgE binding at different temperatures. Mouse *lz*-CD23$^{139–331}$ **(*A*)** or *lz*-huCD23$^{45–321}$ **(*B*)** were incubated with 100 ng of ^{125}I-labeled mouse or human IgE, respectively, at the temperatures indicated. After 30 min, RBL-2H3 **(*A*)** or RBL-2H3 expressing human FcεRIα **(*B*)** were added after another 1-h incubation, cell-bound radioactivity was determined, and the inhibitory effect was determined.

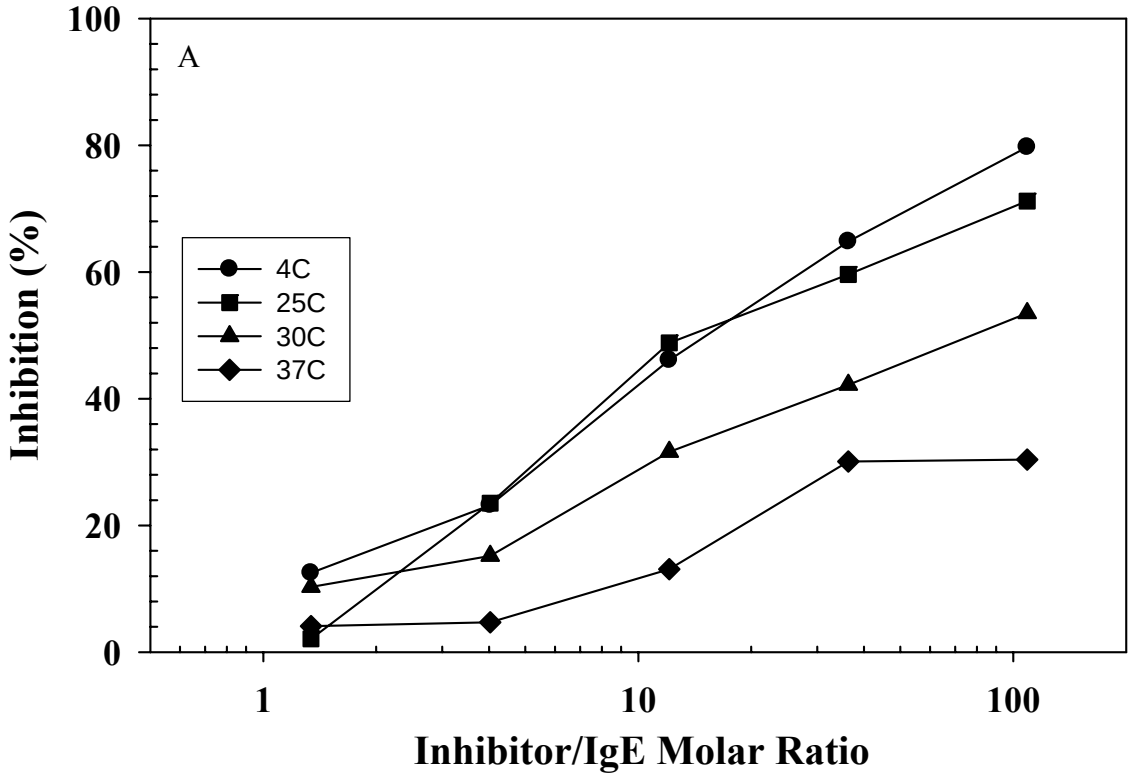
A
100
80
60
40
20
0
Inhibition (%)
4C
25C
30C
37C
1
10
100
Inhibitor/IgE Molar Ratio

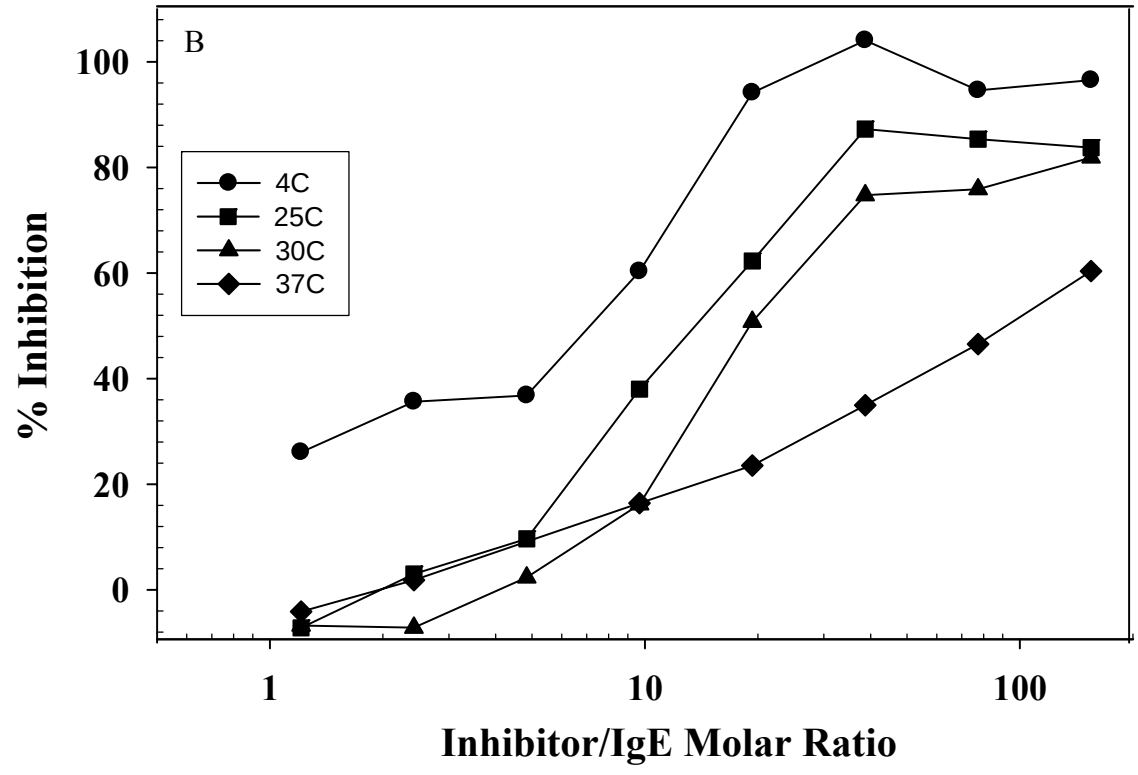
B
100
80
60
40
20
0
% Inhibition
4C
25C
30C
37C
1
10
100
Inhibitor/IgE Molar Ratio

With increasing temperature, the retention of CD23 to IgE diminishes. As can be seen at 4˚C, 20-fold molar CD23 excess over that of IgE reaches it maximal inhibition of near 100%. However, if the temperature is raised to 37˚C the inhibition is reduced markedly to only 20%. Similar observations are seen in the mouse system (**Figure 6A**). As the temperature rises the inhibition to prevent IgE from preferentially binding its high affinity receptor on the RBL cell is lost. This led to the conclusion that the IgE molecule has two conformations of the open and closed IgE structures found by crystallography, and that they interact differentially with the two IgE receptors.

Rabbit polyclonal antibodies directed against the CD23stalk bind to 8866 cells in a dose dependant manner. I sought to determine if the oligimerization of CD23 found on the surface was important in influencing the production of IgE under IL-4/antiCD40. As had been reported previously in our lab, monoclonal antibodies targeting the mouse stalk were able to reduce the production of IgE. It is thought that the destabilization of the molecule potentiates the cleavage of the stalk at one of it cleavage sites by an as yet unknown metalloprotease, although preliminary results in our lab point to this metalloprotease as a member of the ADAM family of disintegrins. Because CD23 is known to be a down regulator of IgE production when bound by an IgE-antigen complex, I wished to ascertain if antibodies targeting the stalk might be able reduce IgE production. Rabbit IgG was generated in a rabbit model targeting the stalk region of human CD23. Serum was collected and the IgG fraction was purified by 40% ammonium sulfate precipitation. Once purified and concentration determined, binding

to constitutively expressed CD23 on RPMI-8866 cells was determined. $1x10^6$ 8866 cells were incubated with increasing concentrations of rabbit anti-CD23stalk collected from one rabbit (RAS1) **(Figure 7A)**. Starting from 10µg/ml and increasing to 100µg/ml RAS1 binds in a dose dependent manner. Another rabbit was also challenged with CD23stalk (RAS2) and its binding efficiency was compared to that of RAS1 (**Figure 7B**). As can be seen equal concentrations of RAS have different binding to CD23, with RAS2 binding about 5-fold higher than the isotype control, but over one $\log_{10}$ lower than RAS1. RAS1 has a similar but still slightly lower binding than the positive control of the mouse monoclonal antibody targeting the lectin-head, EBV-CS2. I would expect, based on the binding that any effects on IgE production would be more pronounced with RAS1 due to its greater binding to CD23 than RAS1. I also sought to determine if the presence of RAS would influence IgE binding to CD23.

Rabbit anti-CD23stalk antibodies pre-incubated with HuCD23 inhibits CD23 binding to plate bound huIgE. *lz*-CD23 is prevented from binding plate bound human IgE in a dose dependent manner in the presence of preincubated RAS-CD23 complexes. Increasing concentrations of both RAS1 and RAS2 were preincubated with 8nM *lz*-CD23 for 1 hour at 4ºC. After incubation the mixture was added in 50µl aliquots to ELISA plates preincubated with 5µg/ml IgE. The RAS-CD23 mixture incubated with the IgE for one hour at 4ºC. After washing goat-anti-rabbit-HRP antibodies (1:1000) were added and OneStep TMB substrate was added and relative inhibition was determined by spectrophotomety. Both the RAS1 and RAS2 antibodies inhibited *lz*-

CD23 from binding (**Figure 8**). Similar to binding to the native surface CD23 on 8866 cells, RAS1 had ~5-fold better efficacy in inhibition than that of RAS2.

Figure 7: Rabbit anti-huCD23stalk antibodies bind with differing capacity on constitutively active CD23 expressing RPMI-8866 cells. Relative maximal binding between the two rabbit anti-huCD23stalk antibodies was compared. **(A)** $1x10^6$ RPMI-8866 cells expressing constitutively the CD23 surface antigen were incubated with increasing rabbit anti-CD23stalk antibodies. Rabbit anti-stalk #1 (RAS1) was added at 10ngml (——), 25ng/ml (——), and 100 ng/ml (——), respectively, or not at all (——) to determine at which concentration would saturate the CD23 present on the surface. **(B)** 100ng/ml RAS1 (——) was chosen for comparison with 100ng/ml RAS2 (——). Also shown are rabbit IgG isotype control (——), cells alone (——) and in orange is the anti-CD23 lectin-head antibody mouse EBV-CS2 used as a positive control.

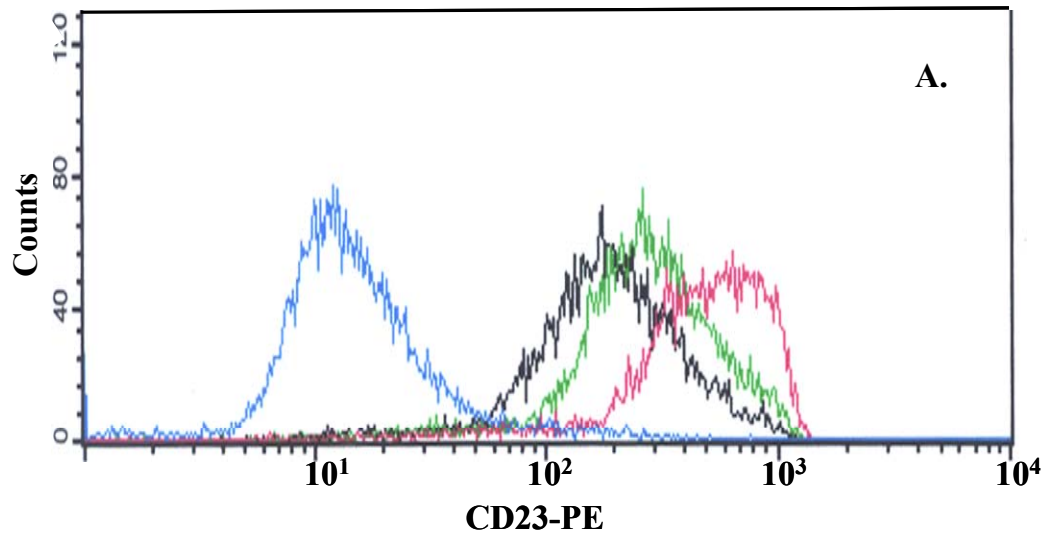
A.
Counts
0
40
80
10^1
10^2
10^3
10^4
CD23-PE

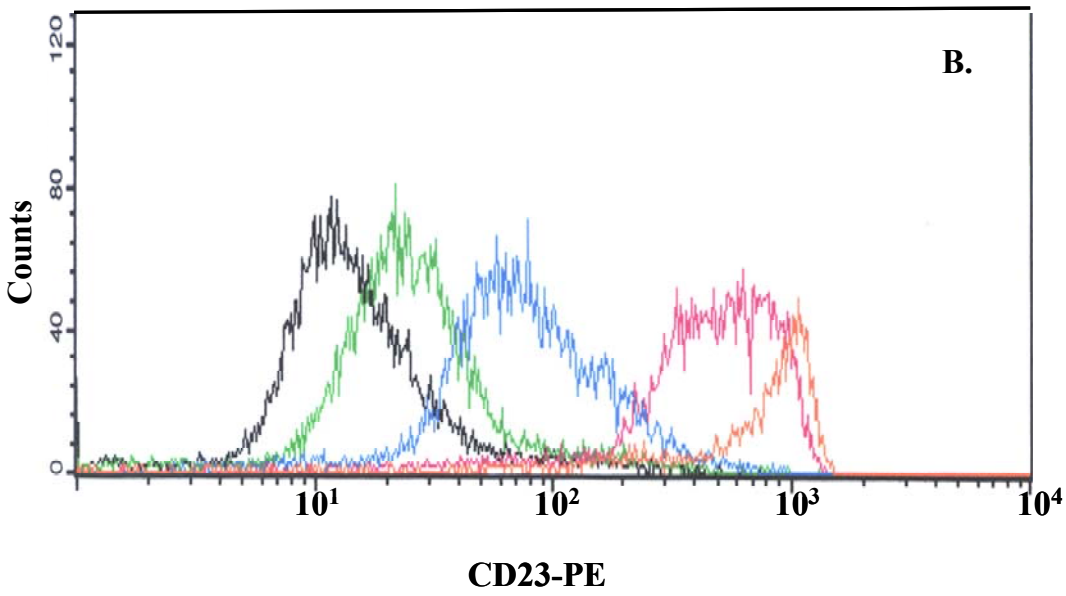
B.
Counts
0
40
80
120
10^1
10^2
10^3
10^4
CD23-PE

Figure 8: Rabbit anti-CD23stalk antibodies pre-incubated with HuCD23 inhibits CD23 binding to plate bound huIgE. 8nM of huCD23 was incubated with increasing concentrations of rabbit anti-CD23stalk antibodies, rabbit anti-CD23stalk #1 and #2, RAS1 (●) and RAS2(▲). Increasing concentrations of non-specific rabbit IgG (■) was used as a control. Maximal binding of huCD23 to hu-IgE was determined by the addition of no antibody (♦). The preincubation mixture was then added to plate bound IgE and full length lz-CD23 binding to IgE was assessed.

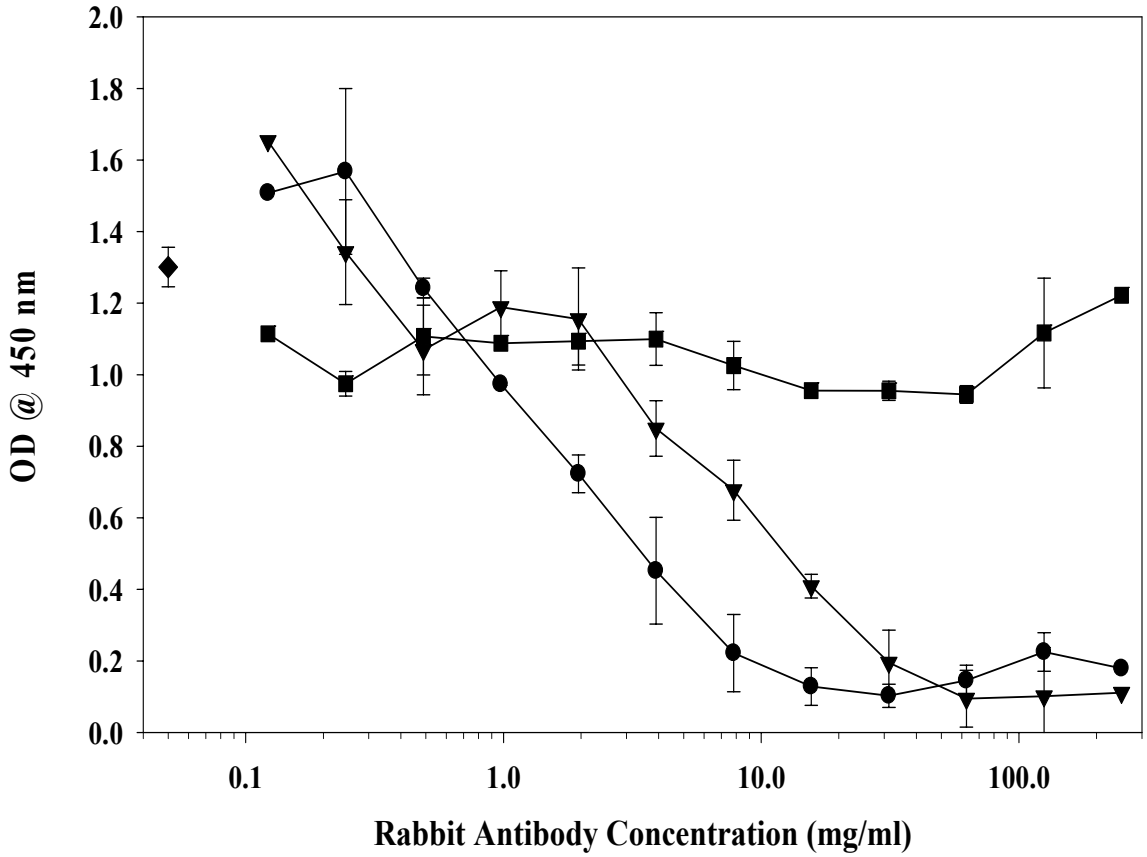
2.0
1.8
1.6
1.4
1.2
1.0
0.8
0.6
0.4
0.2
0.0
OD @ 450 nm
0.1
1.0
10.0
100.0
Rabbit Antibody Concentration (mg/ml)

Rabbit anti-stalk antibodies have reduced expression dependent on time on 8866 cells. I hypothesized that the antibodies might facilitate the destabilization of the CD23 trimer, exposing cleavage sites to a metalloprotease, or CD23 sheddase. As had been previously shown in our lab, a monoclonal anti-mouseCD23stalk antibody increase serum levels in *in vivo* mouse studies. In this preliminary study (**Figure 9**) I treated 8866 cells with a constant amount of 10μg/ml of RAS1. The cells were incubated in complete culture media for increasing times ranging from 1 hour to 24 hours. After each time point the cells were collected and washed and resuspended in buffer and stained with goat anti-rabbit FITC. The intensity with each increasing time point was determined and shows that the total count of cells at a given intensity decreased as the time increase (**Figure 9a**). Although not significant, there was a loss of intensity as the time of incubation was increased. To investigate if the concentration of RAS1 added might be a contributing factor, a 6 hour incubation time was used for all concentrations used (**Figure 9b**). As can be seen although there is increasing intensity with increasing concentration of RAS, there is no appreciable reduction in counts in the lower concentrations of antibody added, indicating that either there is no loss of antibody, or that the antibody had been internalized .

Endocytosis is unlikely in RAS1/CD23 interaction. It has been shown that CD23 can be involved in CD23 endocytosis in phagocytosis on monocytes and macrophages, and involved in internalizing antigen, and is involved in intracellular antigen processing. I sought to compare the differences between cells treated with RAS1 at both 4ºC and 37

ºC and compare expression of RAS1 after a series of time points. (At that time it was uncertain if the trimer would behave in a manner that would have the stalk bound tightly at the membrane together with its other members of the trimer. This would mean that the stalk could freely move as individual units above that point and would be able to be readily bound at all three stalk portions that were targeted by the antibodies. Also the differences in temperature were only beginning to be explored and the results here were of a fortuitous nature.) As can be seen from Fig.10, there

Figure 9: Binding Experiments of RAS to 8866 Cells. To determine the optimal concentrations of rabbit anti-CD23stalk antibodies on 8866 cells titrations of different concentrations were assessed. Also time course kinetics on binding was assessed. Finally, the binding of RAS to 8866 cells was analyzed in regards to temperature. **(A)** $1x10^6$ 8866 cells were incubated for 1 hour at 37˚C (grey), 6 hours (dashed) or overnight (16 hours) (solid black) with 10µg/ml RAS1. Cells were collected and washed and stained again with goat anti-rabbit FITC. **(B)** Due to the high CD23 expression by 8866 cells, the concentrations were increased. Time course of 6 hours at 37˚C with 10µg/ml (black), 25 µg/ml (dashed), and 100 µg/ml (grey). Isotype control is shown as fine dashes in all figures.

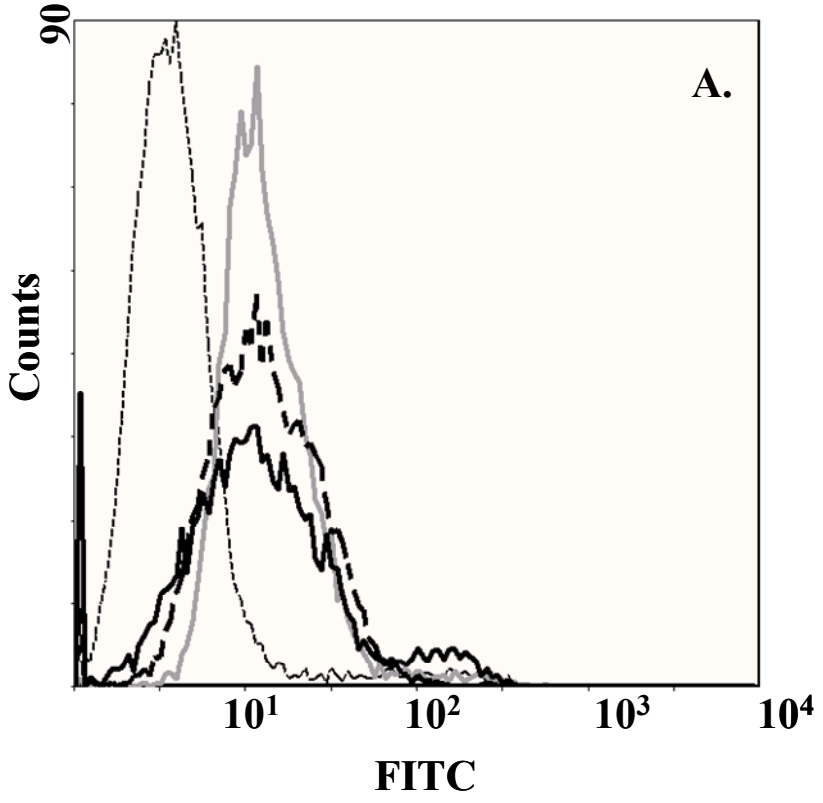
90
A.
Counts
10¹
10²
10³
10⁴
FITC

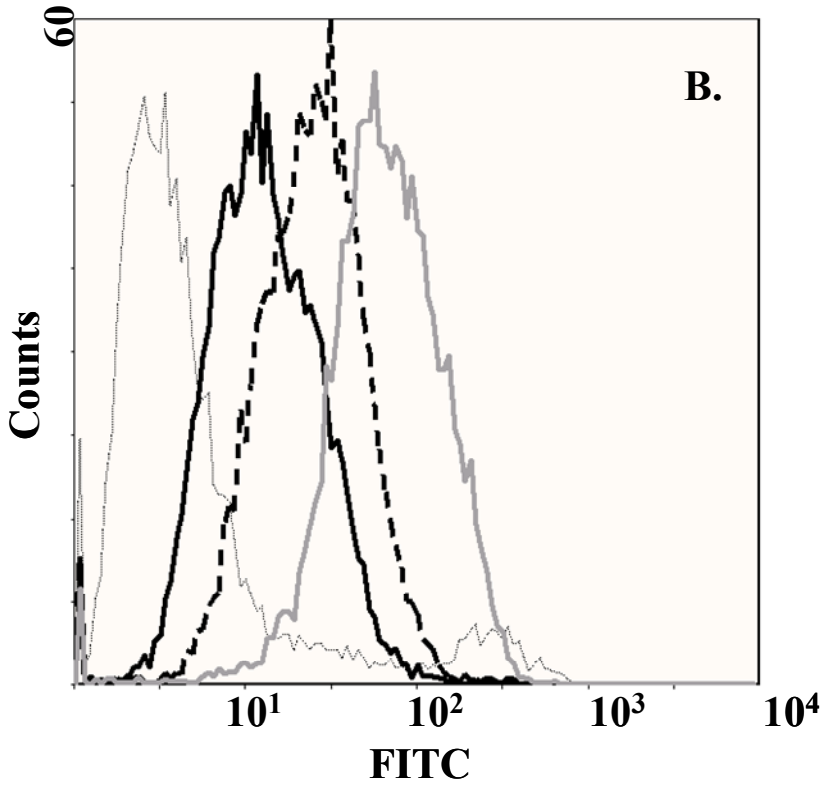
60
B.
Counts
10¹
10²
10³
10⁴
FITC

Figure 10. Endocytosis is not involved in anti-stalk antibody/CD23 interaction. To analyze any effects due to possible endocytosis of the CD23 molecule RAS1 complex, the overnight binding assay of 100μg/ml RAS1 was performed at differing temperatures of 4˚C (solid black) and 37˚C (dashed black). Other times at 37˚C were also studied at 6 hours (grey) and one hour (heavy dot). Isotype control is shown as fine dashed in all figures.

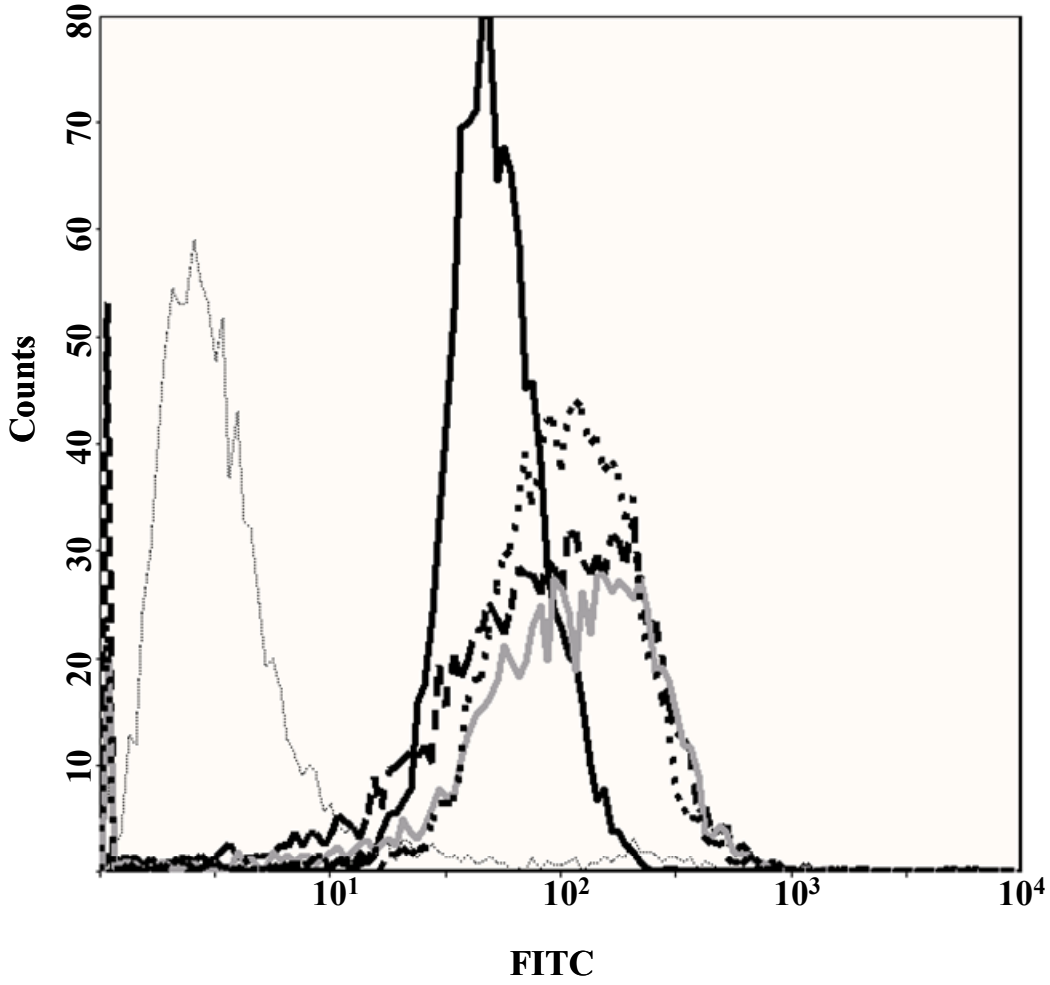
Counts
10
20
30
40
50
60
70
80
10^1
10^2
10^3
10^4
FITC

is a significant increase in the mean fluorescence intensity (MFI) when the rabbit anti-stalk (RAS1) antibody is allowed to bind at 37ºC for one hour (13.1) as compared to the binding MFI that occurs under 4ºC conditions (5.6). My initial hypothesis that the additional temperature would lead to a reduced expression due to the cells being incubated at physiological conditions, allowing normal functioning of the cell to occur were not seen. Even if the incubation times were increased to 6 hours (MFI 14.3) and 24 hours (MFI (11.8), this was not realized. Our initial intention of trying to observe if the addition of the RAS antibodies would lead to a reduction in surface expressed CD23 due to the increased temperature to physiological conditions did not manifest. In fact the opposite occurred, leading to the conclusion that perhaps the trimeric model of CD23 allows for the receptor to be both trimeric and monomeric (all three monomers bound at the base of the stalk, yet opening up as the distance between the membrane increases). As the temperature indicates, there is roughly a 2-3 fold increase in the MFI at 37ºC as compared to the MFI at 4ºC. This suggests that the CD23 molecule is open at physiological temperatures exposing three stalks to binding. At the 4ºC condition the trimer is perhaps complete from membrane base to lectin-head, preventing that antibodies from binding either to loss of epitope exposure or steric hinderance.

sCD23 is increased in supernatants from IL-4/antiCD40 PBMCs when in the presence of RAS1 and RAS2. From the observations that I received in the temperature study, I sought to determine if the increased binding seen at physiological temperatures indicated increased exposure of the CD23 homotrimers to proteolytic cleavage.

Peripheral blood was collected and stimulated with IL-4 and anti-CD40. Cells were plated at 200k cells/ml and either RAS1 or RAS2 were added in increasing concentrations. After 12 days the supernatants were collected and analyzed for sCD23 release (**Figure 11**). At the highest concentrations of both RAS1 and RAS2 there was a significant increase of sCD23 present in the supernatant as determined by ELISA. The data suggests that at concentrations that are effective in reducing IgE secretion by IL-4/antiCD40 stimulated B cells, RAS antibodies also contribute to increasing the shedding of surface CD23. This suggests that the CD23 trimer is altered in such a way as to expose cleavage sites for proteolytic degradation.This data supports that supposition that the anti-stalk antibodies may induce cleavage of the oligomer of CD23.

Rabbit anti-CD23stalk antibodies inhibit IgE production in PBMCs treated with IL-4/antiCD40 in a dose dependent manner. Human peripheral blood was collected and the buffy layer was purified by density gradient centrifugation. Cells were plated at 200k cells/well and treated with IL-4 and antiCD40 in complete RPMI-1640 media. RAS1 and RAS2 were added in increasing concentrations and after 12-14 days the supernatant was collected and centrifuged to remove any contaminating cells and debris. IgE content was assessed by ELISA. As can be seen in **Figure 12**, RAS1 has near total inhibition of IgE secretion in stimulated PBMCs at 100µg/ml. By 1µg/ml the inhibition is still reduced with the loss of inhibition finally occurring when 0.1µg/ml is added. RAS2 was also able to inhibit IgE secretion, albeit not to the extent that RAS1 was able to. Only at the highest concentration of 100µg/ml was any significant

reduction of IgE secretion seen. By 10μg/ml, the inhibitory effect was essentially gone. The fact that the RAS2 did not have the same ability to reduce IgE synthesis as effectively is not particularly surprising as binding studies showed that RAS2 did not bind to CD23 as effectively as did RAS1.

Figure 11: RAS1 and RAS2 added to IL-4/antiCD40 stimulated PBMC increase the sCD23 found in the supernatant after 12 days. PBMC was collected and plated at 200k cells/well and treated with IL-4 and antiCD40 (black dot). Some conditions were treated with either increasing RAS1 (black bar), RAS2 (med grey bar). Rabbit isotype control is shown in the dark grey bar. $p < 0.002$

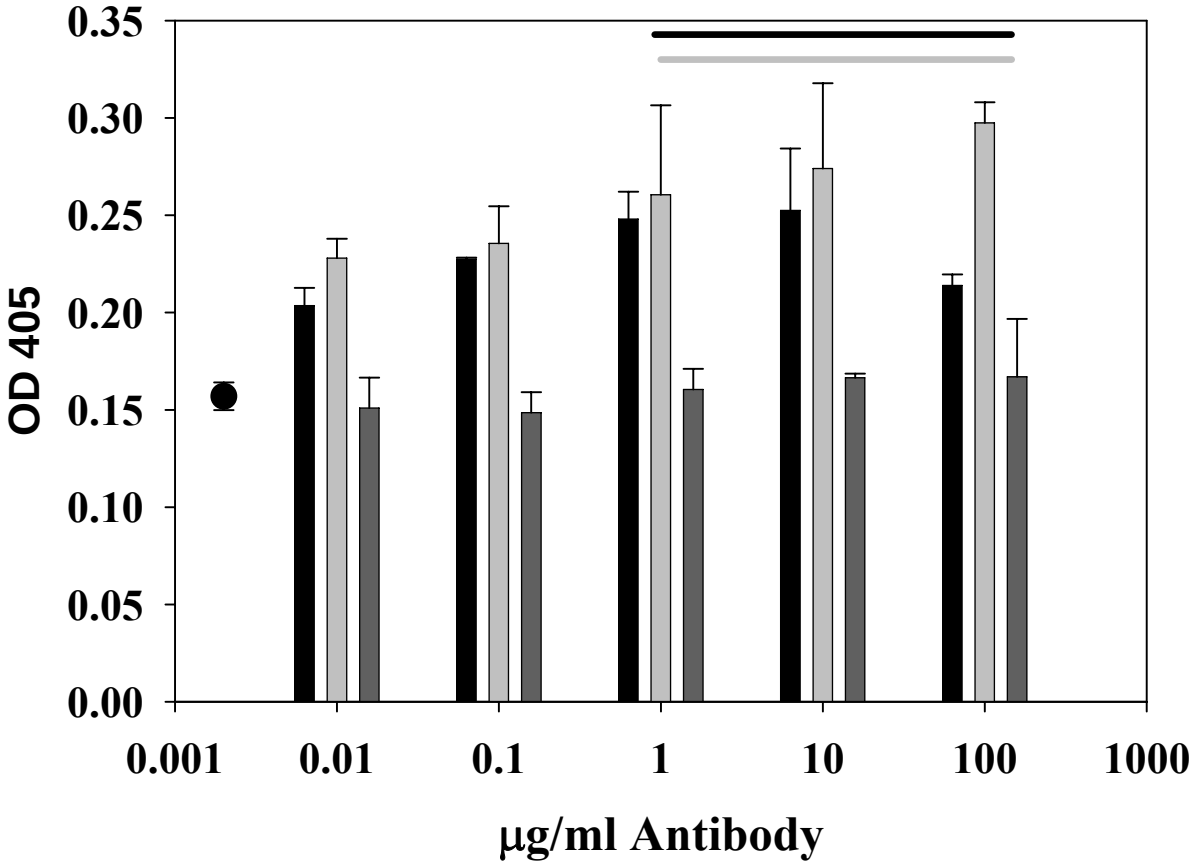
0.35
0.30
0.25
0.20
0.15
0.10
0.05
0.00
OD 405
0.001
0.01
0.1
1
10
100
1000
µg/ml Antibody

Figure 12. Rabbit anti-humanCD23 stalk antibodies inhibit IgE production from IL-4/antiCD40 stimulated PBMCs in a dose dependent manner. Human peripheral blood was collected and non-granular lymphocytes were plated at 200k cells/well. Increasing concentrations of RAS1 (black) and RAS2 (medium grey) were added to the cells. Cells were incubated for 12 days and after that time the supernatants were analyzed for IgE content by ELISA. Rabbit isotype control (dark grey) and no antibody control (faint grey) are shown.

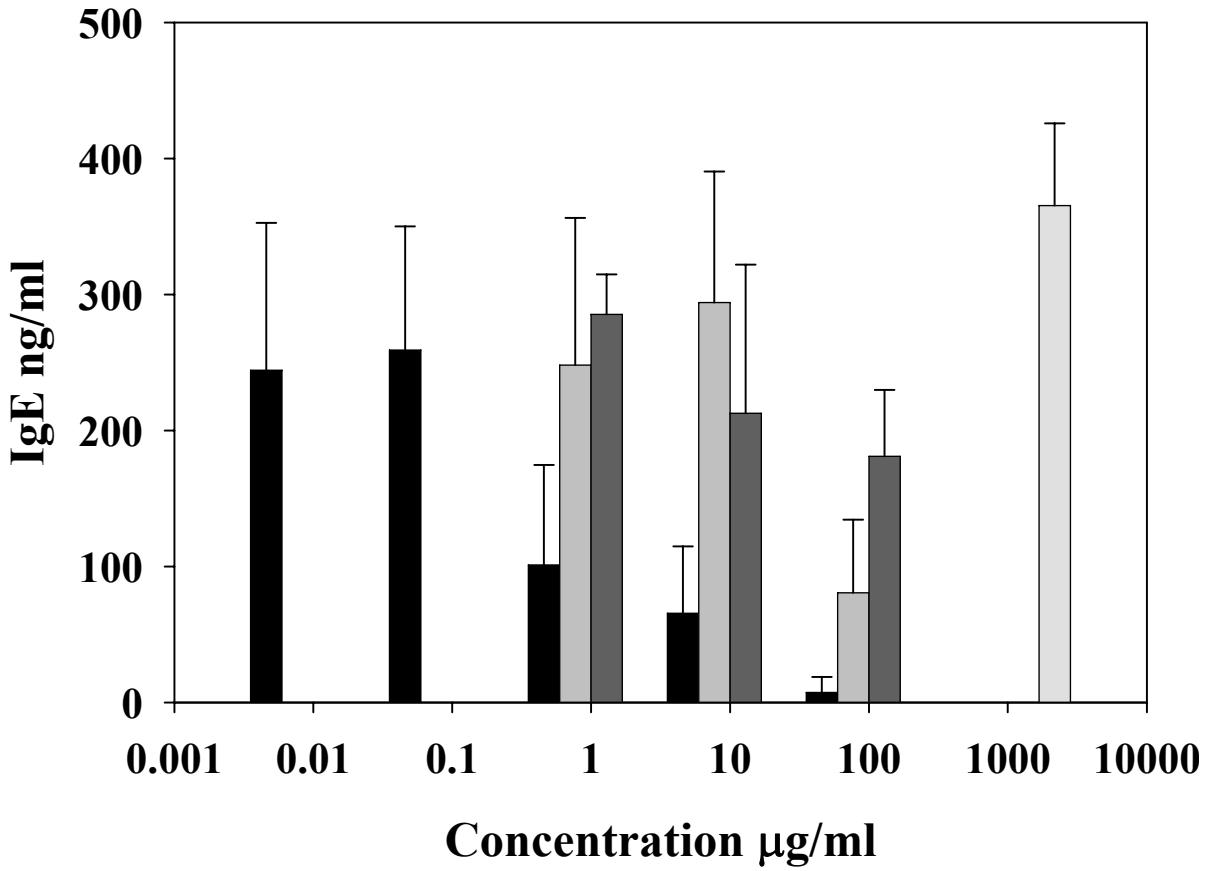
500
400
300
200
100
0
IgE ng/ml
0.001
0.01
0.1
1
10
100
1000
10000
Concentration μg/ml

Affinty purified Rabbit antiCD23 antibodies do not show markedly increased inhibition of IgE production in IL-4/antiCD40 stimulated cells. I hypothesized that if the antiCD23stalk antibodies in the rabbit anti-CD23stalk pool were affinity purified, it would provide a significant improvement of IgE inhibition. It was also thought that by working with the purified antiCD23stalk antibodies, all subsequent studies would be made more relevant as only those antibodies specific to the stalk would be used in the study. To do this a large quantity of CD23 stalk was made. I started with growing up the *E.Coli* BL21-huCD23stalk$^{48\text{-}153}$ overnight in 100 mls media with 100µg/ml ampicillin. A total of 4L of Luria Broth (LB), with 100µg/ml ampicillin, with 25mls of each being added to a single liter of LB was prepared. To determine the best time for adding IPTG, absorbance was taken at each hour and at A_{280}=0.4 1mM IPTG was added. After 4 hours the cells were spun down and the pellet resuspended in 200mls buffer A (25mM Tris (pH7.5), 1mM EDTA, 1mM DTT, and 0.01% Triton X-100). The cells were homogenized as to disrupt the cells. Following a freeze thaw cycle, the insoluble material was pelleted by centrifugation for 30 minutes. A Q-fast flow 16cm XK20 column was equilibrated with 0.1M NaCl in buffer A. Half of the supernatant was loaded at 2.5ml/min and the human CD23stalk was eluted with 600 ml gradient of 0.1 NaCl to 1.0M NaCl in buffer A. Human CD23stalk$^{48\text{-}153}$ was found in the column wash and low salt fractions. This was repeated a second time to ensure the removal of bacterial DNA and protein contamination. The volume was concentrated on an Amicon concentrator using a YM3 membrane. As the concentration of CD23stalk increased the material precipitated. 6M GnHCl in 0.1M Tris pH 7.5 was added and the stalk

redissolved. The purified huCD23stalk was purified by gel filtration on a Sephacry S-200 HR 100cm column with 6M GnHCl and 0.1MTris. Fractions containing the stalk were identified by SDS-PAGE. These were pooled and diluted with 4 volumes of 0.1M NaCl, 25mM Tris (pH 7.5) and 1mM EDTA. This was concentrated on a YM 3000 membrane. Samples were diluted and concentrated one more time to remove residual guanidine hydrochloride. The resulting purified antibody was added in increasing concentrations to PBMC that had been treated with IL-4 and anti-CD40. As can be seen from **Figure 13**, RAS3, like RAS1 and RAS2, inhibited the production of IgE. What it did not do however, was significantly increase the inhibition beyond what the unpurified RAS3 was capable of doing. The total reduction in IgE inhibition is ~75% compared to no buffer alone or rabbit isotype control. While this was a bit of a disappointment, it did illustrate the importance of using the monoclonal antibodies that I had started to generate in rats and subsequent to that, in mice.

Figure 13: Rabbit anti-CD23stalk antibodies purified over CD23stalk column gained little IgE Inhibition in IL-4/antiCD40 stimulated PBMC. Rabbit anti-CD23stalk #3 (RAS3) was further purified to retain only anti-CD23stalk antibodies. PBMC was collected and stimulated with IL-4 and antiCD40. Increasing concentrations of affinity purified RAS3 was added. After 12 days the supernatants were collected and IgE contained in the supernatants were determined by ELISA. Affinity purified RAS3 is shown in black, Rabbit isotype control is shown in light grey. Circle represents no antibody added.

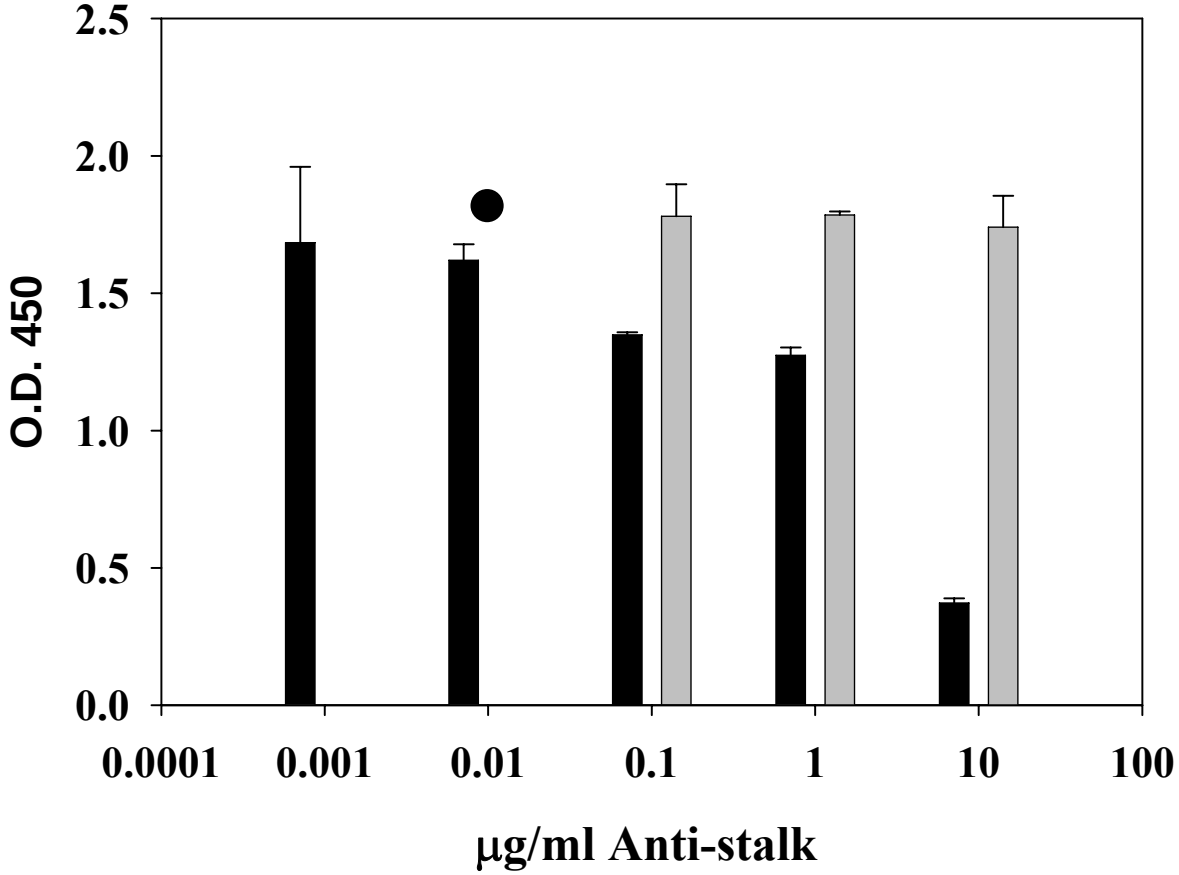
2.5
2.0
1.5
1.0
0.5
0.0
O.D. 450
0.0001
0.001
0.01
0.1
1
10
100
μg/ml Anti-stalk

IgE secretion inhibition due to rabbit anti-CD23stalk antibodies is determined by the Fc portion. The influence of the Fc receptor, FcγRIIb, must be taken into consideration when working with intact antibodies. The FcγRIIb is an inhibitory surface receptor that has an ITIM motif. To determine if the inhibitory effect of IgE synthesis in IL-4/antiCD40 stimulated PBMCs is due to the ITIM engagement, some of the RAS antibodies were subjected to pepsin degradation. The antibodies were then run over size exclusion columns and the fractions were collected and protein content determined by spectrophotometry. The fractions containing the proteins were analyzed for IgE binding by ELISA. As expected the larger $F(ab')_2$, was found in the early peak. The antibodies were concentrated in an Amicon protein concentrator and dialyzed. Concentration was determined by spectrophotometry. PBMCs were collected and the lymphocytes were purified, washed and resuspended in complete media. Cells were stimulated with IL-4 and anti-CD40 and treated with increasing concentrations of either intact RAS or RAS $F(ab')_2$. As seen in **Figure 14**, the inhibition of IgE synthesis in IL-4 antiCD40 stimulated cells using intact rabbit anti-CD23stalk antibodies is lost when the Fc domain is removed and only the $F(ab')_2$ is used. This implicates that the effect seen in IgE secretion reduction is dependent on perhaps the FcγRIIb inhibitory receptor and most likely not due to the CD23 molecule exclusively. The RAS1 is shown here although similar results with RAS2 were also seen (data not shown).

Rabbit anti-CD23stalk antibodies bind to CD23 8866 dependent on temperature roughly 2-3-fold higher. I sought to determine if the binding of rabbit anti-CD23stalk

antibodies would influence the stability of the CD23 trimer by stabilizing it or by destabilizing it. If the CD23 molecule could be destabilized, and opened, allowing proteolytic cleavage one would expect that

Figure 14. The inhibitory capacity of Rabbit anti-humanCD23stalk is dependent on an intact antibody. Rabbit anti-CD23stalk antibodies were treated with pepsin and purified over a sepherose column. The $F(ab')_2$ pool was purifed and added to IL-4/antiCD40 stimulated PBMC (▲). Intact RAS1 antibodies were also added to cells treated with similar conditions (●) and significantly reduced IgE production with 1μg/ml of antibody added. After 12 days of incubation the supernatants were collected and IgE content was analyzed.

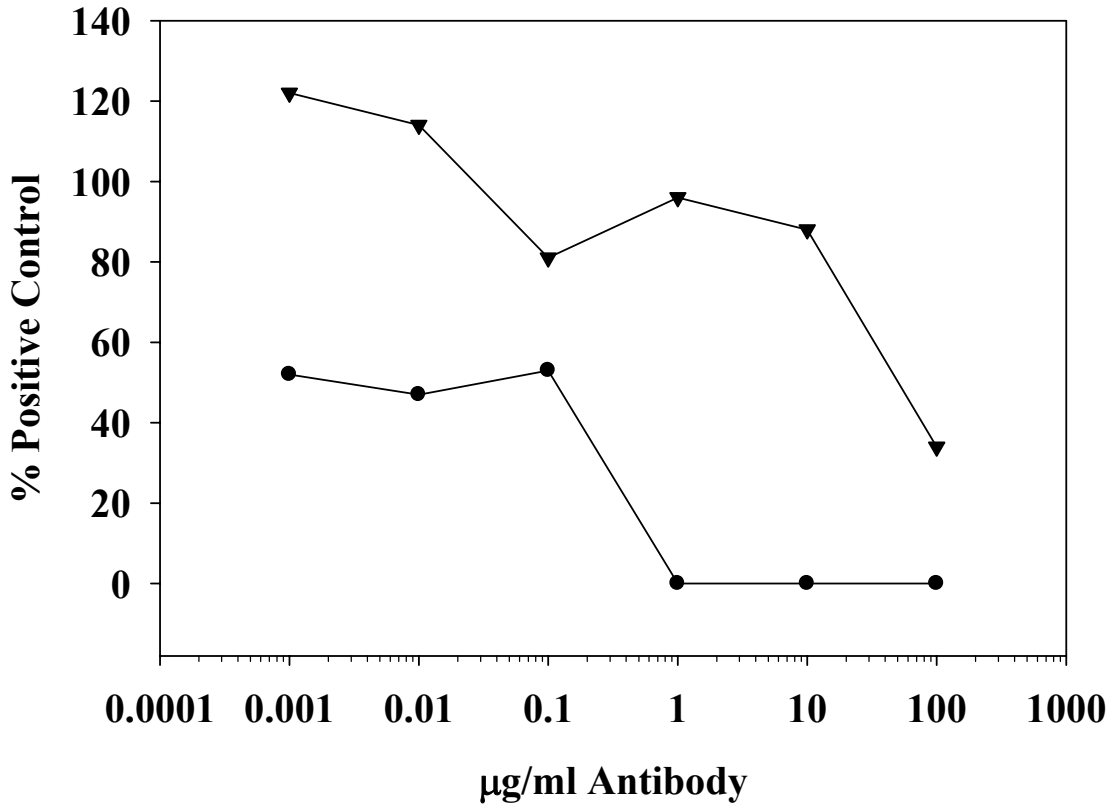
140
120
100
80
60
40
20
0
% Positive Control
0.0001
0.001
0.01
0.1
1
10
100
1000
µg/ml Antibody

there would be an increase in IgE production. If however, the presence of the anti-stalk antibodies could block the cleavage site and stabilize the CD23 trimer, IgE production might be found to increase, allowing for an exciting model for studying increased IgE production. As I had discovered that the presence of either RAS antibodies added to IL-4/antiCD40 stimulated cells actually reduced the production of IgE and increases CD23, I began to expect that there should be a concomitant increase in sCD23, regardless of the data that the loss of the Fc portion seemed to be largely responsible for what inhibition that occurred. RPMI-8866 cells were incubated with 100μg/ml of various RAS antibodies for one hour at either 4ºC or 37 ºC (**Figure 15**). Cells were then washed and centrifuged and stained with a goat-anti rabbit-FITC and binding was determined. As seen in **Figure 15a** and **Figure 15b**, RAS1 and RAS2 both have significant more binding at 37ºC than at 4ºC. Much less difference can be seen in the EBV-CS1, the anti-stalk mouse monoclonal in **Figure 15c**. However, as expected, the anti-lectin head mouse monoclonal EBV-CS2 (**Figure 15d**) had a significant increase in binding at 37ºC. Similar studies were performed on rat monoclonals that had been prepared in the lab as seen in **Figure 16**. Three rat isotypes, IgG2b (**Figure 16a**), IgG1 (**Figure 16b**), and IgM (**Figure 16c**) had varying degrees of binding, but all had increased binding at 37ºC than at 4ºC. The mean fluorescent intensity (MFI) was compared and the results tabulated in **Table 1**. I was looking for an even 3-fold difference that could be easily explained by all three monomers of the CD23 trimer being equally exposed due to the higher temperature based upon data shown by Kilmon *et al.* using the rat monoclonal targeting the mouse CD23stalk [88] (**Figure 17**). However, only RAS1 and the Rat

IgG2b had an increase of ~3-fold at 37ºC over that of 4ºC. The others had lower increases. I was surprised by the results of EBV-CS2 as that is a lectin head antibody and would be expected to have a more ready exposure to its binding site.

Figure 15. Temperature influences binding of anti-CD23stalk antibodies. $CD23^{+}$ RPMI-8866 cells were incubated with the anti-stalk antibodies at 37˚C (blue) or 4˚C degrees (green). Isotype controls were used and are shown at 37˚C (black) or 4˚C degrees (red). **(A)** RAS1, **(B)** RAS2, **(C)** EBV-CS1, and **(D)** EBV-CS2. A goat anti-rabbit FITC or goat-anti mouse FITC was used as a secondary antibody and was analyzed on a flow cytometer.

A.

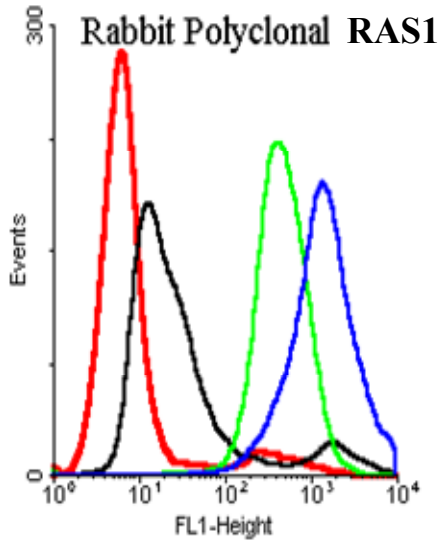
Rabbit Polyclonal RAS1
300
Events
0
10^0 10^1 10^2 10^3 10^4
FL1-Height

B.

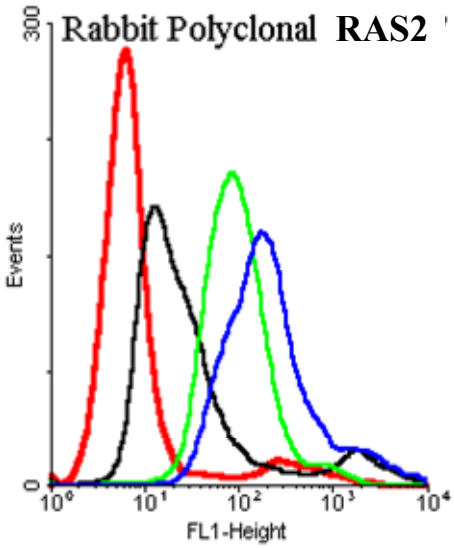
Rabbit Polyclonal RAS2
300
Events
0
10^0 10^1 10^2 10^3 10^4
FL1-Height

C.

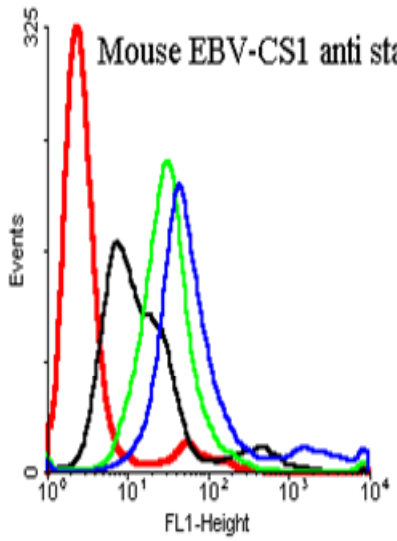
Mouse EBV-CS1 anti stalk
325
Events
0
10^0 10^1 10^2 10^3 10^4
FL1-Height

D.

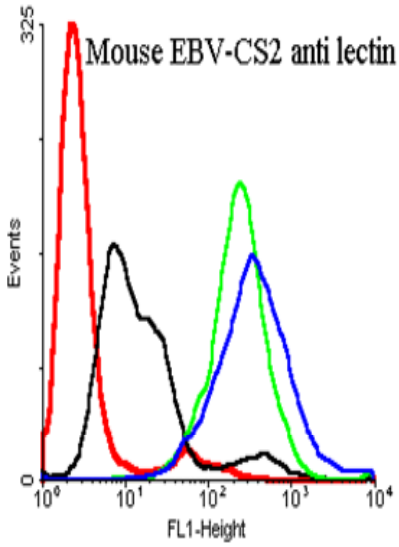
Mouse EBV-CS2 anti lectin
325
Events
0
10^0 10^1 10^2 10^3 10^4
FL1-Height

Figure 16: Temperature influences the binding of rat anti-CD23stalk antibodies. Rat anti-CD23 monoclonal antibodies of varying isotypes of **(A)** IgG2b, **(B)** IgG1, and **(C)** IgM were incubated with 8866 cells at varying temperatures of 37˚C (blue) or 4˚C degrees (green). Isotype controls were also run at varying temperatures of 37˚C (black) or 4˚C degrees (red).

A.

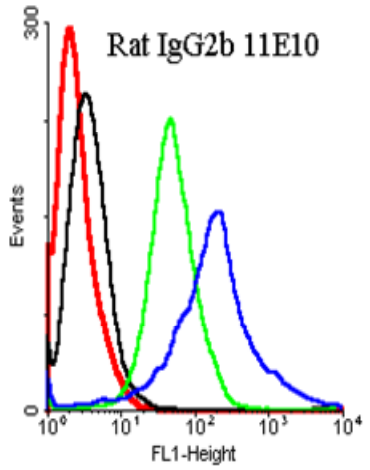
Rat IgG2b 11E10
300
0
Events
10^0 10^1 10^2 10^3 10^4
FL1-Height

B.

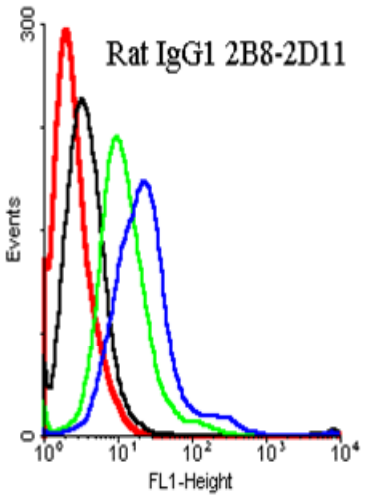
Rat IgG1 2B8-2D11
300
0
Events
10^0 10^1 10^2 10^3 10^4
FL1-Height

C.

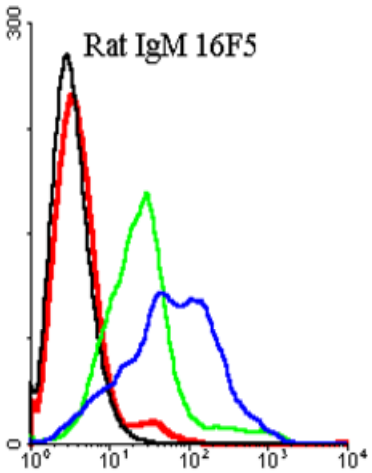
Rat IgM 16F5
300
0
10^0 10^1 10^2 10^3 10^4

Relative Binding is Increased at Higher Temperature

TABLE 1.

ANTIBODY	**4°C**	**37°C**
11E10 IgG2bκ Rat	1x	3.32x
2B8-2D11 IgG1κ Rat	1x	1.94x
16F5 IgMκ Rat	1x	2.48x
Rabbit Polyclonal "Red"	1x	2.89x
Rabbit Polyclonal "Purple"	1x	2.08x
EBV-CS1 (anti-stalk) mouse	1x	1.43x
EBV-CS2 (anti-lectin) mouse	1x	2.06x

This table shows the ratio of the Mean Fluorescence Intensity at the two temperatures.

Numbers were calculated from (37°C mean Ab - 37°C isotype mean control) /(4°C mean Ab-4°C isotype mean control) from the FACS. 4°C was arbitrarily set to 1x

Figure 17. Proposed Structure of CD23 at 4°C and 37°C in the presence of anti-CD23stalk antibodies. (**A**) The trimeric stalk at 4°C is tightly wound together preventing multiple epitopes from being accessed by the anti-CD23stalk antibodies. (**B**) The trimeric stalk at 37°C is loosely associated allowing all three epitopes to be accessed by the anti-CD23stalk antibodies.

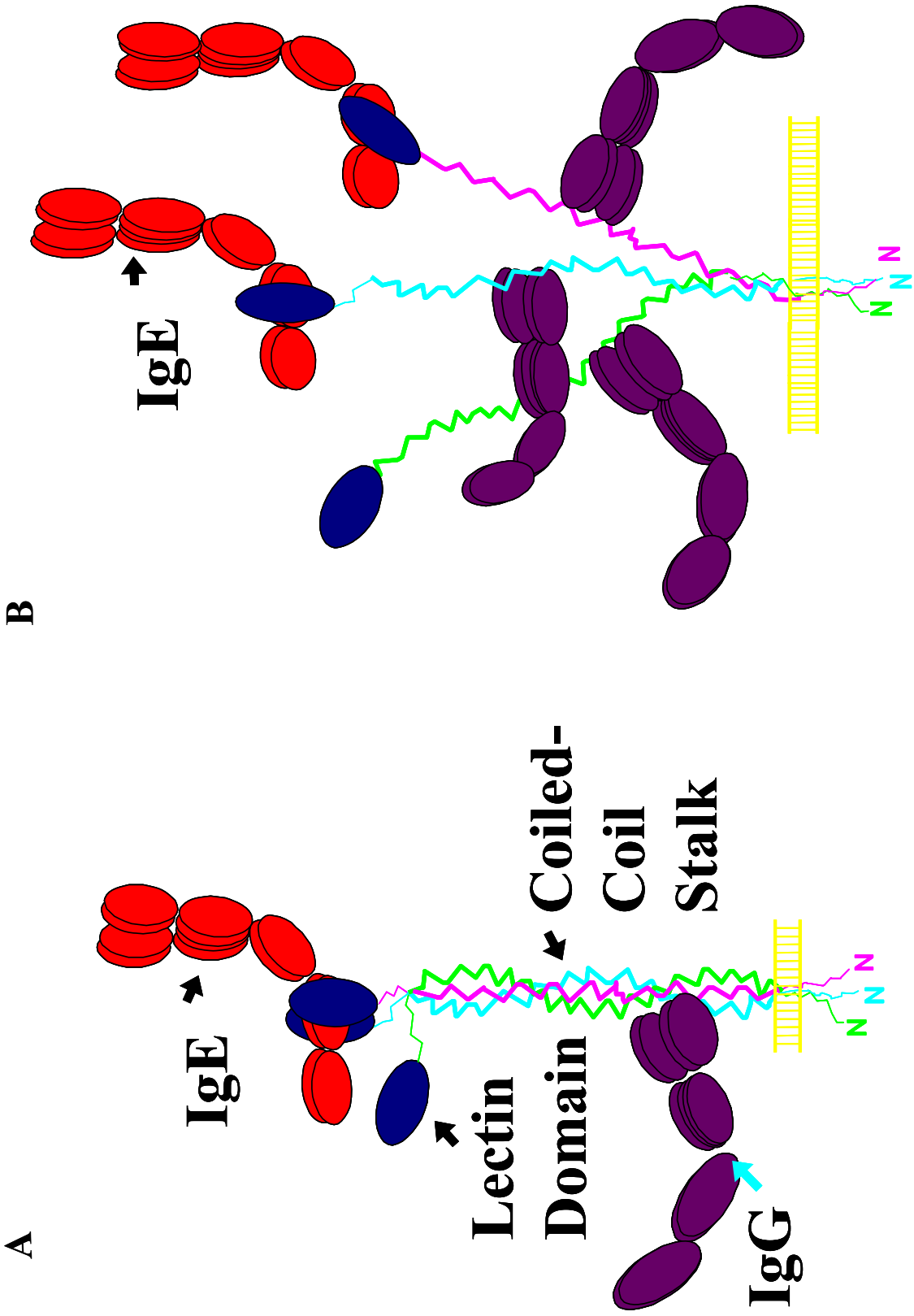
A
IgE
Lectin
Domain
Coiled-
Coil
Stalk
IgG
B
IgE

Binding Inhibition to Immobilized IgE is similar between all anti-CD23stalk antibodies tested. I sought to determine if the relative similarities seen in the RAS antibodies as well as mouse antibodies targeting the stalk would also be seen in the rat monoclonal antibodies that were made. As can be seen in **Figure 18**, all antibodies tested, when preincubated with *lz*-CD23, CD23 prevented binding to immobilized IgE which had been plated in an ELISA plate.

Monoclonal mouse anti-CD23stalk antibodies are both inhibitory as well as stimulatory in IgE production on both PBMCs and tonsilar B cells. One of my goals was to move from the polyclonal rabbit antibodies to monoclonal, single epitope antibodies to more clearly define the role of the interaction between the antibody and the CD23 stalk. Monoclonal antibodies were first made by taking purified human CD23stalk and injecting 100µg of antigen in 150µl of complete Freund's adjuvant (CFA) into the dermis of the rat. A second and third injection 3 weeks apart, were injected into the rat both subcutaneously and intramuscularly keeping the total to 150µg for each occasion in incomplete Freund's adjuvant (IFA). A final injection one week after the third was given with 50µg of stalk in IFA. Three days before the animal is to be sacrificed the final injection was given intraperitoneally in PBS with a final 100µg of stalk. PBS is chosen as the vehicle of delivery as this will allow a very rapid dispersement unlike the slow release of antigen when delivered in CFA or IFA. Intravenous delivery would be preferred as the route to introduce the antigen to the

spleen the fastest, but in terms of time and ease, the IP route was decided on as the preferential route of delivery.

Mice were bled after the third delivery to ensure that the antigen reactivity and tantibodies were indeed being produced. To determine the presence of specific antibodies in the blood, the serum fraction of the blood was plated on ELISA. Once it had been determined that the mice were producing antigen specific antibodies the mice were sacrificed and the spleen was harvested, washed, and centrifuged. Spleen cells were mixed 3:1 to IR983F myeloma cells (spleen cells:myeloma cells). The mouse splenic cells were fused to the myeloma cells using polyethylene glycol (PEG). Stepwise removal of PEG by slowly adding media ended the fusion process. The fused spleen/myeloma cells were then plated at several concentrations of 300k cells/well, 100k cells/well and 30k cells/well in complete culture media containing HAT and 10% hybridoma cloning factor. After ~4 days the media was refreshed and this was repeated every three days until colonies began to become visible around day 21. Aliquots of supernatant were taken from wells that had only one visible colony and content of mouse anti-humanCD23stalk antibodies was determined by ELISA. The antibodies that tested positive were 1D1, 6C5, 11F2, 13A6, 14F5, 16C5, 17E1, 18B1, 19G10 and 23C6. These were grown up and injected IP into either LouM rats or nude mice that had been primed with Pristane (Sigma) with 1.0 or 0.5mls, respectively. Ascites were collected by abdominal puncture. Antibody content was collected by 40% ammonium sulfate precipitation and purified by a combination of ion exchange and gel filtration or

by Protein G affinity chromatography. Isotype of each antibody was determined by a mouse isotyping kit from BD BioSciences.

Figure 18: *lz*-CD23 binding to immobilized IgE (PS) is inhibited by all anti-stalk antibodies tested. Varying concentrations of antibody were preincubated with lz-CD23 at 37˚C for one hour. After one hour, mixture of CD23/anti-CD23 was added to IgE immobilized on an ELISA plate and binding of CD23 to IgE was assed. All antibodies tested, mouse anti-lectinCD23 (■), rat 11E10 (IgG1) (●), rat 16F5 (IgM) (▲), and RAS1 (♦) displayed similar inhibition of binding although that mouse monoclonal antibody targeting the lectin head predictably had the greatest inhibition.

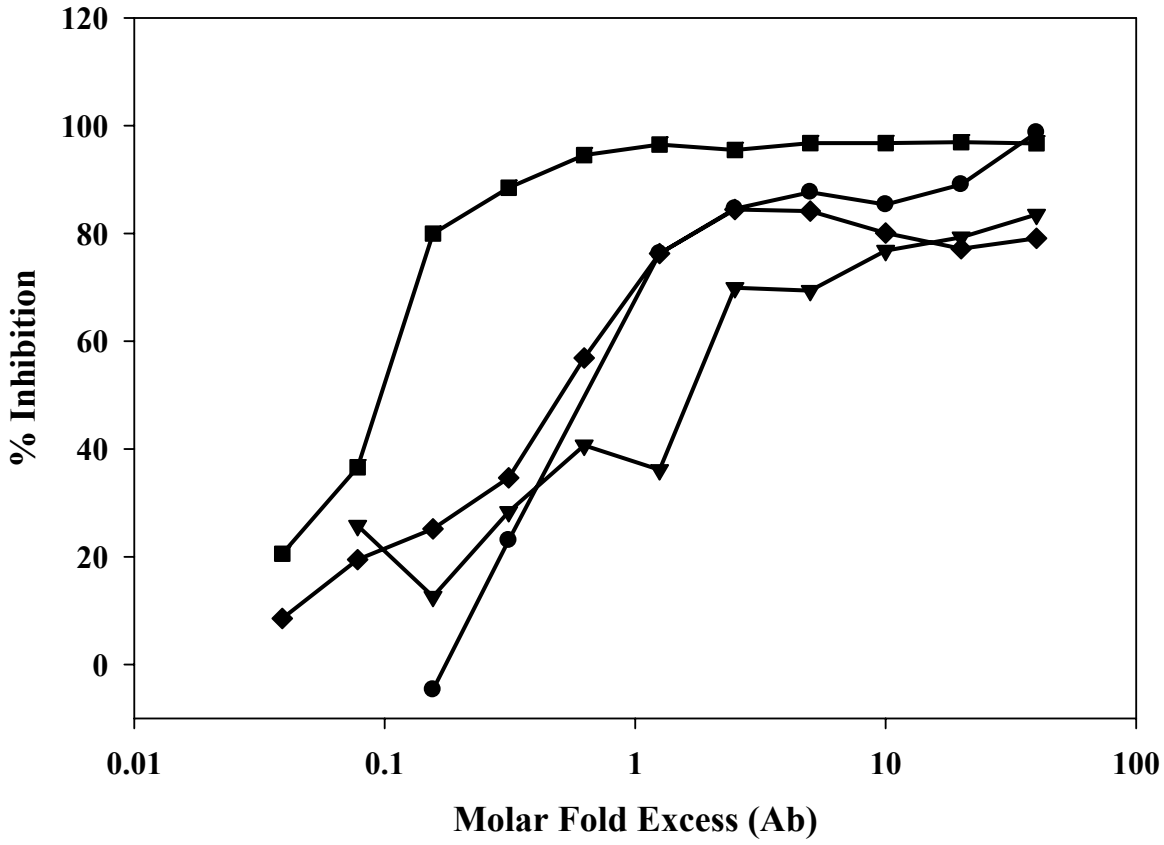
120
100
80
60
40
20
0
% Inhibition
0.01
0.1
1
10
100
Molar Fold Excess (Ab)

After purification, the mouse monoclonal antibodies were added to either PBMC or purified tonisilar B cells that had been stimulated with IL-4 and anti-CD40. Increasing concentrations of mouse monoclonal antibodies were added. After 12-14 days, the supernatants were collected and IgE was determined by ELISA. As can be seen from **Figure 19**, some of the monoclonal antibodies had a stimulatory effect on IgE production while others did not. I was very encouraged by this as I now had a tool that would allow us to have two competing models to study IgE regulation involving both the up regulation of IgE dependent on CD23 stimulation as well as down regulation of IgE. Unfortunately, the up regulation and down regulation of B cell IgE production from either B cells from peripheral blood or purified from tonsil was highly variable (**Figure 19**). As can be seen in **Table 2** where several experiments were compiled showing the effects of the anti-CD23stalk monoclonal antibodies, some occasions produced IgE that has higher than the baseline IL-4/antiCD40 stimulated cells (green) whereas others produced lower (red). Still other times there would be no change in IgE production when cells were treated with mouse anti-CD23stalk antibodies as compared to IL-4/antiCD40 IgE production (yellow)

Mouse Monoclonal AntiCD23stalk antibodies that Enhanced IgE production inhibited IgE binding in a temperature dependent manner. It had been hypothesized that the ability to interfere with IgE binding to the CD23 molecule would be cause for modulation of IgE synthesis. It had been shown using the rabbit polyclonal antibodies, that their addition to IL-4/antiCD40 stimulated PBMC inhibited IgE production in all

RAS tested. It was also shown that the pre-mixture of RAS with IgE prevented the IgE from binding and that this was temperature dependent. It was therefore thought that with monoclonal antibodies that enhanced the production of IgE, the relative binding might be opposite from that seen with the rabbit antibodies that inhibited IgE production. Purified monoclonal mouse anti-CD23stalk antibodies were added to cells in increasing concentrations. After washing ^{125}I-IgE was added and allowed to incubate. As can be seen from **Figure 20**, the addition of the antibodies that were providing the most consistent IgE enhancement, behaved similarly to the rabbit anti-CD23stalk antibodies.

In mouse #17E1, #18B1, and #23C6, all cases in the presence of pre-bound anti-CD23stalk antibodies prevented rather then enhanced the binding of IgE. This was somewhat surprising because I was anticipating that those antibodies that increased IgE production would behave differently from those antibodies that inhibited IgE production. However, as it was determined that the loss of the Fc portion from the rabbit antibodies (RAS) also resulted in the loss of capacity to inhibit, it is reasonable to assume that the binding capacity to disrupt IgE might be secondary to IgE synthesis modulation than the FcγR.

One predominant epitope on the Human C23stalk was found common to all mouse monoclonals, and another epitope was found to be targeted by one monoclonal. We sought to determine if the variability seen in the IgE production in the IL-4/antiCD40 stimulated cells could be explained by the epitopes that were being targeted

by the anti-CD23stalk antibodies. It was my original intention to make a series of stalk deletions from the *lz*-CD23$^{45\text{-}321}$ chimera. The chimera lz-CD23$^{148\text{-}321}$, had significant stalk removed as can be seen from the diagram in **Figure 3b**. However, the attempts to make the other stalk mutants seen in **Figure 3c** proved to be unsuccessful. From those results, I decided that surface plasmon resonance (SPR) would be means to try and see if there was any epitope over lap between the various antibodies. The premise was to bind the *lz*-CD23 to the CM5 biosensor chip, by activating both the dextran bound chip as well as the M15 anti-*lz* antibody and bind the M15 covalently to the chip, and then adding the *lz*-CD23 to the M15 antibody. Then add an anti-CD23 stalk antibody in this case the mouse anti-CD23stalk #18B1. Once the readings had stabilized, an additional anti-stalk antibody would then be added. The binding by the additional anti-CD23stalk would indicate that the second antibody bound to a different epitope. As can be seen from control **Figure 21a** the addition of IgE to mouse #18B1 resulted in no increase in binding as was expected based on the binding inhibition data seen from the rat monoclonals that were able to inhibit the binding of IgE to the CD23stalk after the rat had already been bound to the stalk as seen in a **Figure 18**. Also, as expected, the addition of #18B1 to #18B1 as seen in another control, **Figure 21b,** resulted in no further increase in binding, indicating that the initially bound #18B1 had saturated the stalk epitope. However, in **Figure 21c** the addition of #17E1 to the #18B1-CD23 complex also resulted in no increase in binding as seen from the relative response units output on the abscissa. The binding value remains constant at ~11,000. The lack of increase in binding as indicated when #17E1 was bound to #18B1 indicates that #17E1

is incapable of binding to its epitope. While the SPR does not completely rule out the possibility that the binding epitopes are unique, it does indicate that the epitopes for #18B1 and #17E1 are proximal enough to each other that the presence of one already on the stalk will prevent the other from binding to its epitope. The #18B1 in addition to preventing #17E1 also prevented binding of several other monoclonal antibodies such as 1D1, 6C5, 13A6, 14F5,16C5, and 19B1 (data not shown).These results were identical to **Figure 21c**, indicating that they, too, like #17E1 had epitopes that were the same or proximal to, the epitope of #18B1. However, as can be seen in **Figure 21d**, the addition of #23C6 showed a significant increase in relative binding, indicating that #18B1 and #23C6 had unique and separate epitopes from each other.

Figure 19: Mouse monoclonal anti-CD23stalk antibodies have both inhibitory and stimulatory capablilities on human PBMC. Human peripheral blood was collected and stimulated with IL-4 and anti-CD40. A battery of mouse monoclonal antibodies targeting the stalk portion of human CD23 were analyzed for capacity to influence IgE production. 10μg/ml (light bar) or 100μg/ml (black bar) of antibody were added and after 12 days the supernatants were collected and IgE concentrations were determined by ELISA. Data is the mean of three individual wells. Horizontal bar is amount of IgE produced with no antibody added.

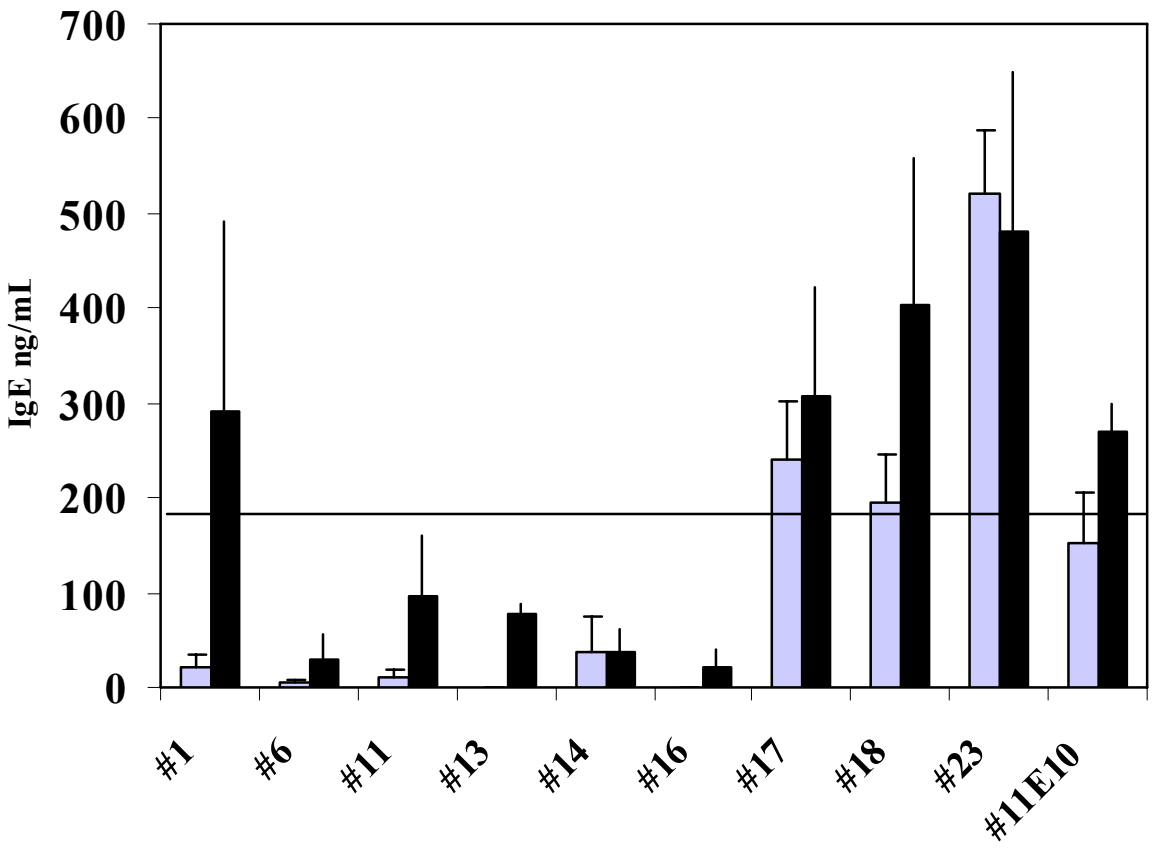
700
600
500
400
300
200
100
0
IgE ng/ml
#1
#6
#11
#13
#14
#16
#17
#18
#23
#11E10

Table 2

IgE Enhancement or Inhibition as compared to IL-4/anti-cD40

Stimulation in sixteen experiments.

*First experiment is only expressed in OD_{450}. All others are ng/ml of IgE and relative percent increases (green) or decreases (red) or no change (yellow)

Shown are four Rabbit (RAS), a rat, an anti-lectin head, and eight mouse anti-CD23stalks monoclonal antibodies.

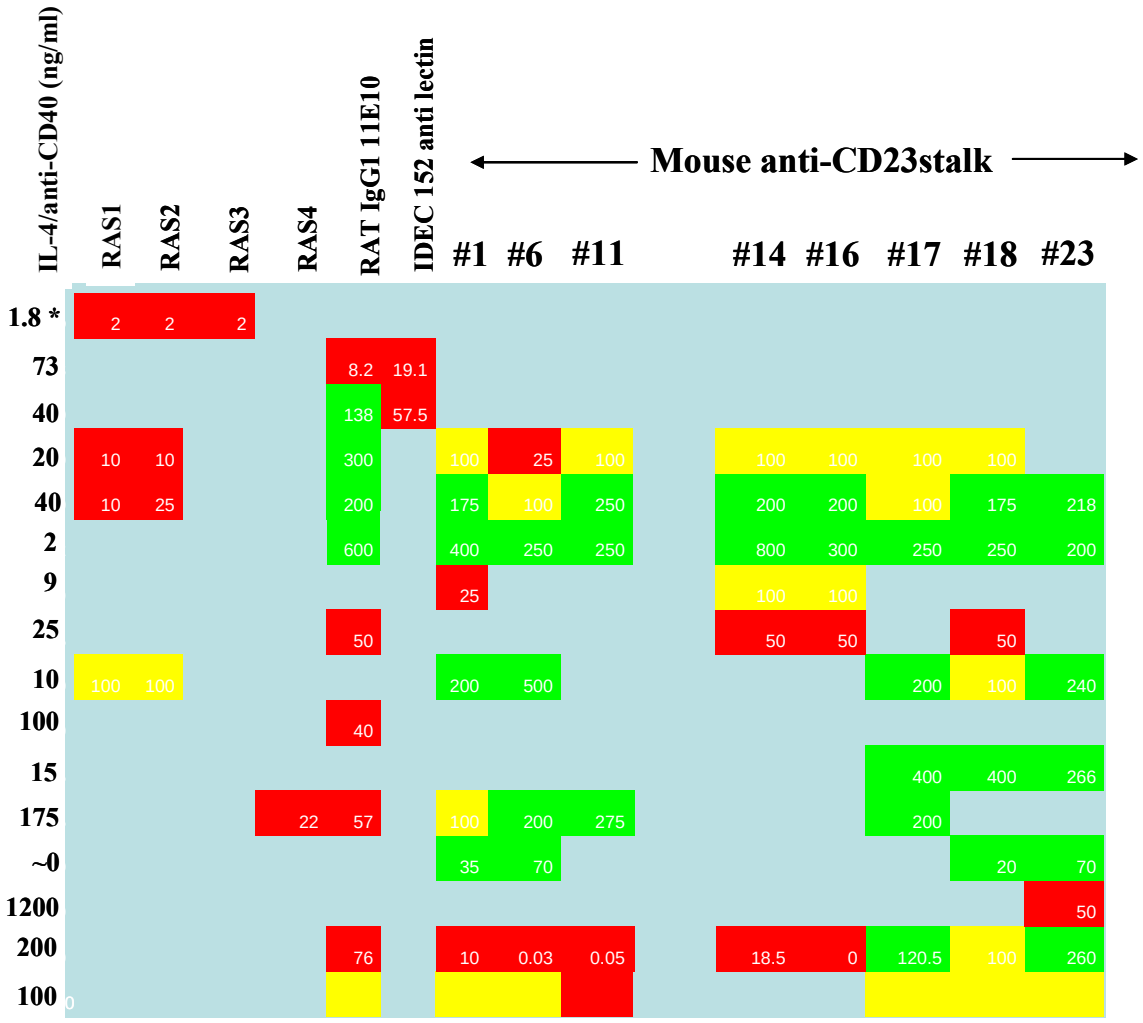
IL-4/anti-CD40 (ng/ml)
RAS1
RAS2
RAS3
RAS4
RAT IgG1 11E10
IDEC 152 anti lectin
Mouse anti-CD23stalk
#1
#6
#11
#14
#16
#17
#18
#23
1.8 *
73
40
20
40
2
9
25
10
100
15
175
~0
1200
200
100
2 2 2
8.2 19.1
138 57.5
10 10
10 25
300
200
600
100 25 100
175 100 250
400 250 250
25
50
100 100
200 500
40
22 57
100 200 275
35 70
76
10 0.03 0.05
100 100 100 100
200 200 100 175 218
800 300 250 250 200
100 100
50 50 50
200 100 240
400 400 266
200
20 70
50
18.5 0
120.5 100 260

Figure 20. The presence of mouse anti-CD23 stalk antibodies prebound on CD23$^+$ 8866 cells prevent the binding of IgE in a dose dependent and temperature dependent manner. Cells were kept at a constant temperature of either 4ºC (black) or 37ºC (open) when being incubated with mouse anti-CD23stalk antibodies (A) #17E1, (B) #18B1, and (C) #23, as well as the second incubation with radiolabeled ^{125}I-IgE. As can be seen at 37ºC, the addition of the antibodies all prevented binding of IgE to the CD23 molecule.

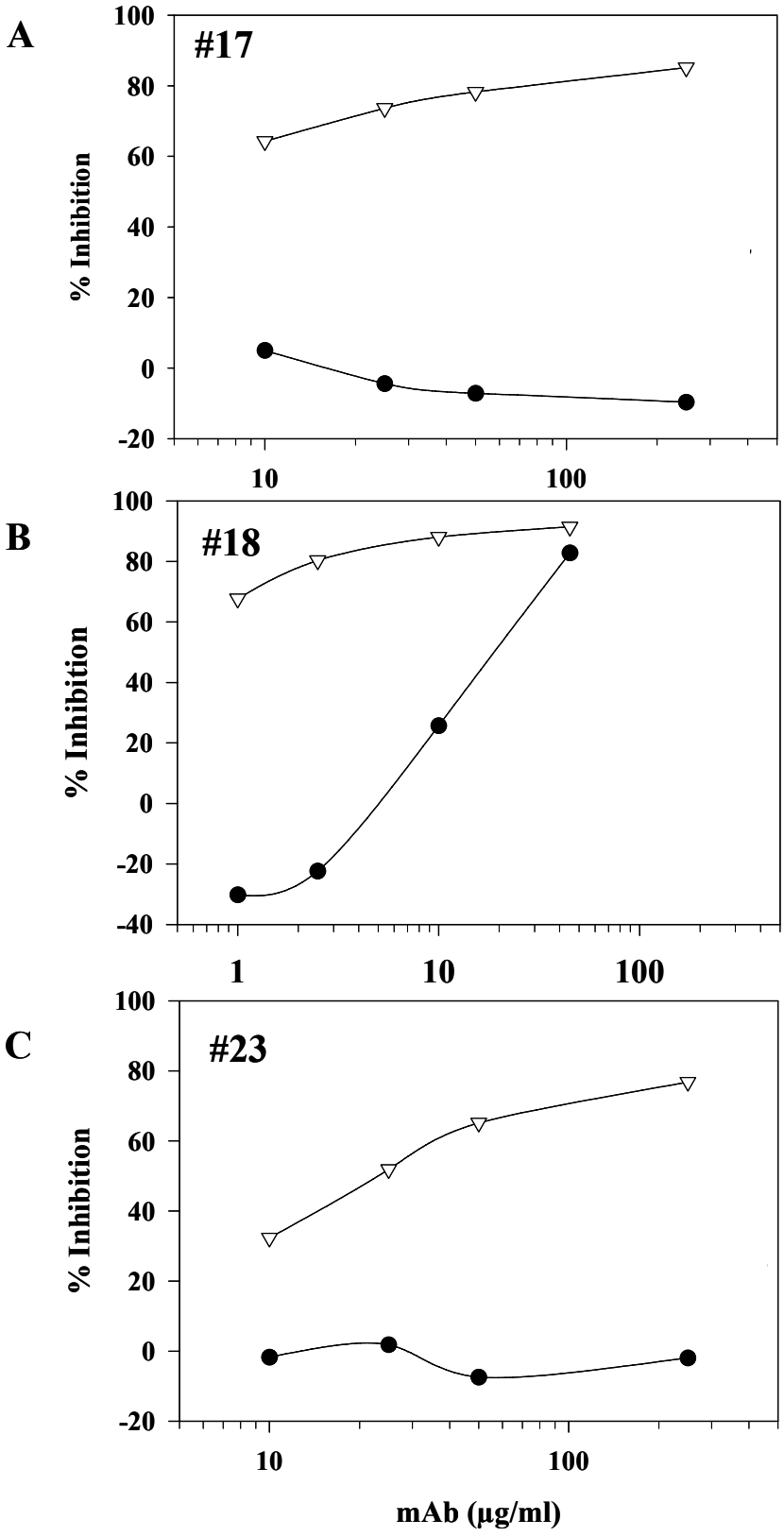
A
#17
100
80
60
40
20
0
-20
% Inhibition
10
100
B
#18
100
80
60
40
20
0
-20
-40
% Inhibition
1
10
100
C
#23
100
80
60
40
20
0
-20
% Inhibition
10
100
mAb (µg/ml)

Figure 21. All mouse monoclonal antibodies bind to a similar region on the stalk of CD23 as mouse #18B1, except for mouse #23C6 as determined by surface plasmon resonance (SPR) analysis. Anti-*lz* M15 was covalently bound to the biosensor chip (1) and allowed to equilibrate. Then full-length human CD23-lz chimera was added and allowed to equilibrate (2). Then mouse monoclonal anti-CD23stalk #18B1 was added to the chip and allowed to equilibrate (3) **(A-D)**. Then either IgE (**A**), #18B1 again (**B**), #17E1 (**C**), or #23 (**D**) were added and the relative change (if any) was determined. After binding was determined glycine-HCl (pH 2.0) was added and the chip was washed of everything except the covalently bound M15.

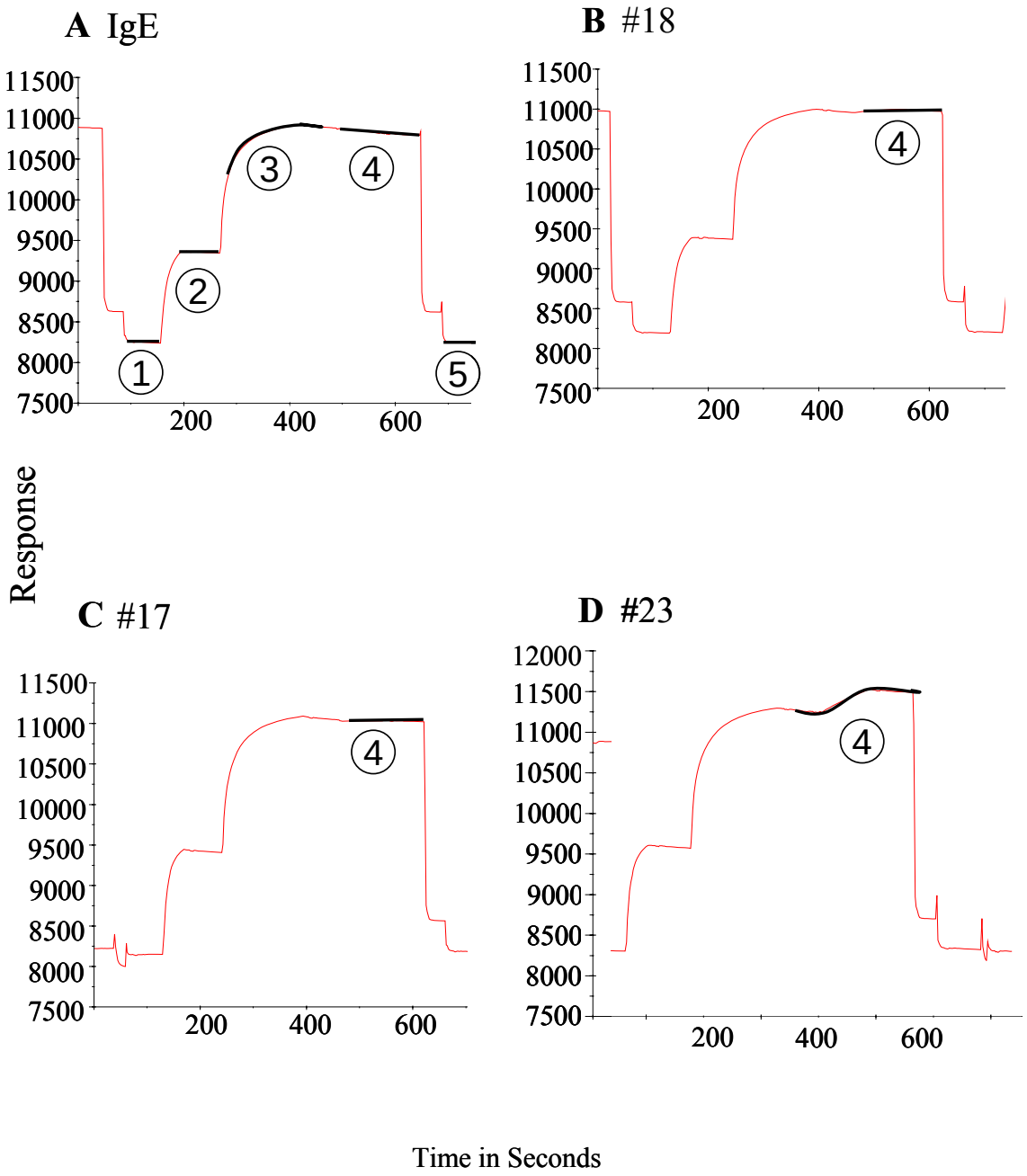
A IgE
B #18
C #17
D #23
Response
Time in Seconds
11500
11000
10500
10000
9500
9000
8500
8000
7500
12000
200
400
600
1
2
3
4
5

Human IL-21 rationale and preparation: During the studies with the RAS and mouse anti-CD23stalk antibodies, problems developed in generation of IgE. I examined several contributing factors that were involved in my IgE production model to try and answer what the problems were in getting consistent IgE generation that could be of significant, measurable quantities from IL-4/antiCD40 stimulated cells. Different companies of IL-4 were tried at varying concentrations of IL-4. The source of the antiCD40 antibody both G28-5 generated and purified from ascites and 5C (ATTC) were tried. The different antibodies were also used at increasing concentrations, from as low a 1 ng/ml up to 1000ng/ml. I found that that concentration was the best production using 1000ng/ml, and in all future experiments this concentration was used. Different FBS was tried and different concentrations. I received from Dr. Natalie McClosky details that in their IgE systems insulin and transferrin were used successfully. Still however, the consistent IgE production that I was seeking was missing. At this time, interest in IL-21 as an important contributor to B cell proliferation became prevalent in the literature and I explored the use of this cytokine to help try and get a solid working system to continue work on the antibodies that I had generated against the stalk. I was especially intrigued in both the increased IgE as well as the conditions that decreased IgE. However, without a reliable system to produce quantities of IgE that were of significance, the ability to measure any decrease would be made problematic due to the extremely low production of IgE that was mysteriously occurring with some regularity. Therefore, I investigated whether IL-21 might provide the necessary IgE production in order to continue with my goals of the antiCD23stalk study.

As T cells are the source of IL-21, I acquired tonsils from Henrico Doctor's Hospital with the kind assistance of Dr. Linda McGovern and her staff. T cells were purified from the tonsils using the MACS cell sorting system and were stimulated with PMA and ionomycin and incubated overnight. RNA was isolated and RT-PCR was performed using the appropriate primers. The resulting IL-21 cDNA was cloned into a plamid, grown up, sequenced, and confirmed. Once confirmed, the cDNA was inserted into the pEF4MycHisA plasmid and transfected into human embryonic kidney cells (HEK)293T cells. Transfected cells were incubated for 3-4 days and supernatants were collected. Collected supernatants were pooled and then aliquoted and stored in -70Cº.

Confirmation that human IL-21 enhances B cell proliferation. When this project was initiated, human IL-21 was not commercially available. Thus, human IL-21 was cloned by RT-PCR, and supernatants from transfected HEK293T cells were used as the source of IL-21. As can be seen in **Figure 22**, addition of increasing levels of IL-21 transfected HEK293T supernatant resulted in increased B cell proliferation, when used in conjunction with anti-CD40 and IL-4. No proliferation was induced by HEK293T control supernatant alone (data not shown), while B cell proliferation was increased 13 fold by the inclusion of IL-21, compared to IL-4/anti-CD40 (**Figure 22**). In addition, the presence of IL-21 caused massive aggregation of the growing B cells in culture (**Figure 23 a-c**). I determined that the increase in was due to IL-21 contained in the

supernatant, as the addition of soluble IL-21R-chimera abrogated the effect in a dose dependant manner, and that the supernatant alone had no effect (data not shown).

Figure 22: IL-21 Supernatants increase purified human B cell proliferation in a dose dependent manner. Purified human B cells from PBMC were cultured with IL-4 (10 ng/ml) and anti-CD40 (10^3 ng/ml) for 96 hrs in the presence of IL-21 supernatant (25ng/mL (□), 2.5ng/mL (■), 0.25ng/mL (○), or no IL-21 (●)). Cells were pulsed with 1μCi ^{3}H-thymidine/well for the last 16 hrs of a 96 hr culture.

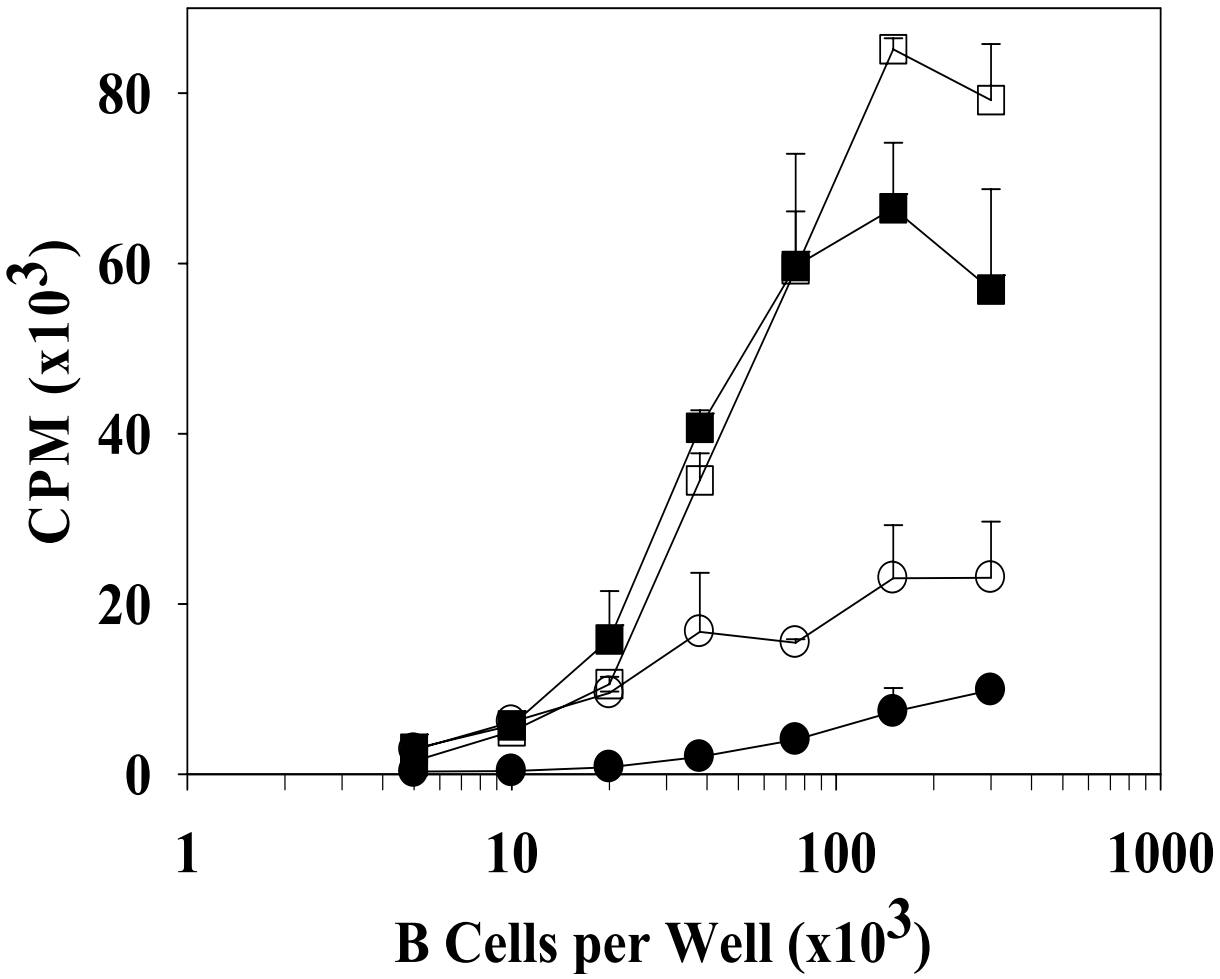
80
60
40
20
0
CPM (x10^3)
1
10
100
1000
B Cells per Well (x10^3)

Figure 23. 10x magnification a 5 day culture of IL-4/anti-CD40 activated CD19^{+} B cells purified from PBMC. Cultures were treated with **(A)** 2.5ng/mL, **(B)** 25ng/mL, and **(C)** 125ng/mL IL-21 supernatant, respectively.

A.

B.

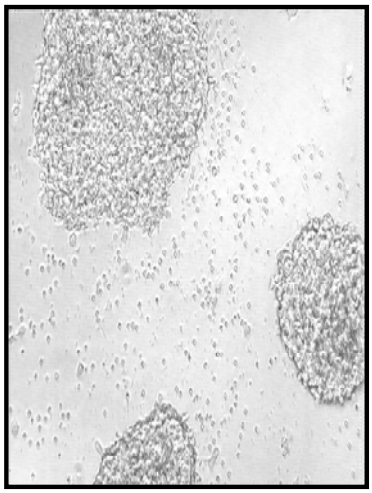

C.

Figure 24: IL-21 Inhibited by IL-21 receptor-Fc chimera. Purified IgD^+ B cells were cultured and pulsed with IL-4 (10 ng/ml) and anti-CD40 (10^3 ng/ml) for 96 hrs. Receptor-Fc chimera was added where indicated at 50μg/mL, 10μg/mL, 1μg/mL, and 0.1μg/mL respectively. Error bars represent one standard deviation (SD) (***,** $p<0.02$). Experimental results representative of two of similar design.

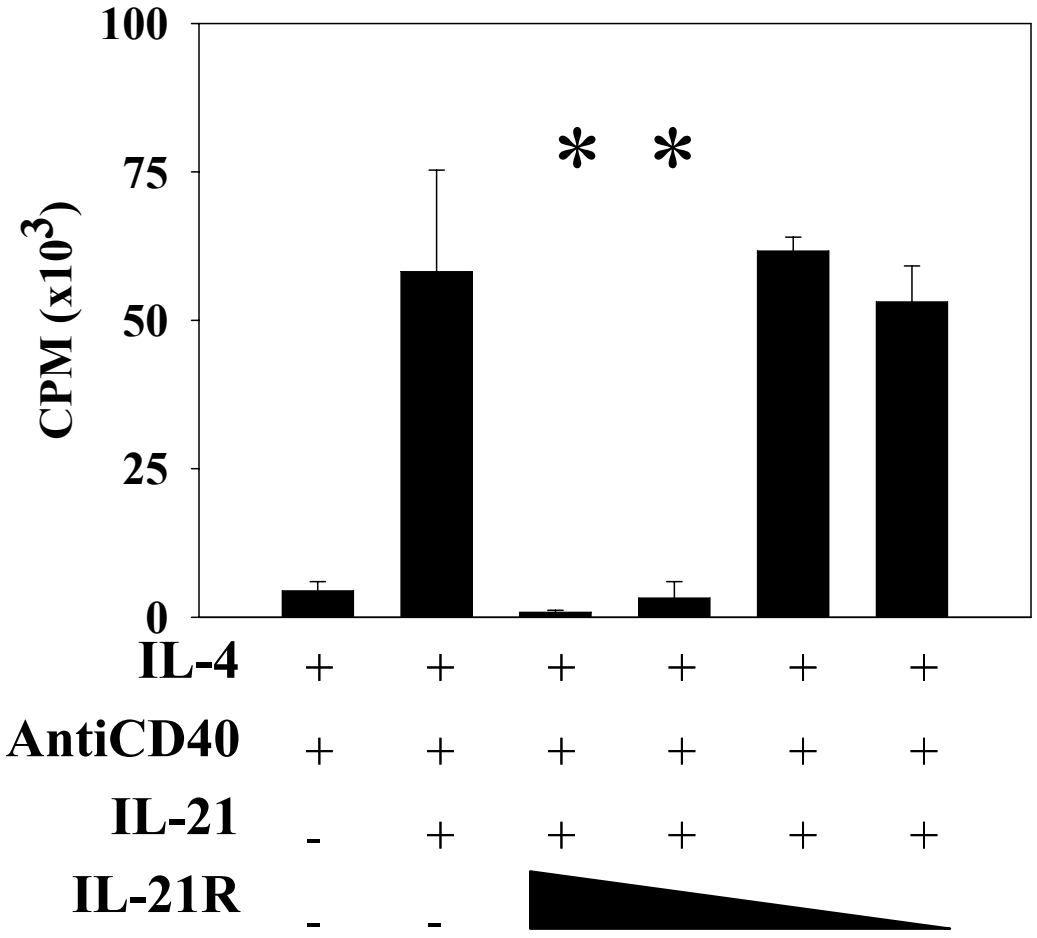
100
75
50
25
0
CPM (x10^3)
* *
IL-4 + + + + + +
AntiCD40 + + + + + +
IL-21 - + + + + +
IL-21R - -

Enhancement of antibody production is seen at low cell densities. In order to determine the effect of IL-21 on antibody production in the human system, IgD^+ tonsilar B cells were purified (>98%) and cultured at increasing cell densities in the presence of anti-CD40, IL-4 with increasing concentrations of IL-21. Analysis of IgE levels in supernatants after 14 days of culture revealed that the inclusion of IL-21 resulted in increased IgE production (**Figure 25a**). Note that the highest level of IgE was obtained at 3000 cells per well in the additional presence of IL-21, one quarter of the cell number that produces maximum IgE when cells are cultured in IL-4/anti-CD40 alone. The **inset** shows an expanded plot of the IgE production seen in the absence of IL-21, shown to emphasize the dependence on cell concentration. The maximum production of IgE occurred at a higher cell density in the absence of IL-21. Controls in which cells were stimulated with IL-4 alone, or IL-4 plus IL-21 only, produced no IgE, indicating that preformed IgE did not contribute to detected IgE levels (data not shown). To emphasize the dramatic increased IgE at low cell concentrations, this data is redisplayed as a function IgE produced per B cell in the presence of IL-21 (**Figure 25b**). In addition to IgE, production of other isotypes was also influenced by the inclusion of IL-21 in the culture. **Figure 26a** shows production of IgG and **Figure 26b** IgM in the presence and absence of IL-21 as a function of cell density. The data are plotted as the Ig produced per B cell plated, and the increased production of both IgG and IgM is evident. Thus, the presence of IL-21 resulted in increased immunoglobulin production at low input cell concentrations for all isotypes tested. It is therefore clearly seen that in humans the production of IgE is cell density dependent. As expected HEK293 untransfected cell

supernatant produced no increase in IgE in IL-4/antiCD40 stimulated cells (data not shown).

Figure 25: IL-21 significantly increases IgE production in purified human IgD^+ B cells. (**A)** The indicated concentrations/well of IgD^+ B cells were stimulated with IL-4 and anti-CD40 in the presence of 25ng/mL (□), 10ng/mL (▲), 2.5ng/mL (○) or no IL-21 (●).IgE was measured by ELISA on 12 day supernatants. Data are represented as total IgE production (A) or IgE production/cell **(B)**. **(Inset)** Enlargement of IL-4/anti-CD40 only conditions, showing optimal IgE in absence of IL-21 is also cell concentration dependent. Error bars represent ± one SD. Experiment results representative of four of similar design.

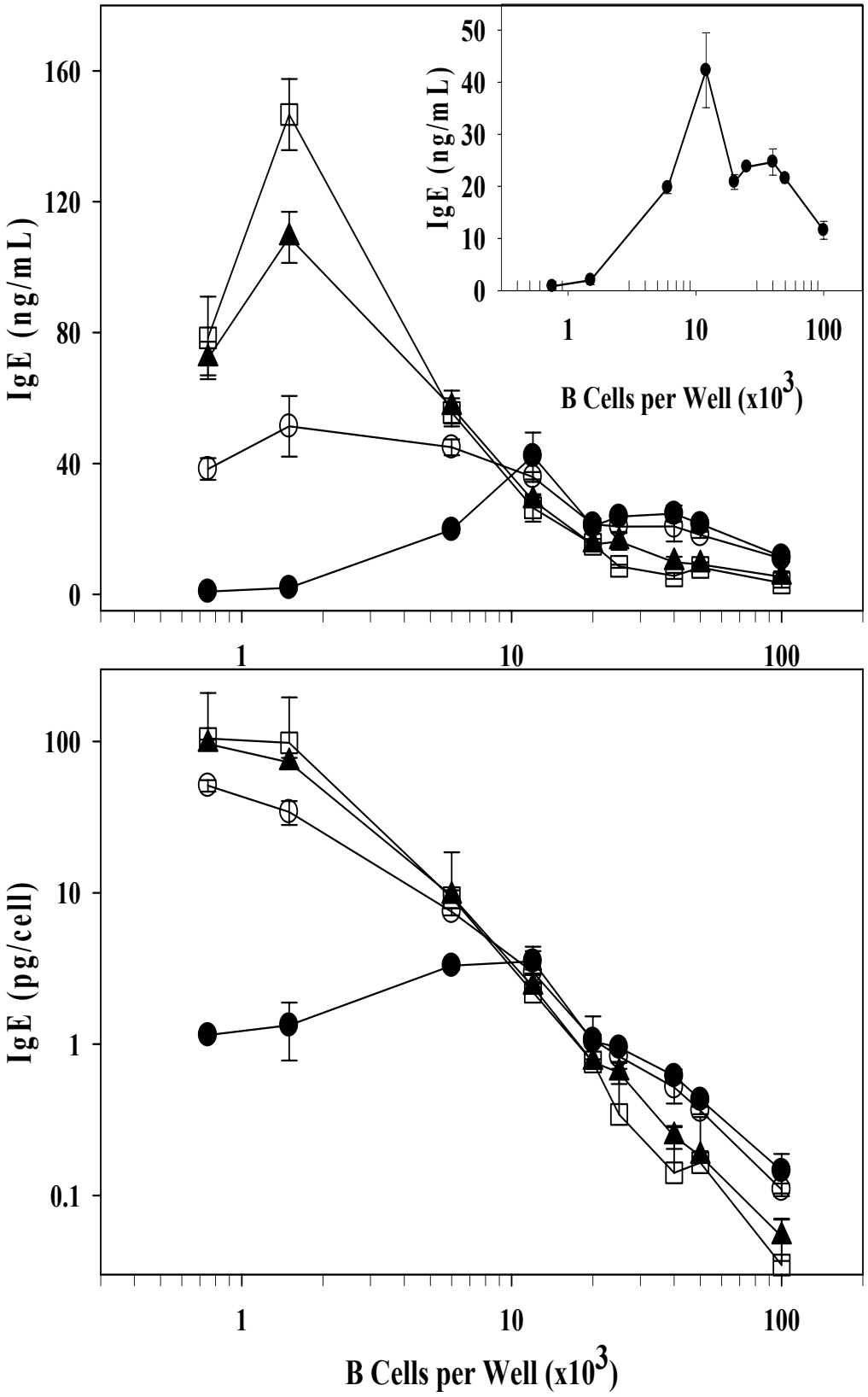
IgE (ng/mL)
160
120
80
40
0
1
10
100
IgE (ng/mL)
50
40
30
20
10
0
1
10
100
B Cells per Well (x10^3)
IgE (pg/cell)
100
10
1
0.1
1
10
100
B Cells per Well (x10^3)

Figure 26: IL-21 increases IgG and IgM production in human *in vitro* cultures. IgD^+ B cells were stimulated with IL-4 and anti-CD40 in the presence of 25ng/mL (□), 2.5ng/mL (■), 0.25ng/mL (○) or no IL-21(●). Day 12 supernatants were collected and the concentration of secreted IgG (A) or IgM (B) was determined by ELISA and plotted as amount produced/cell. Error bars represent one SD. Experiment representative of three of similar design.

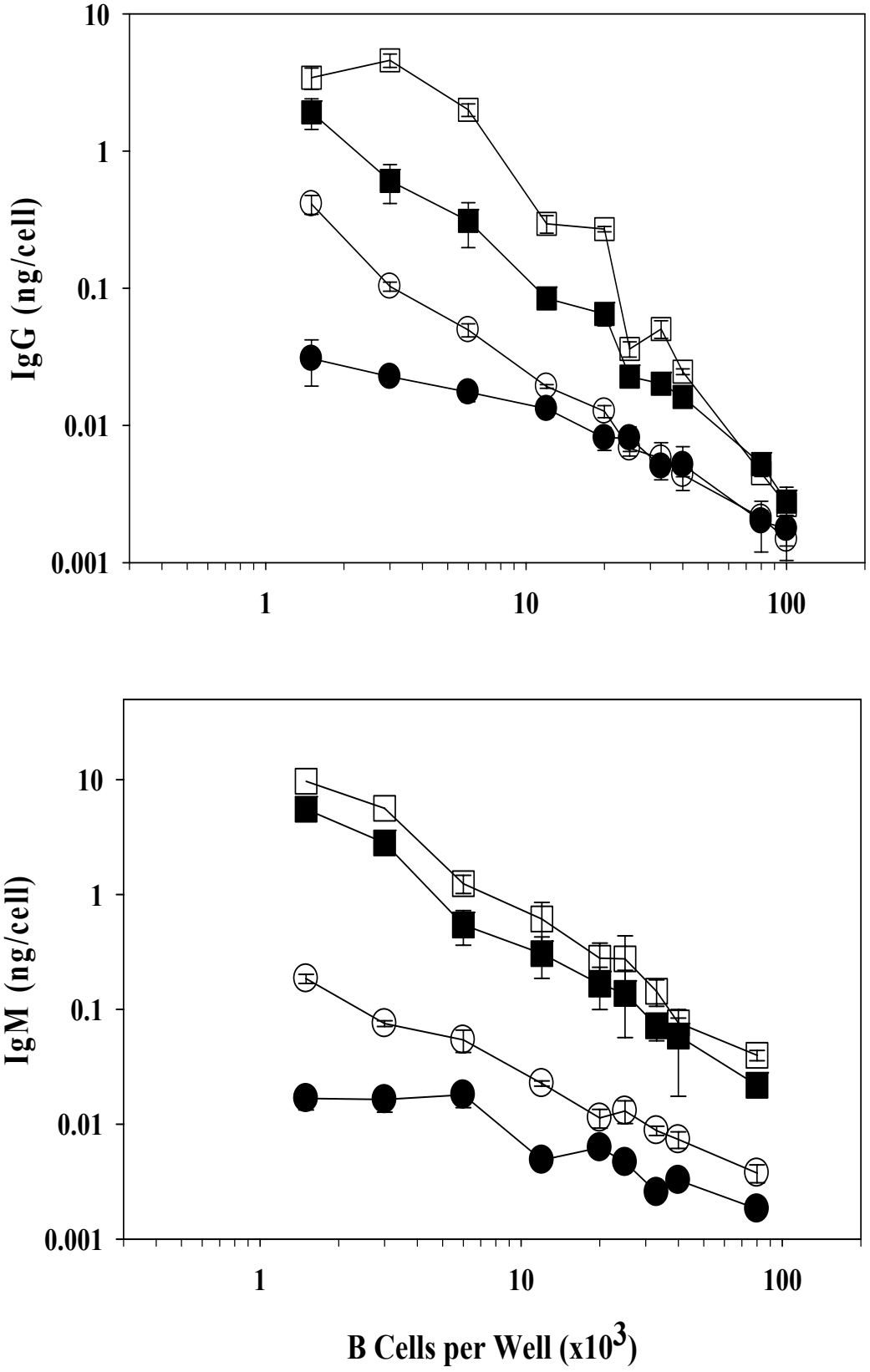
IgG (ng/cell)
10
1
0.1
0.01
0.001
1
10
100
IgM (ng/cell)
10
1
0.1
0.01
0.001
1
10
100
B Cells per Well (x10^3)

Nutrient depletion does not explain differences in IgE production. As can be seen in **Figure 27** cells that were treated with IL-4 and anti-CD40 and 25ng/mL IL-21 have barely detectable IgE levels at 100k cells per well. This is compared to the 100k cell per well conditions of IL-4 and anti-CD40 which are near peak levels of IgE production. To ensure that the increase of IgE from the IL-21 treated cells found at the low density conditions was not merely a result of nutrient depletion, nutrient replenishment was examined. IL-4/anti-CD40/IL-21 stimulated cells were plated at 100k cells per well and had 100μL media with IL-4/anti-CD40 alone or also with IL-21 replaced on day 5. (Day 5 was chosen because of my previous proliferation studies where significant proliferation due to the addition of IL-21 did not occur until days 3-4 (data not shown)). As can be seen in **Figure 27**, the replacement of media and nutrients did increase the levels of IgE produced but the levels were not significant when compared to the optimal cell concentrations. Other conditions examined were double the amounts of stimulation in various combinations to see if any one of the stimulatory reagents were limiting. These had no further increase on IgE production (data not shown). Interestingly, although perhaps only coincidence, the highest IgE levels at 100k found from media/stimulation replenishment were never higher than the highest IgE levels found from the IL-4/anti-CD40 treated cells (data not shown).

Increased cell division occurs at low cell inputs in the human *in vitro* system. Given the correlation between cell division and isotype-specific antibody production, I investigated the contribution of IL-21 to cell division at increasing cell concentrations.

Cell division was assessed by culturing CFSE-labeled human B cells with anti-CD40 and IL-4 in the absence (**Figure 28 a-b**) or presence of IL-21 (**Figure 28 c-d**). Because discrete peaks at each cell division were not clearly evident, estimated cell divisions were determined by dividing the histograms into equally spaced intervals, with the brightest peak (far right) representing cells

Figure 27: Media and cytokine replacement does not explain cell density effect. To determine whether the loss of IgE production at higher cell densities as compared to lower cell densities of IL-4/anti-CD40/IL-21 treated cells (○) was due to nutrient depletion (A), IL-4/anti-CD40/IL-21 treated cells were plated at100k. After five days, half the volume (100μL) of media was replaced containing either IL-4 and anti-CD40, or IL-4, anti-CD40, and 25ng/mL IL-21. Although higher than IL-21 treated cells without a media change, the increase is statistically insignificant to the optimum IgE concentrations (B). Experiments were repeated three times with media change experiments having 10 replicates each and non-media changes results done in triplicate. Figures A and B are derived from three separate experiments. Figure A represents one of them. * p=0.002

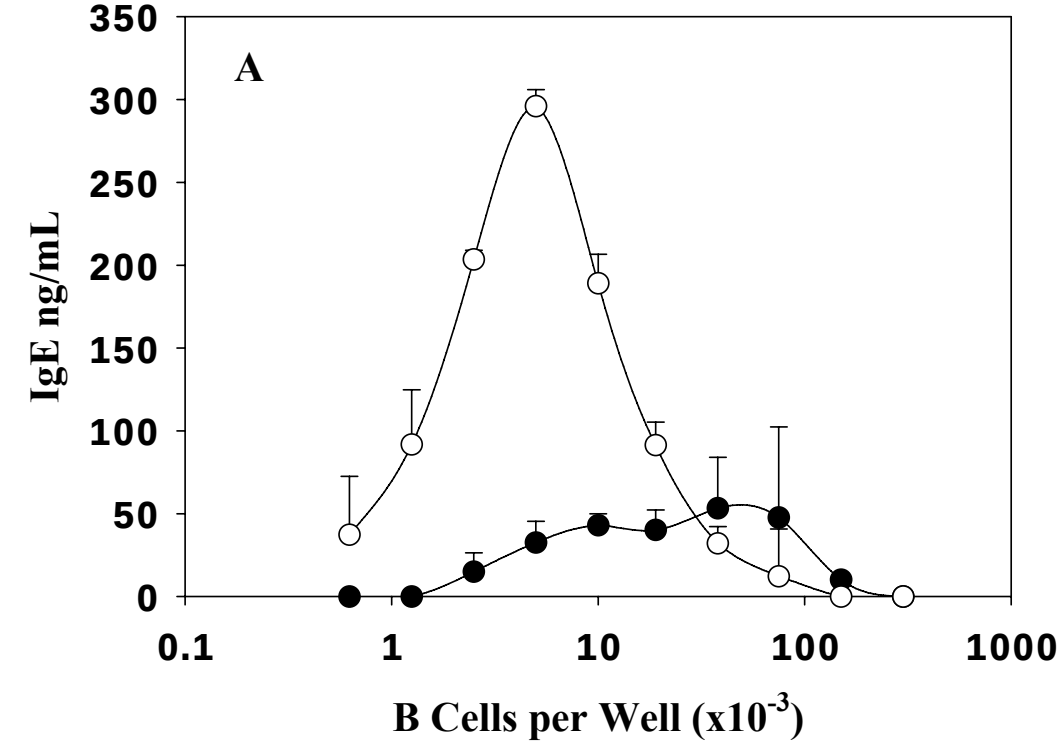

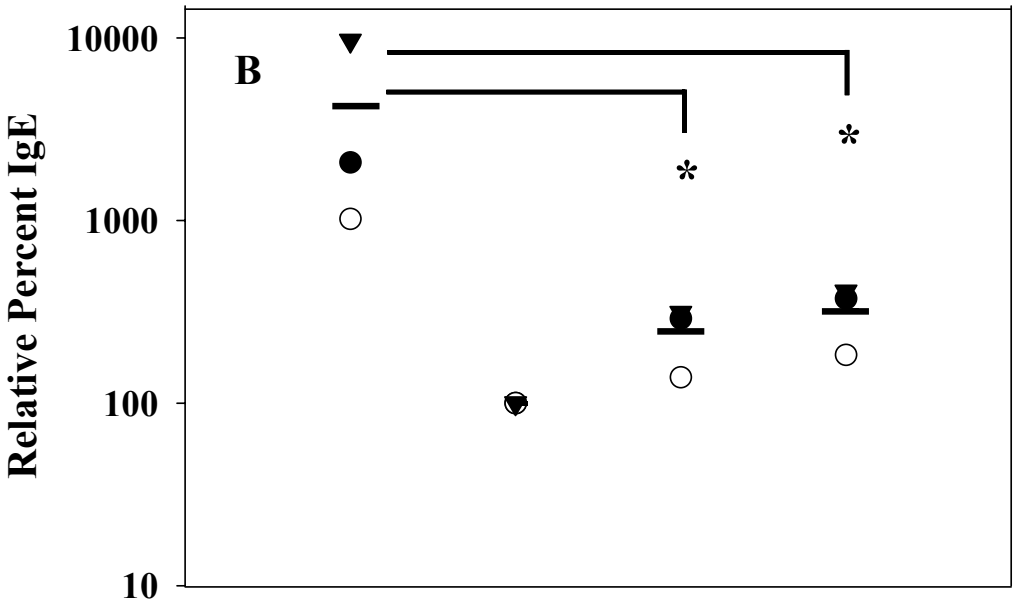

IL-4	**N/A**	**N/A**	**+**	**+**
αCD40	**N/A**	**N/A**	**+**	**+**
IL-21	**N/A**	**N/A**	**--**	**+**
Media Δ	**No**	**No**	**Yes**	**Yes**
Cell Num	**~7k**	**100k**	**100k**	**100k**

Figure 28: Cell Division is Correlated to Cell Density: Human tonsilar IgD^+ B cells were labeled with CFSE/PBS for 15 minutes, washed, and cultured for 8 days with IL-4/anti-CD40, without **(A,B)** or with **(C,D)** 25ng/mL IL-21. (**A,C)** flow histograms of cells plated at 10^5 (·····) or 10^3 (——) cells/well. **(B,D)** show same data plotted as a function of cell division (see Materials and Methods), again with 10^5 (○) and 10^3 (■) cells/well. This experiment is representative of four of similar design.

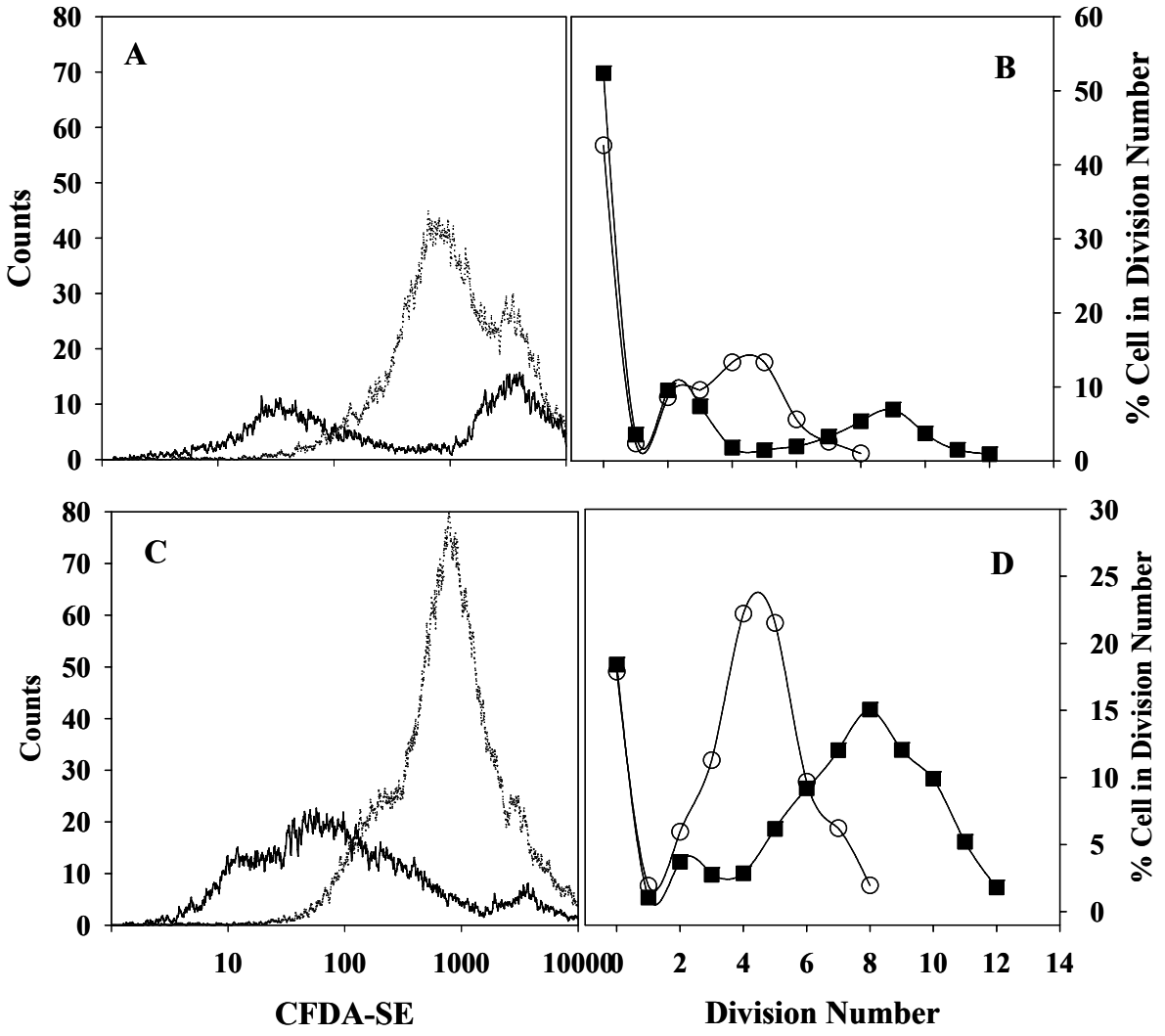
A
B
C
D
Counts
% Cell in Division Number
CFDA-SE
Division Number
80
70
60
50
40
30
20
10
0
10
100
1000
10000
0
2
4
6
8
10
12
14
25
15
5

which had not divided. Increased rounds of cell division, as evidenced by reduced CFSE concentration, were seen when starting cultures had a lower cell input (Compare dark lines of **Figure 28 a** and **c**, and open symbols of **Figure 28 b** and **d**). These data were used to calculate the proportion of total cells in each round of cell division by partitioning the histogram as described above (**Figures 28b** and **28d**). The increase in cell division with IL-21 addition was clearly seen, with dramatically higher cell division evident at lower initial cell inputs (**Figure 28c**, solid line). In addition, inclusion of IL-21 resulted in a higher percentage of cells that underwent at least one division, as seen by the lower percentage of cells remaining in an undivided state (**Figure 28d**). Culture conditions that exhibited the highest levels of cell division correlated with highest IgE production), consistent with previous data for IgG and IgE in the mouse [71] and total IgG in the human systems [75].

IL-21 increases IgE production by IL-10/IL-4/anti-CD40 stimulated PBMC and purified Tonsilar IgD$^+$ cells. IL-10 has been shown to increase *in vitro* IgE production in IL-4 and anti-CD40 stimulated PBMC [89]. I sought to determine whether IL-21 further enhances the amount of IgE produced in cells treated with IL-4/IL-10/anti-CD40 cells. PBMC were treated with IL-4/anti-CD40 plus IL-10. As seen in **Figure 29a**, the addition of both IL-10 and IL-21 to IL-4/anti-CD40 treated cells shows higher proliferation than when only IL-21 or IL-10 alone is added. As shown in **Figure 29b** and **Figure 29c**, IL-10 resulted in an increase in IgE production, with the higher amount of IL-10 (10ng/mL) (**Figure 29c**) giving a 4-fold increase in IgE production, compared

to IL-4/anti-CD-40 alone. Indeed at this concentration IL-10 was more effective than IL-21 alone in inducing IgE production. The addition of both cytokines further increased IgE production in an additive manner. However, when the lower (1ng/mL) of IL-10

Figure 29: IL-10 and IL-21 increase proliferation in PBMC, and increase IgE when added alone and synergistically increase IgE when combined with PBMC or IgD^+ tonsilar B cells. IL-4 and anti-CD40 (4/40) treated PBMC were plated at 300,000 cells per well and treated with buffer, IL-10, IL-21, or IL-10 and IL-21 combined. 25ng/mL IL-21 was used in all conditions. **(A)** Proliferation was determined by ^{3}H-thymidine incorporation. (**B,C)** IgE was determined from PBMC activated as in (A); with IL-10 concentrations of **(B)** 1ng/mL or **(C)** 10ng/mL, respectively, with IL-21 added as indicated. **(D)** IgE production from 75k cells per well IL-4/anti-CD40 stimulated IgD^+ tonsilar B cells that were treated with IL-10 (10ng/mL), IL-21(25ng/mL), or IL-10 and IL-21 combined was determined. In **B-D**, IgE levels were determined by ELISA from day 14 supernatants. Cultures were plated in duplicate, collected on day 14, pooled and determined by ELISA. These two results are representative of seven experiments. Statistics were paired student's t-test (* = $p<0.05$, ** <0.01, ***<0.001).

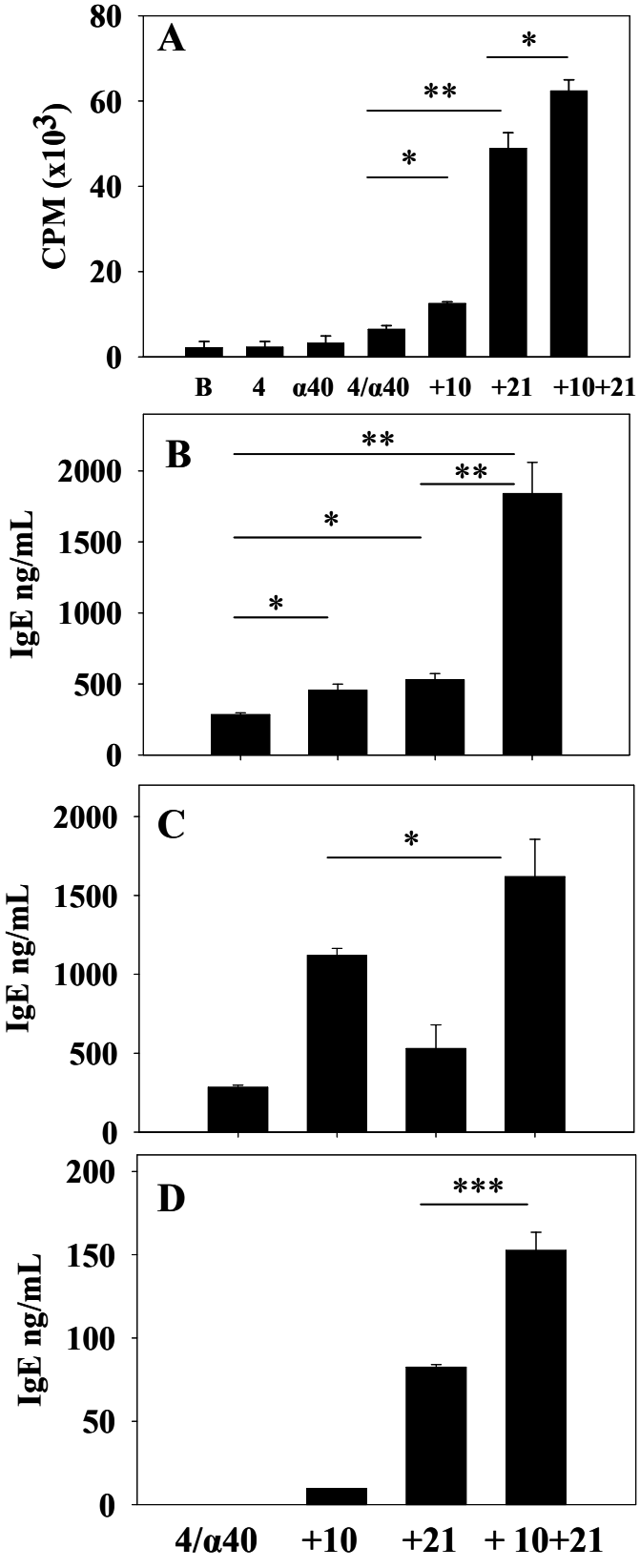
A
CPM (x10^3)
80
60
40
20
0
*
**
*
B
4
α40
4/α40
+10
+21
+10+21
B
IgE ng/mL
2000
1500
1000
500
0
**
**
*
*
C
IgE ng/mL
2000
1500
1000
500
0
*
D
IgE ng/mL
200
150
100
50
0
***
4/α40
+10
+21
+ 10+21

were used (**Figure 29b**), the addition of both cytokines increased IgE production synergistically. In order to determine whether synergy or addition would be found in B cells, purified tonsilar B cells were cultured with IL-4/anti-CD40 in the presence or absence of IL-10 and IL-21. As seen in **Figure 29d**, IL-21 had a greater effect on IgE production compared to IL-10. As seen with PBMC, IL-10 and IL-21 added together to IL-4/anti-CD40 cells resulted in a synergistic increase in IgE. The levels of IgE produced by IL-4/anti-CD40 alone were 2ng/mL.

`

IL-10 increases IgE production in purified tonsilar B cells and causes a modest increase in cell division. Purified tonsilar B cells were labeled with CFSE and activated with IL-4/anti-CD40 in the presence of IL-10. IL-10 also correlated IgE production with cell division, albeit to a lesser degree (**Figure 30a** and **30b**), than to the studies with IL-21 (**Figure 30c** and **30d**), When both IL-10 and IL-21 were added together to IL-4/anti-CD40 stimulated cells there was a further increase in total IgE production as seen in **Figure 31**. Interestingly, the increase in IgE production seen with the double cytokine addition did not correlate with further cell division (**Figure 32**).

In order to determine the generality of this finding, seven tonsils were collected and IgD+ cells were purified and treated with IL-4/anti-CD40 in the presence or absence of IL-10 and 21, added together or separately. IgE production is shown in **Figure 31**. In six of the tonsils there was an increase of IgE over IL-4/anti-CD40 alone when 10ng/mL IL-10 was added. In one case, IgE production with IL-4/anti-CD40 ± IL-10 was below levels of detection. Interestingly, in that tonsil, the production of IgE

was very good with the addition of IL-21 (145ng/mL) and IL-10/IL-21 (340ng/mL). The average IgE production is shown and a significant increase is seen with IL-10/21 as compared to IL-21 alone; note that the average increase is synergistic rather than

Figure 30: IL-10 increases IgE production in IL-4/anti-CD40 stimulated tonsilar B cells and correlates with increased cell division as does IL-21: IgD^+ B cells were treated with IL-4/anti-CD40 and increasing concentrations of IL-10 **(A+B)**. IgE **(A)** and cell division **(B)** was determined. Cells from the same experiment were plated and treated similarly except were also treated with CFSE and analyzed by flow cytometry on day 8. **(C,D)** represents similar conditions as in **(A,B)** except IL-21 was used. In **(B)** the dotted line, light grey, med grey, and black lines represent 4/40, or 4/40 plus 0.1, 1,10 ng/mL IL-10, respectively. In **(D)** the dotted line, light grey, med grey, and black lines represent 4/40, or 4/40 plus 5,25,50 ng/mL IL-21, respectively.

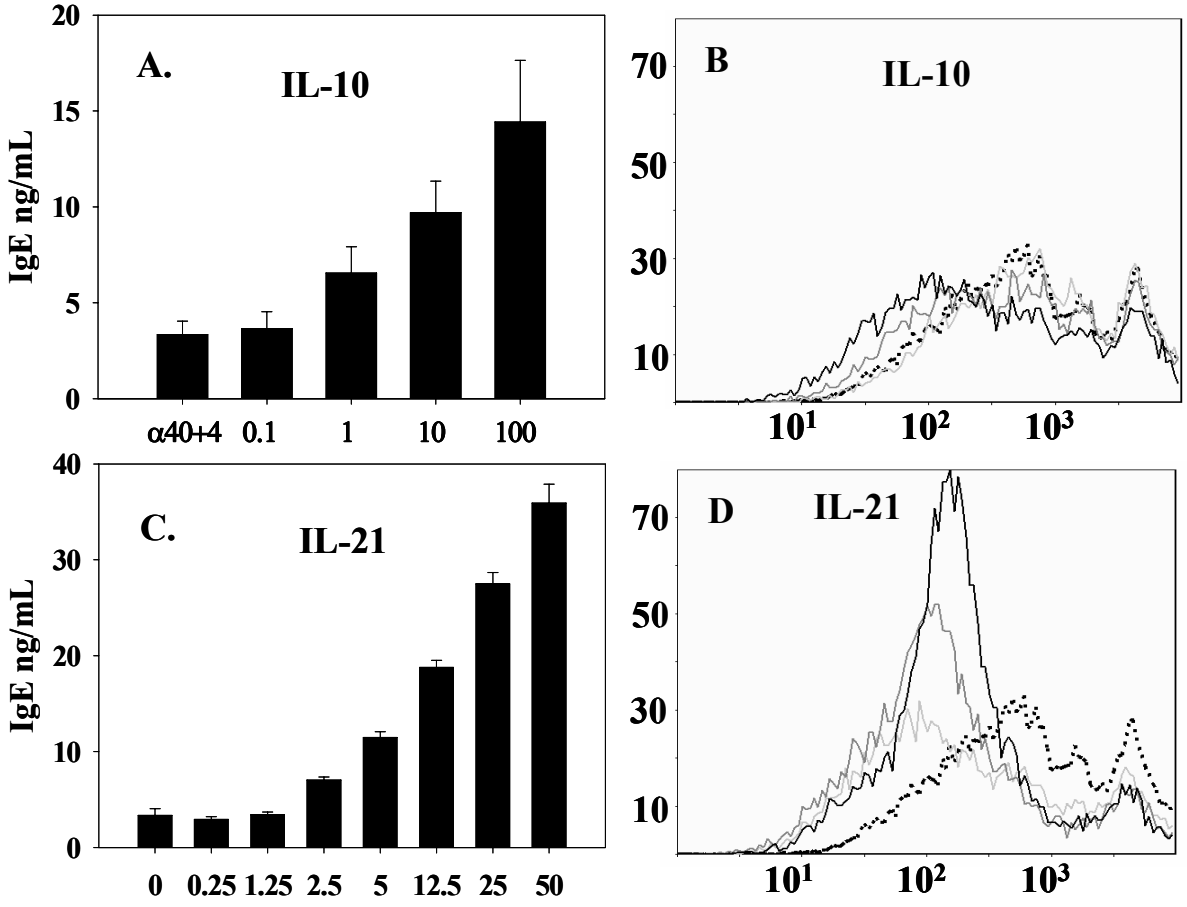
A.
IL-10
IgE ng/mL
20
15
10
5
0
α40+4
0.1
1
10
100
B
IL-10
70
50
30
10
10¹
10²
10³
C.
IL-21
IgE ng/mL
40
30
20
10
0
0
0.25
1.25
2.5
5
12.5
25
50
D
IL-21
70
50
30
10
10¹
10²
10³

Figure 31: IL-10 added to IL-21 conditioned cells treated with IL-4/antiCD40 increases IgE production Mean IgE values from seven IgD^+ B cell tonsil preparations were plotted; conditions shown are 4/40 or 4/40 plus IL-10 (10 ng/ml), IL-21 (50ng/mL) or same levels of both IL-10 and IL-21. IgE levels were determined by ELISA on day 14. Student's paired t-test ($p<0.05$).

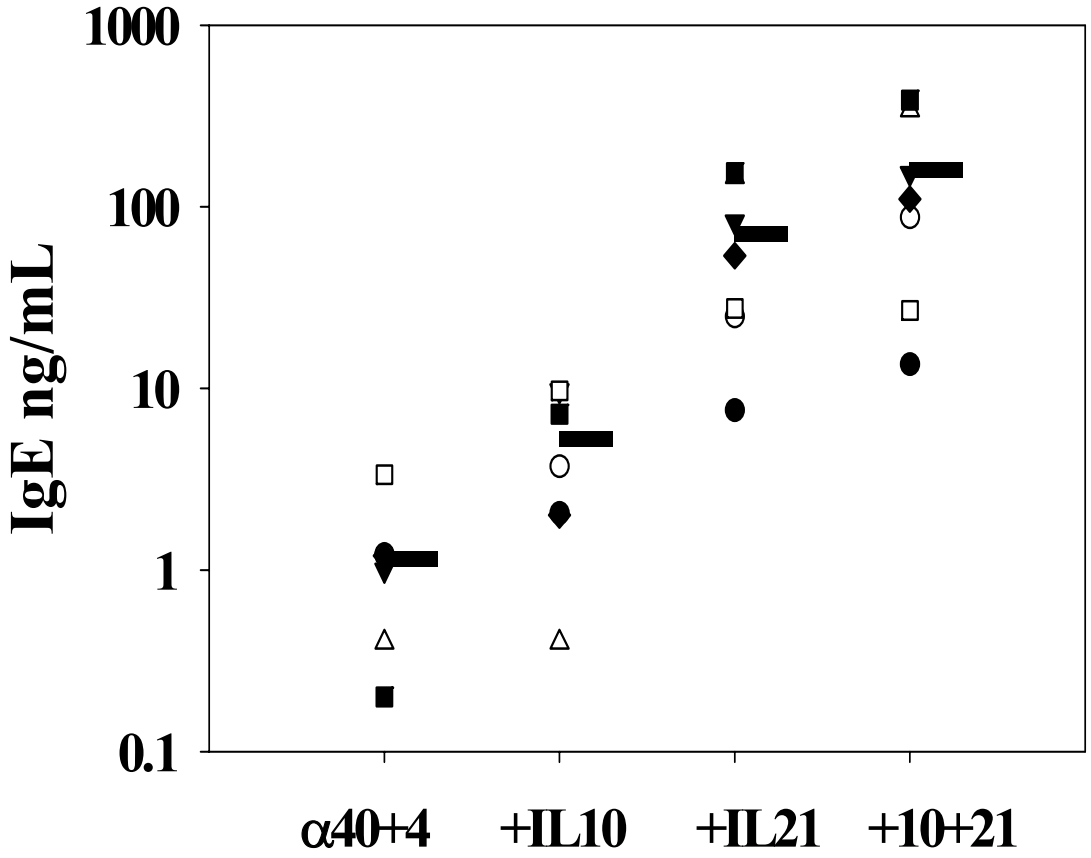
1000
100
10
1
0.1
IgE ng/mL
α40+4
+IL10
+IL21
+10+21

Figure 32: Addition of IL-10 to IL-21 stimulated cells has no further effects on cellular Division. Mean Fluorescent Intensity (MFI) values were plotted from one CFSE-labeled tonsil B cell culture representative of two; IL-10 (ng/ml) or IL-21 (ng/mL) levels are shown. Flow analysis was done on day 8.

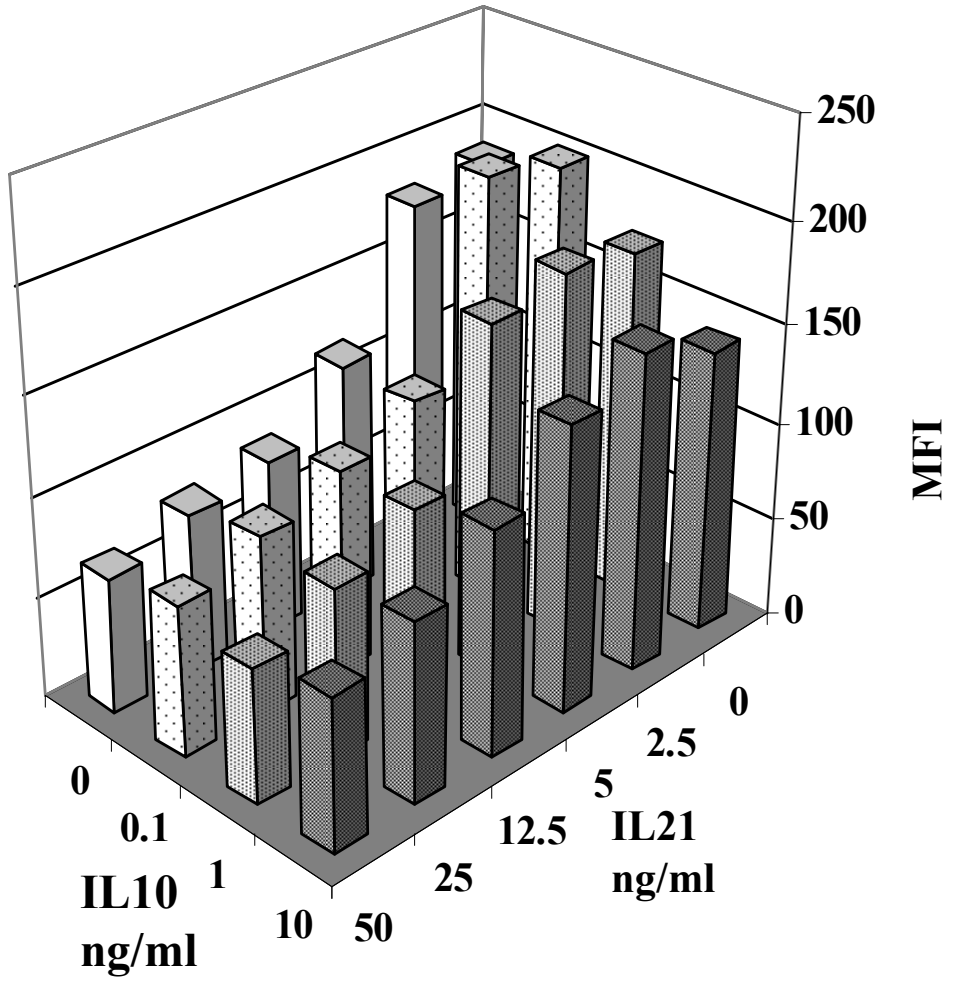
250
200
150
100
50
0
MFI
0
0.1
1
10
50
IL10
ng/ml
0
2.5
5
12.5
25
IL21
ng/ml

additive. Although there was an increase of IgE when both IL-10 and IL-21 were added to IL-4/anti-CD40 stimulated cells, there was no further cell division at the higher IL-21 concentrations added as seen by the CFSE results, **Figure 32**. As can be seen, the highest level of IL-21 resulted in a mean fluorescent intensity (MFI) to around 60; addition of IL-10 did not result in a further decrease in MFI, indicating no additional cell division was occurring.

Mouse B cell proliferation is also enhanced by IL-21, but IgE production is inhibited at the peak production values. Current literature indicates that IL-21 is inhibitory to IgE production in the mouse, while stimulatory in humans [32;57], however the relationship of mouse IL-21 and cell density has not been examined. In order to better compare the human and mouse system, I cultured mouse B cells with CD40LT, IL-5, IL-4, and M15 (anti-LZ) in the presence or absence of mouse IL-21. As was seen with the human system [53], the addition of mouse IL-21 to activated B cell cultures, also resulted in increased B cell proliferation (data not shown). Analysis of antibody production in response to different initial B cell input indicate that IgE production was influenced in a biphasic manner by the inclusion of IL-21 in the cultures (**Figure 33a**). At high cell concentrations, IL-21 inhibited IgE production; however, some enhancement was seen at low cell inputs. While mouse IgG_1 and IgM production were not inhibited by the addition of IL-21 at any concentration, the bulk of IgG_1 production was shifted towards lower cell density (**Figure 33b**). Mouse IL-21 had minimal effect on the cell concentration dependence for IgM production (**Figure 33c**).

In order to determine whether changes in cell division explained the inhibitory effects of IL-21, CFSE labeled mouse B cells were incubated with CD40LT, IL-4, IL-5 ± IL-21. After 4 days of culture, cell division numbers were examined by flow cytometric analysis. Trends of increased cell division was evident at the low cell input numbers when compared to the higher cell input numbers (**Figure 34a** and **34b**), but these differences were not statistically significant. IL-21 addition seemed to further increased cell division, especially at these low cell inputs, analogous to what was seen in the human B cell cultures.

Figure 33: mIL-21 has a biphasic effect on IgE and IgG_1. (A) IgE levels, **(B)** IgG1 levels, or **(C)** IgM levels were measured from resting B cells plated at $1x10^2$-$5x10^4$ cells/well and incubated for 8 days with the cocktail alone (CD40LT/IL-4/IL-5/M15)(●) or cocktail and 25ng/mL mIL-21 (▽). Supernatants from the cells were collected on day 8 and assayed for the respective immunoglobulin by ELISA. Error bars represent one SD. This experiment is representative of three of similar design.

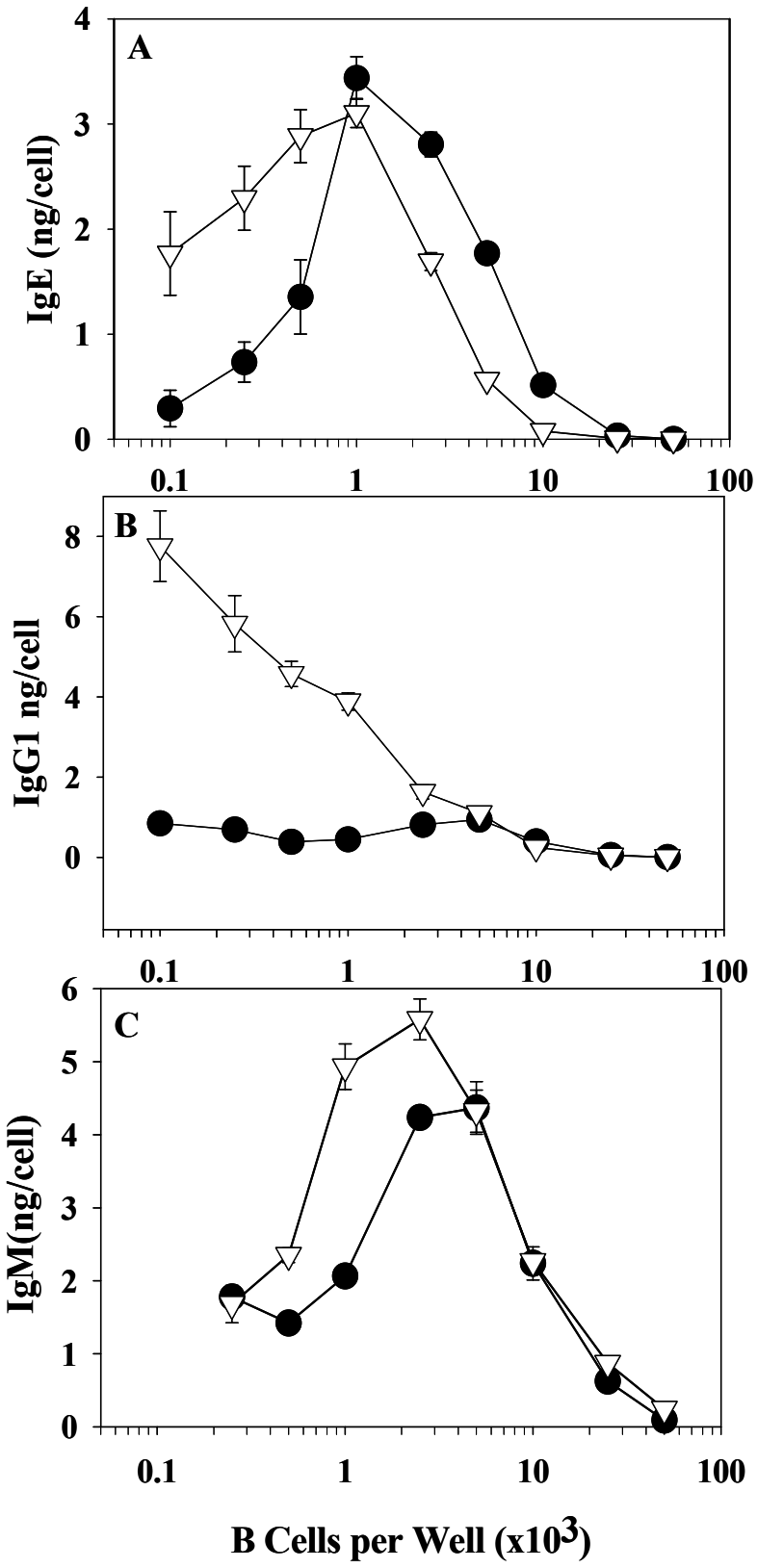
A
IgE (ng/cell)
0
1
2
3
4
0.1
1
10
100
B
IgG1 ng/cell
0
2
4
6
8
0.1
1
10
100
C
IgM(ng/cell)
0
1
2
3
4
5
6
0.1
1
10
100
B Cells per Well (x10^3)

Comparison of the Effects of Cell Density on Human and Mouse systems. In order to directly compare the mouse and human *in vitro* systems, I analyzed the inhibition or enhancement of IgE production as a function of the B cells per well due to the addition of IL-21 relative to IL-4/anti-CD40 conditions alone. This analysis is shown in **Figure 35** and this figure clearly shows that both the human and mouse systems exhibit a similar activity in the presence of IL-21. In order to show the variability that is seen, two experiments are plotted in this manner. Note that the primary difference is that the curve is shifted towards lower cell concentrations in the mouse system, while both systems exhibit enhancement of IgE at low and inhibition at high cell densities, respectively. The mean cell number of the mouse system where an increase of IgE production due to IL-21 was in the hundreds of cells per well (mean=625 cells per well, 2 experiments) The human system also displayed a similar trend of IgE production as was found in the mouse system, but the cell density where that was found was considerably higher. The average of six experiments was 47k cells per well +/- 25k. Whilst there is considerable variability in the human system this is to be expected. However, the differences are almost 2 logs higher that in the mouse system.

Figure 34: Increased cell division is evident at low cell densities in mouse IL-21 containing cultures. Splenic murine B cells were labeled with CFSE and cultured at 500 cells/well for 4 days then analyzed by flow cytometry. **(A)** Histogram of cells cultured with IL-4 only (—), stimulation cocktail (CD40LT/IL-4/IL-5/M15) (— –) or stimulation cocktail plus 5ng/mL mIL-21 (·····). **(B)** Analysis of division numbers from flow data IL-4 only (●); activation cocktail plus IL-21(■), or without IL-21 (▽), respectively. Experiment is representative of three of similar design.

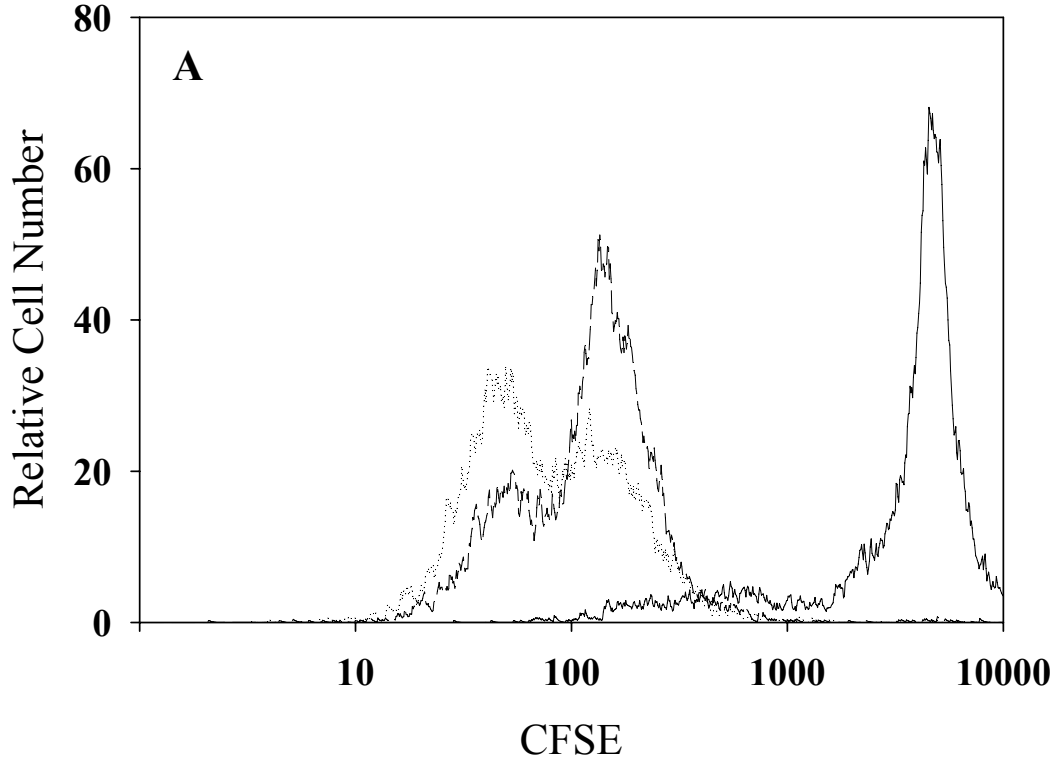
A
Relative Cell Number
80
60
40
20
0
10
100
1000
10000
CFSE

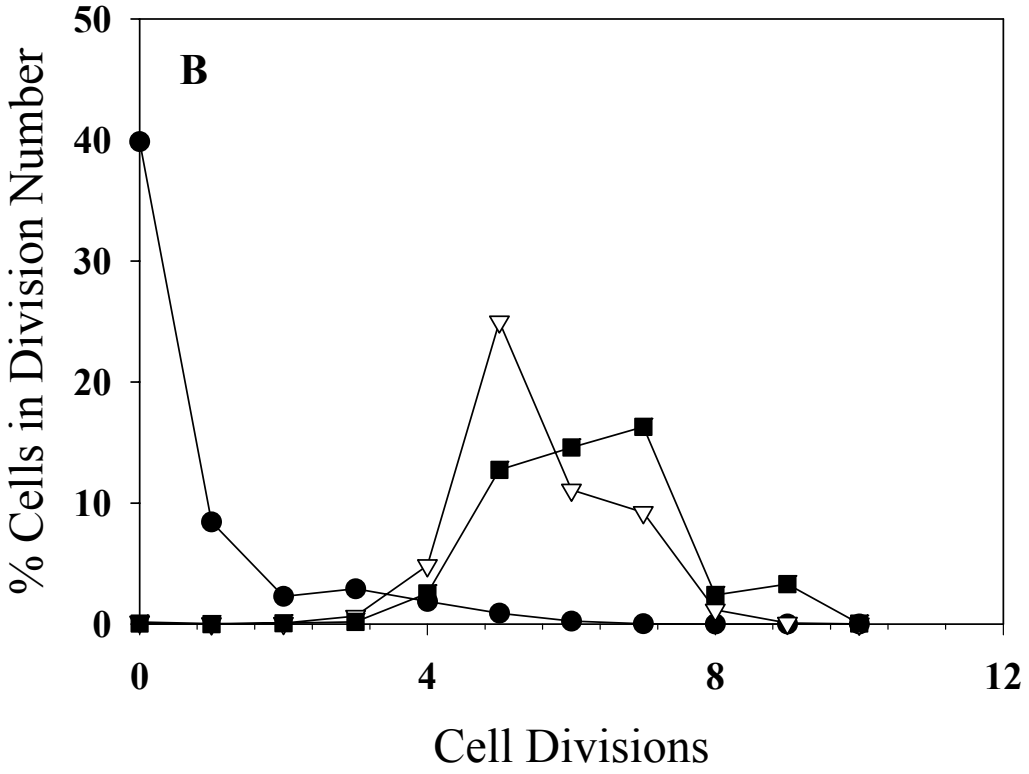
B
% Cells in Division Number
50
40
30
20
10
0
0
4
8
12
Cell Divisions

Figure 35: Comparison of the effect of cell density on human and mouse IgE production. The influence of IL-21 on the amount of mouse (●) or human (■) IgE produced is shown as a function of cell density in order to illustrate that IL-21 causes both enhancement and inhibition of IgE synthesis, depending on the initial cell input. Mouse B cells were activated with CD40LT/IL-4/IL-5/M15 plus 25 ng/ml mIL-21, while the tonsilar B cells were activated with IL-4/anti-CD40 plus 25ng/mL human IL-21 supernatant. The formula used was IgE level at: ((no IL-21 – IL-21)/ no IL-21)*100). Two experimental results for mice are shown. Two experimental results for human cells are shown, representative of seven experiments of similar design.

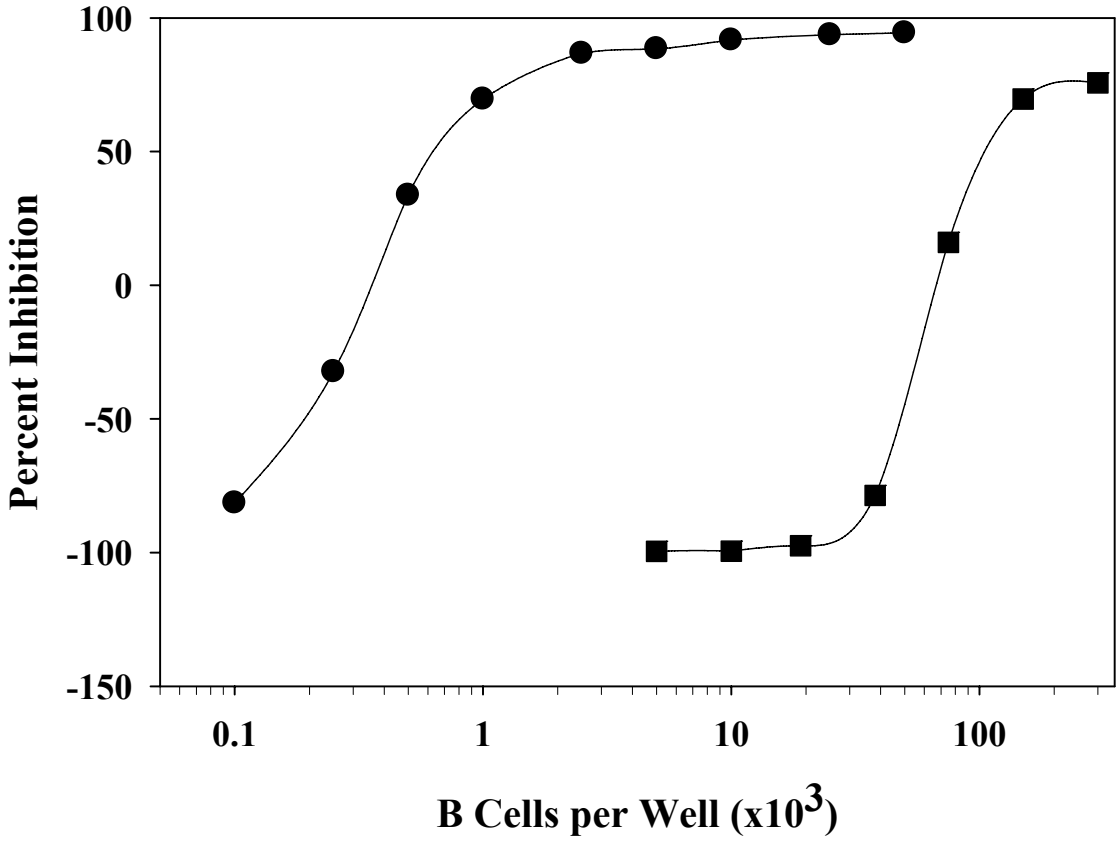
100
50
0
-50
-100
-150
Percent Inhibition
0.1
1
10
100
B Cells per Well (x10^3)

IL-10 CD23 expression influence is cytokine dependent, and IL-21 induced CD23 expression is cytokine dependent and JAK2 dependent. It is known that under certain conditions IL-21 will act in opposing ways depending on stimuli. It has been shown that IL-21 will enhance the IL-4/antiCD40 stimulation but will inhibit the IL-4/anti-IgM stimulation [53;55;62]. As I was working with IL-21 supernatant, I wished to further demonstrate that IL-21 was responsible for the effects that were being attributed. Purified naïve B cells from human tonsils were treated with increasing concentrations of IL-21 **(Figure 36A)** or with increasing concentration of IL-10 **(Figure 36B)** Cells were incubated for four days and after incubation the cells were washed and stained to determined the surface expression of CD23 with anti-human CD23 FITC. The results clearly showed that without a second signal, both IL-21 and IL-10 decreased surface expression as compared to B cells that were unstimulated. However, with IL-4/antiCD40 stimulation it is readily seen that the surface expression is significantly higher and in a concentration dependent manner of IL-10 (**Figure 37a**) and also for IL-21 (data not shown) and that 25ng/ml IL-21 had the greatest increase in expression, higher than the highest concentration of IL-10 tested, 100ng/ml (**Figure 37b**).

IL-21 is reported to be involved with STAT1, STAT3, and STAT5 signaling. Signaling through the STAT3 has been reported due to the IL-21 sharing the common gamma chain (γ_c). To elucidate the role of IL-21 involved in enhanced IgE production it was hypothesized that there would also be an accompanying increase in CD23 expression and this would go through the STAT3 signaling pathway. AG490 is a potent inhibitor of JAK2, which is itself required for STAT3 signaling. I treated IL-4/antiCD40

B cells with increasing concentrations of AG490 to find a concentration that would not effect expression of CD23. As can be seen in **Figure 38a**, 5μM AG490 had little effect on surface CD23 expression in IL-4/antiCD40 treated B cells.

Figure 36: IL-21 and IL-10 both reduce surface CD23 expression in naïve unstimulated B cells. Naïve tonsilar B cells were either untreated (solid red) or treated with increasing concentrations of 1.25ng/ml (——), 12.5ng/ml (——), or 25ng/ml (——) IL-21 **(A),** or increasing concentrations of 10ng/ml (——), 50ng/ml (——), or 100ng/ml (——) IL-10 **(B)**. After four days, cells were collected and stained with CD23-PE and analyzed for surface expression of CD23 by flow cytometry. Shown is one representative experiment of three.

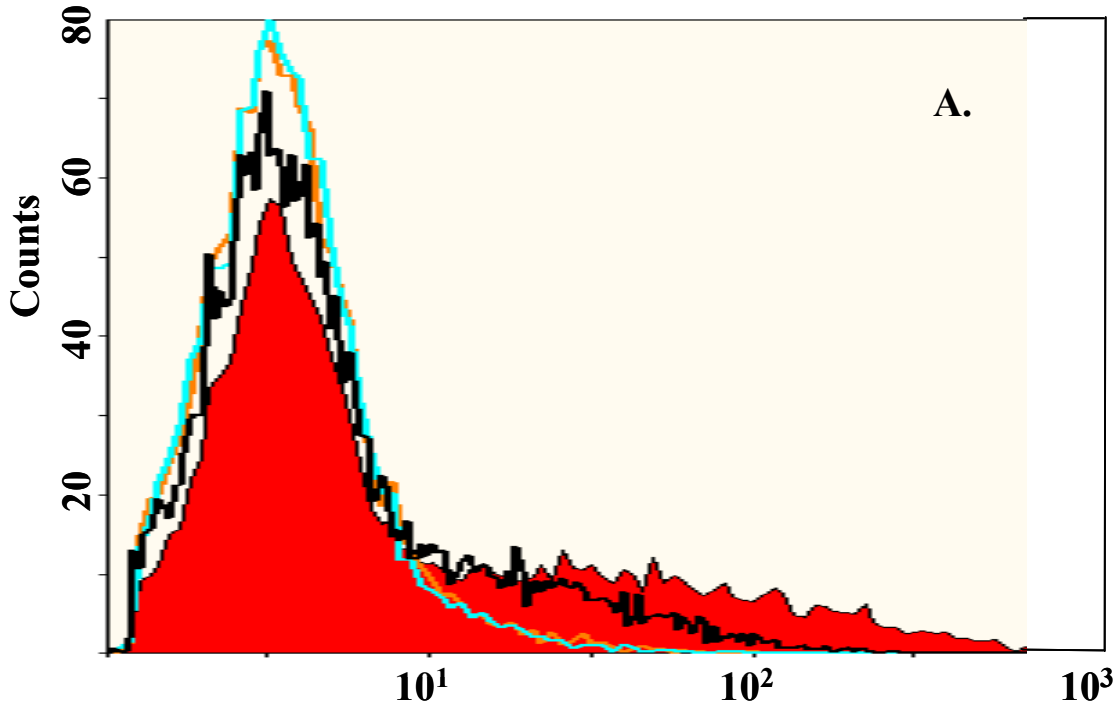
A.
Counts
80
60
40
20
10^1
10^2
10^3

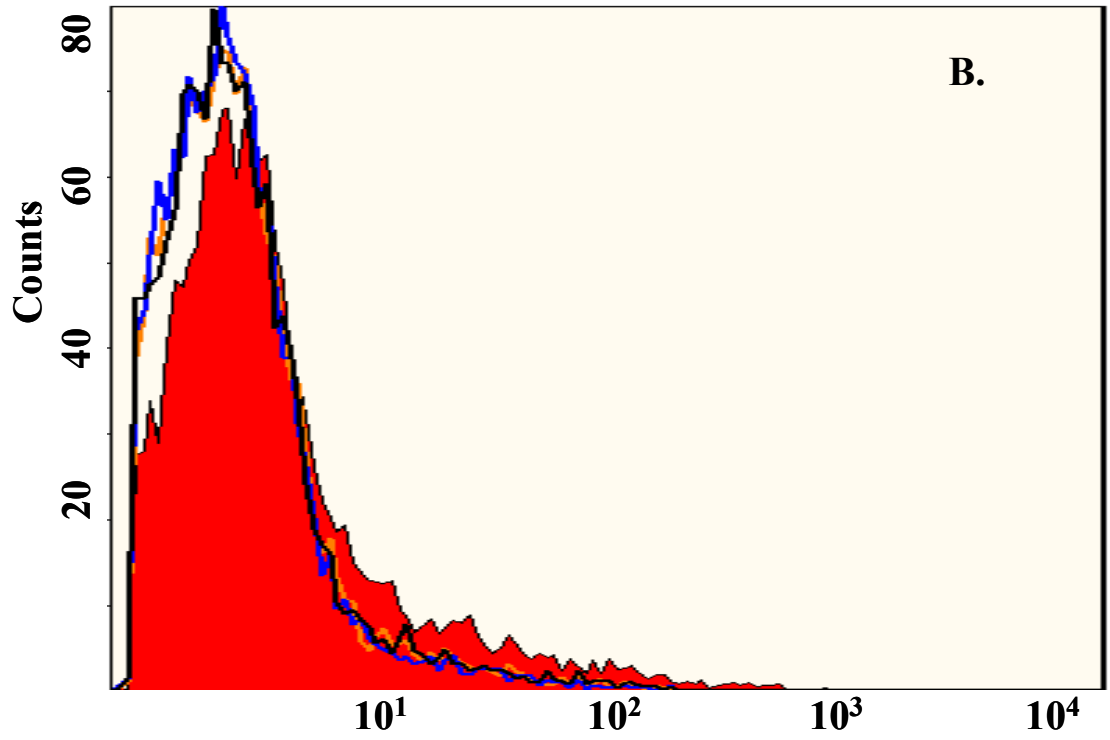
B.
Counts
80
60
40
20
10^1
10^2
10^3
10^4

Figure 37: Surface CD23 on IL-4/antiCD40 stimulated Naïve B cells is increased with IL-10 and IL-21 in a dose dependent manner with IL-21 being the most stimulatory. Naïve B cells were purified from tonsils and treated with IL-4 and antiCD40. Some were treated with increasing concentrations of IL-10 **(A)** and others with IL-21 **(B)**. **(A)** After four days the cells were collected and analyzed for surface expression of CD23 by flow cytometry. IL-10 concentrations of 10ng/ml (——), 50ng/ml (——), or 100ng/ml (——) were added to IL-4/antiCD40 (solid red) stimulated cells and were compared. **(B)** IL-21 25ng/ml (——) had the highest increase in CD23 over all conditions. B cell alone (solid red), IL-4/antiCD40 (——), and 10ng/ml IL-10 (——). Shown is one representative experiment of three.

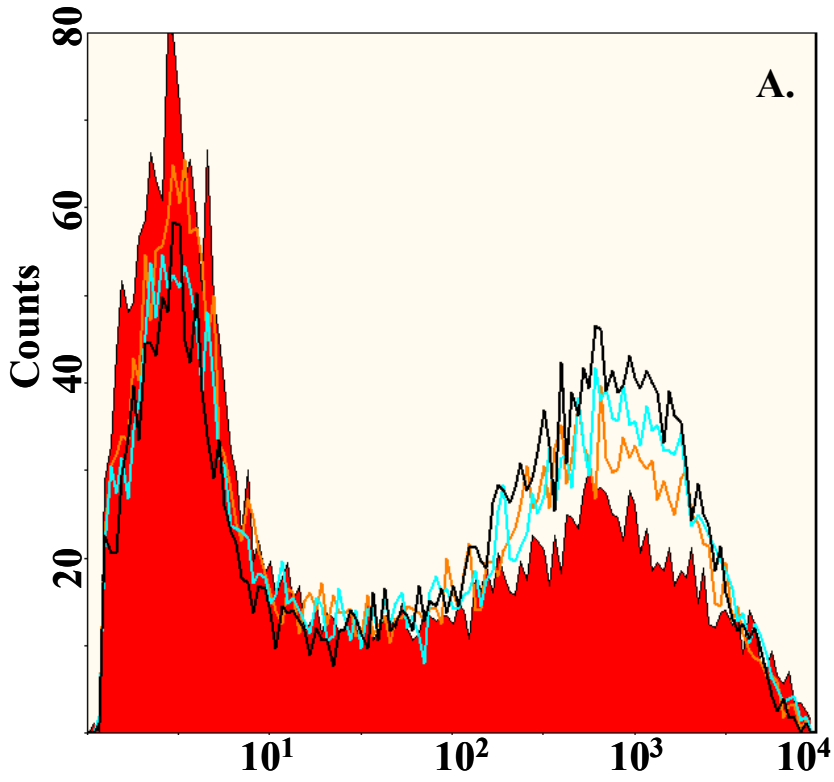
A.
Counts
80
60
40
20
10^1
10^2
10^3
10^4

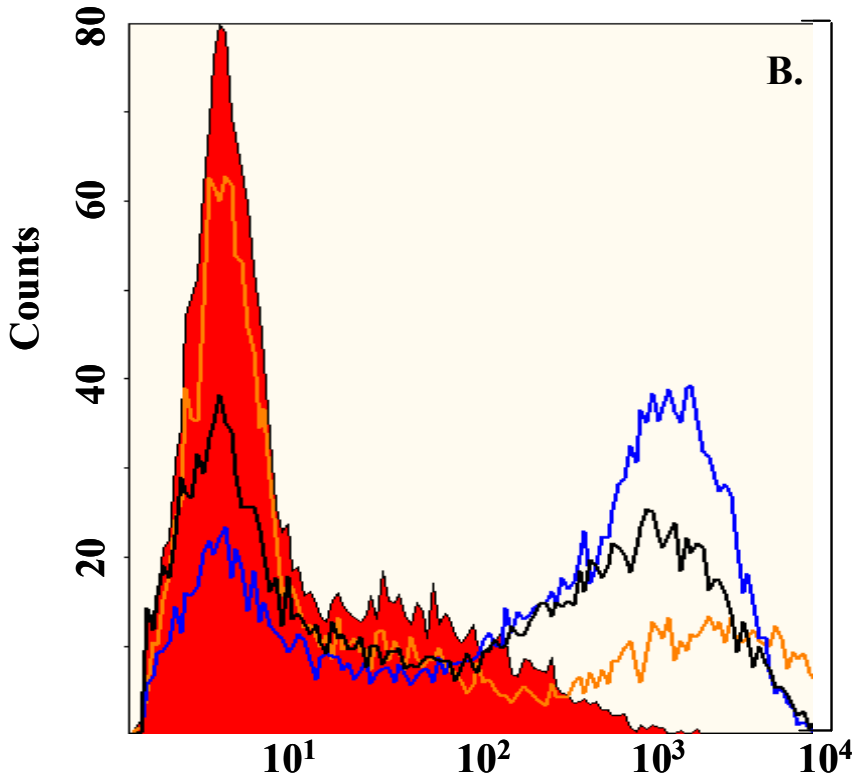
B.
Counts
80
60
40
20
10^1
10^2
10^3
10^4

Figure 38: The Effects of IL-21 on B Cells expression of surface CD23 is dependent on B cell stimuli and is JAK2 dependent. (A) Naïve tonsilar B cells stimulated with IL-4 and antiCD40 as control (solid red), and others were given increasing amounts of AG490, a JAK2 inhibitor, of 5μM (——), 10 μM (——) and 20 μM (——). After four days the cells were collected and analyzed for CD23 expression. 5μM of AG490 was shown to have little CD23 expression effect from that of IL-4/antiCD40 cells that had only vehicle control. **(B)** Naïve B cells were treated with IL-4/antiCD40 (solid red) or the addition of 25ng/ml IL-21 in the presence (——) or absence (——) of 5 μM AG490. 5 μM AG490 control is shown in (——). After four days the cells were collected and analyzed for the surface expression of CD23. Shown is one representative experiment of three.

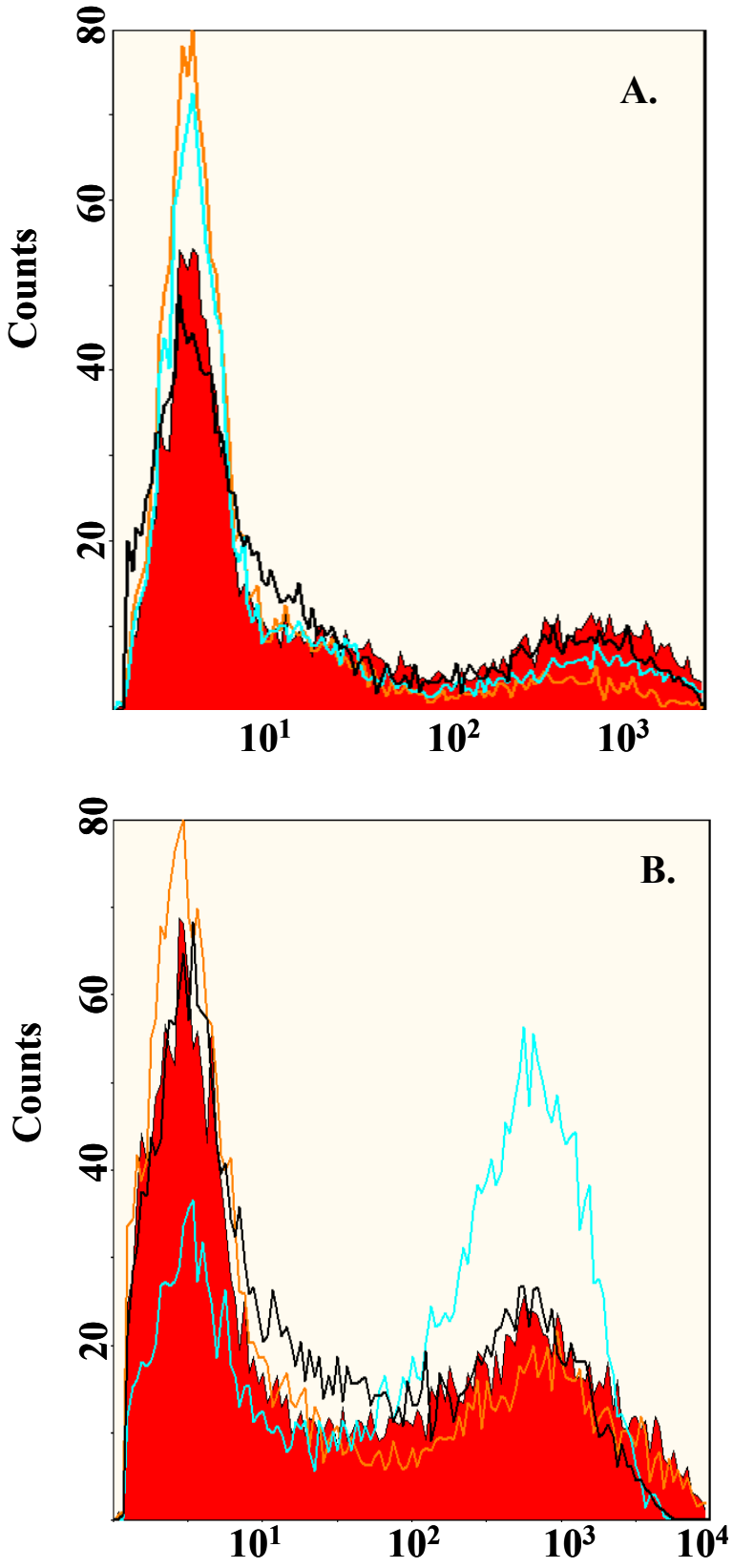
A.
Counts
80
60
40
20
10^1
10^2
10^3
B.
Counts
80
60
40
20
10^1
10^2
10^3
10^4

When IL-21 was added to IL-4/antiCD40 treated cells, the expression of CD23 was significantly higher than that of IL-4/antiCD40, but upon addition of the JAK2 inhibitor, all effects due to IL-21 were lost (**Figure 38b**). This study demonstrated that part of the effects of IL-21, as seen by increased surface CD23 when added to IL-4/antiCD40 treated cells could be abrogated by the addition of the STAT3 inhibitor. Because the STAT signaling pathway is still under investigation in determining the role of IL-21 involved in IgE synthesis, the next step was to try and answer if using the JAK2 inhibitor could be useful. The matter is complicated however, and although IL-4 uses STAT6, it has been shown that both JAK1 and JAK3 are phosphorylated, and AG490 is not only a JAK2 inhibitor but has also been shown to have some effects on JAK1 inhibition as well.

Because of this, I sought to try another approach and target STAT3 signaling itself. As was mentioned earlier, IL-21 has been associated with a variety of STATS, 1,3, and 5, depending on cell type and stimulation. To further elucidate the role if STAT3 in IL-21 mediated increased cell division and increase immunoglobin expression, particularly, IgE, I employed a STAT3 dominant negative plasmid transfection approach using electorporation of human B cells. Using a pCMV-STAT3β-IRES-EGFP plasmid, human B cells were elctroporated using an Amaxa electroporator. A control plasmid without the STAT3β dominant negative portion was used to determine transfection efficiency. As can be seen from **Figure 39**, the control was effectively transfected into the B cells as determined by GFP expression seen by flow cytometry (**Figure 39A and Figure 39B**). However, the GFP was not seen in B

cells that had been transfected with the bicistronic STAT3β-GFP **(Figure 39C and Figure 39D)**. Due to time limitations, I was not able to follow further with this course of study but it remains a powerful tool to understanding and more precisely defining which of the downstream signaling pathways are involved.

Figure 39: Transfection of Human Naïve B Cells with bicistronic dominant negative STAT3-GFP plasmid. $5x10^6$ Human B cells were purified and combined with 3μg control plasmid **(A,B)** pIRES-CMV-IRES-EGFP or experimental **(C,D)** pIRES-CMV-STAT3β-IRES-EGFP and pulsed using the Amaxa Nucleufector II kit. After 20 hours cells were collected and analyzed by flow cytometry for GFP expression. Shown is one experiment representative of five.

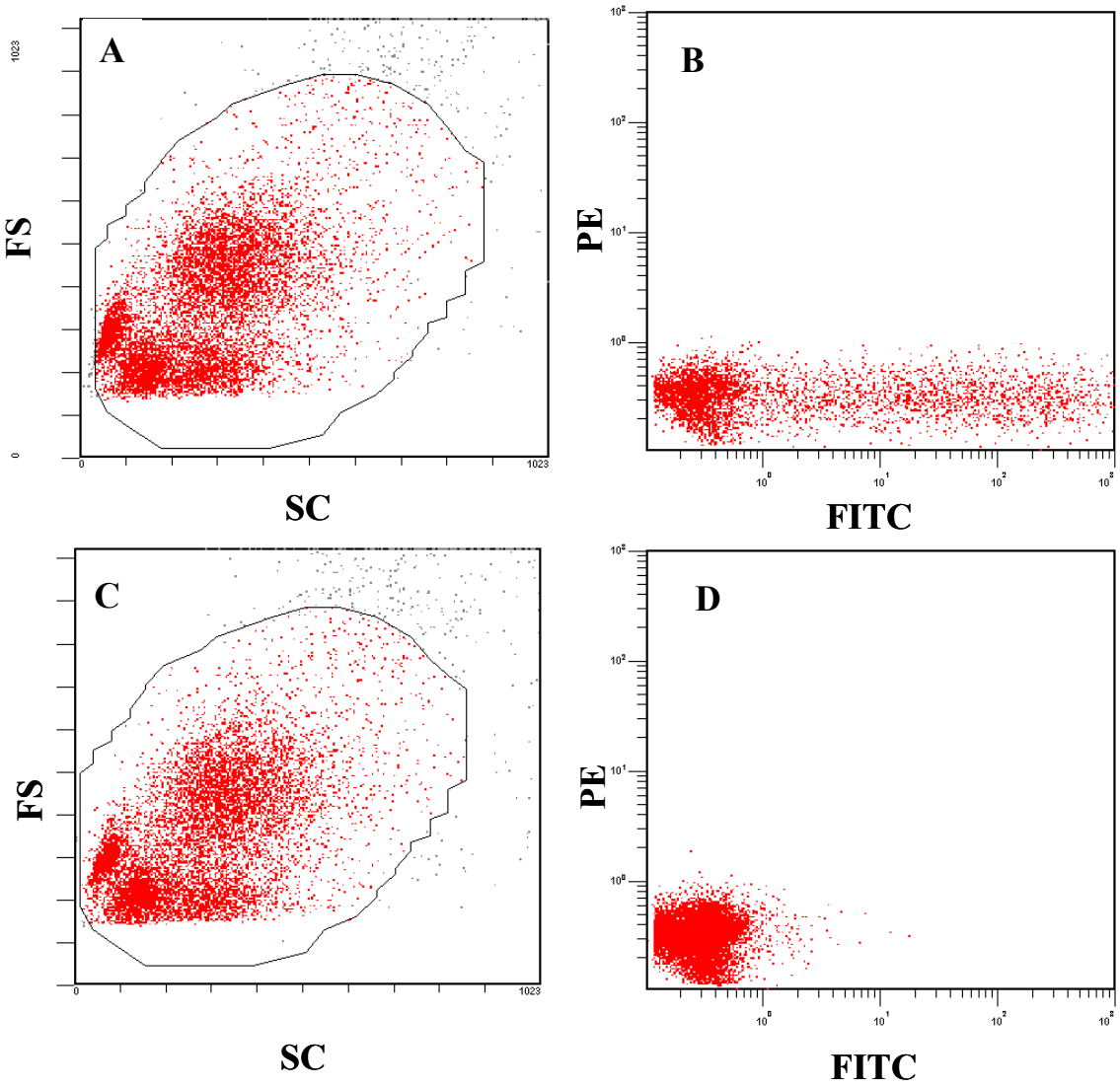
A
B
C
D
FS
SC
PE
FITC
0
1023

Kinetics of differential expression of IgD^+ surface expression and $CD38^+$ surface expression on purified tonsilar B cells. I sought to determine what correlations existed in surface expression of the surface cell markers IgD and CD38. CD38 is a single chain 42 to 46 kDa type II integral transmembrane glycoprotein with a short N terminal cytoplasmic tail. CD38 is highly expressed on thymocytes. It is also expressed by early cells of B and T lineages, NK cells, plasma cells, monocytes and macrophages. Because of its expression on differentiated cells, including plasma cells, CD38 was chosen as a maker of differentiation.

The cells were originally purified using anti-IgD^+ selection to have a pool of purified naïve cells. Naïve cells were plated at varying concentrations of three hundred thousand cells per well and titrated 1:2 in decreasing numbers to the lowest of six hundred cells per well. Cells were treated with IL-4 and anti-CD40, with the second condition having the addition of 25ng/ml IL-21 added. Cells were collected on days 4, 6, and 12 and were stained with both anti-IgD FITC and anti-CD38 PE Cy5. As can be seen from the results on day 4 for the IL-4/anti-CD40 treated cells (**Figure 40**) there is a uniform expression of IgD^+ cells across all the differing cell inputs. These results contrast however to that of the IL-21 treated cells (**Figure 41**). As can be seen the results indicate that there is a an increase in the CD38+ cell expression along with a decrease in IgD^+ surface expression. Also it appears that there is the emergence of a small population of IgD- cells that are found in the two lowest cell populations shown, 5k and 2.5k cells per well. This is not surprising as it is generally found that IgE production, as determined by ELISA on day 12, is highest in the lower cell density

wells. In addition there is also the emergence of a small population that is IgD-CD38^{+} in the 2.5k well.

The development of cellular differentiation along both differing time courses and inverted cell density curves becomes more readily apparent when day 6 is observed. As has been shown in IgE found in supernatant, the levels found in IL-4/antiCD40 stimulated conditions tend to be at the higher cell densities and not at the lower cell densities (**Figure 42**), while the inverse is true for cells with the additional stimulation of IL-21 (**Figure 43**). In these cells the maximal IgE production tends to be found in the very low cell densities. As can be seen from the day 6

Figure 40: IL-4/antiCD40 treated IgD^+ tonsilar cells remain naïve and undifferentiated after four days as determined by high IgD^+ and low $CD38^+$ surface expression over all cell densities. Tonsilar B cells were purified using Milltenyi IgD^+ cell sorting and were then plated at decreasing cellular density titration starting from 300k per well to 0.6k cells per well. The cells were then treated with 10ng/mL IL-4 and 1000ng/mL antiCD40 and incubated for four days. After four days the cells were collected, washed, and stained with 5µl anti-IgD-FITC and 5µl anti-CD38- PE-CY5.

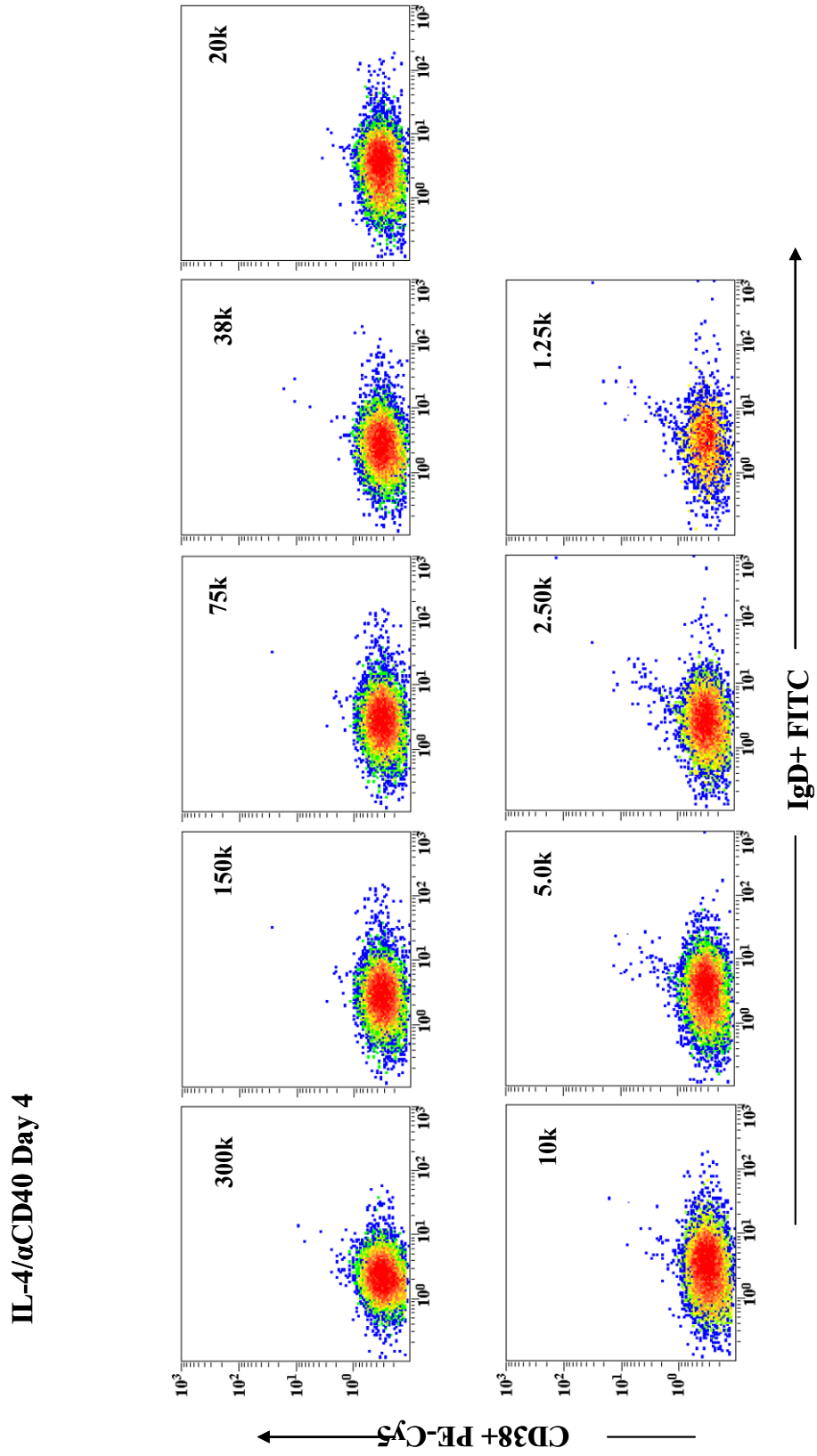
IL-4/αCD40 Day 4
20k
38k
75k
150k
300k
1.25k
2.50k
5.0k
10k
CD38+ PE-Cy5
IgD+ FITC

Figure 41: IL-21 added to IL-4/antiCD40 treated IgD^+ tonsilar cells show increased expression of $CD38^+$ after four days as well as the greatest loss of IgD^+ at the lowest cell densities . Tonsilar B cells were purified using Milltenyi IgD^+ cell sorting and were then plated at decreasing cellular density titration starting from 300k per well to 0.6k cells per well. The cells were then treated with 10ng/mL IL-4,1000ng/mL antiCD40, 25ng/ml IL-21, and incubated for four days. After four days the cells were collected, washed, and stained with 5µl anti-IgD-FITC and 5µl anti-CD38- PE-CY5.

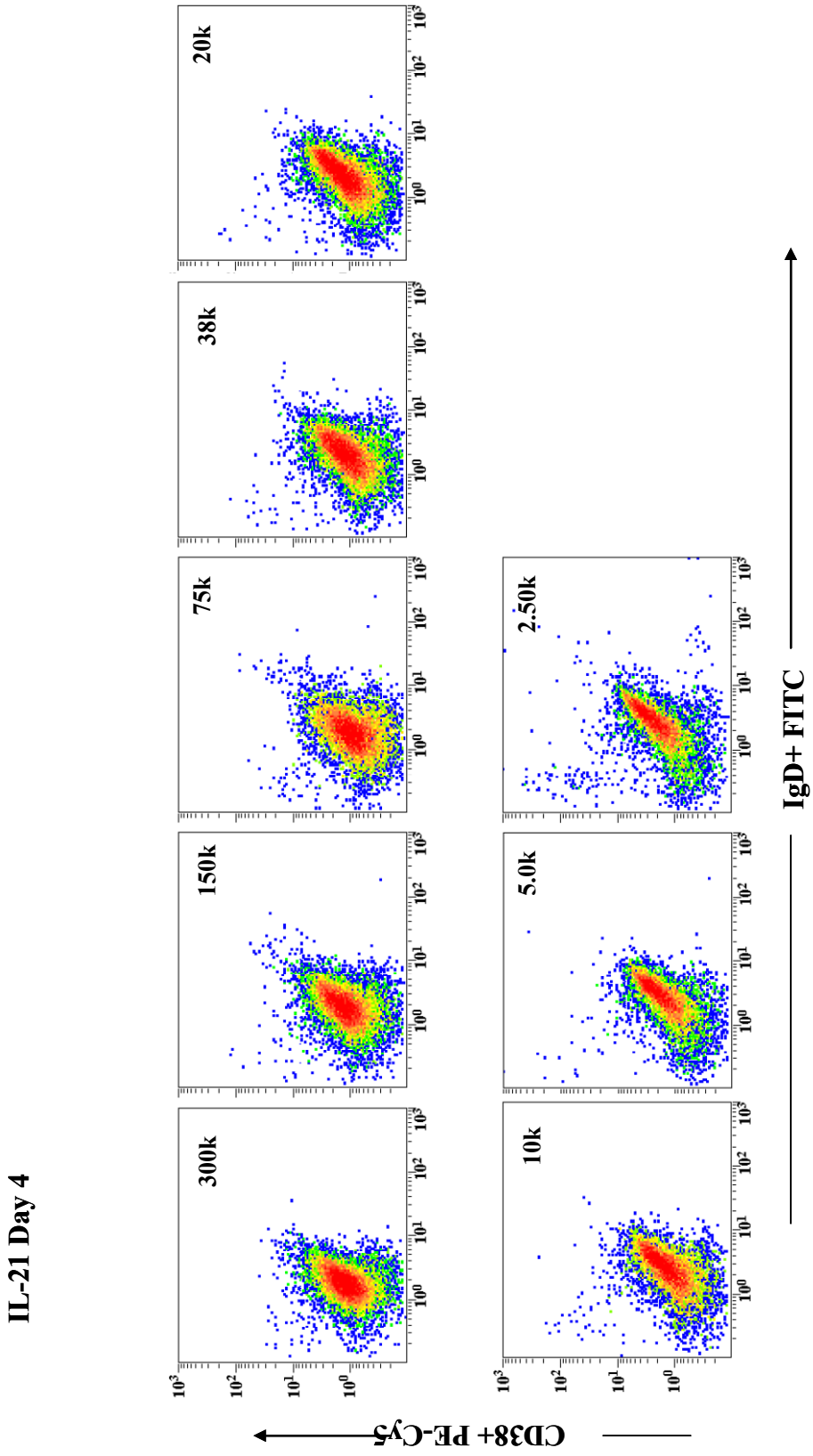
IL-21 Day 4
300k
150k
75k
38k
20k
10k
5.0k
2.50k
CD38+ PE-Cy5
IgD+ FITC

Figure 42: Day 6 IL-4/antiCD40 treated cells show the greatest loss of IgD^+ expression in the higher cell density populations. Tonsilar B cells were purified using Milltenyi IgD^+ cell sorting and were then plated at decreasing cellular density titration starting from 300k per well to 0.6k cells per well. The cells were then treated with 10ng/mL IL-4 and 1000ng/mL antiCD40 and incubated for six days. After six days the cells were collected, washed, and stained with 5µl anti-IgD-FITC and 5µl anti-CD38-PE-CY5.

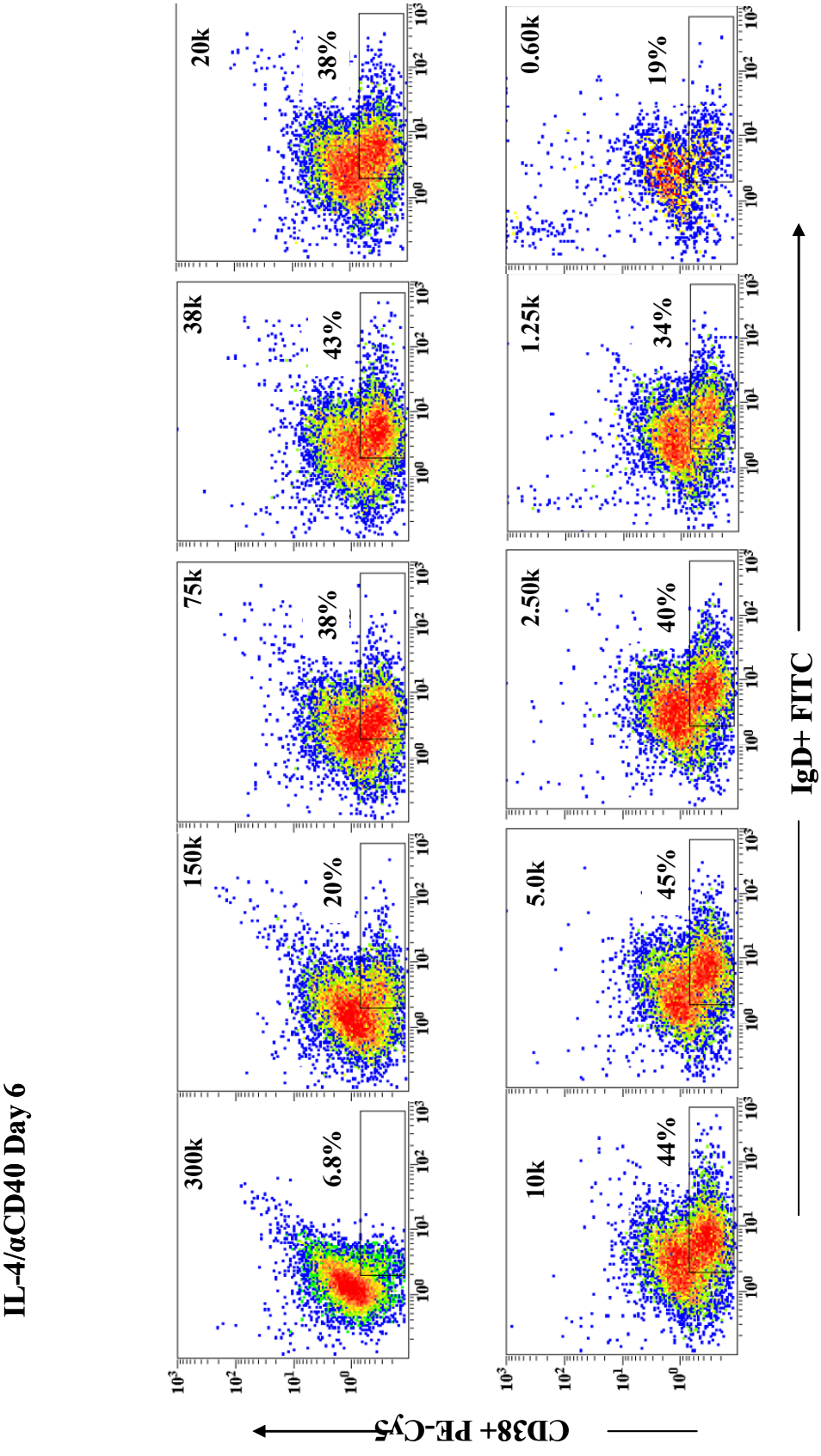
IL-4/αCD40 Day 6
300k
6.8%
150k
20%
75k
38%
38k
43%
20k
38%
10k
44%
5.0k
45%
2.50k
40%
1.25k
34%
0.60k
19%
CD38+ PE-Cy5
IgD+ FITC

Figure 43: IL-21 added to IL-4/antiCD40 treated IgD$^+$ tonsilar cells by day six show differential expression of CD38$^+$, inversely dependent on plating density of cells, as well as decreasing IgD$^+$. Tonsilar B cells were purified using Milltenyi IgD$^+$ cell sorting and were then plated at decreasing cellular density titration starting from 300k per well to 0.6k cells per well. The cells were then treated with 10ng/mL IL-4, 1000ng/mL antiCD40, and 25ng/ml IL-21 and incubated for six days. After six days the cells were collected, washed, and stained with 5µl anti-IgD-FITC and 5µl anti-CD38- PE-CY5.

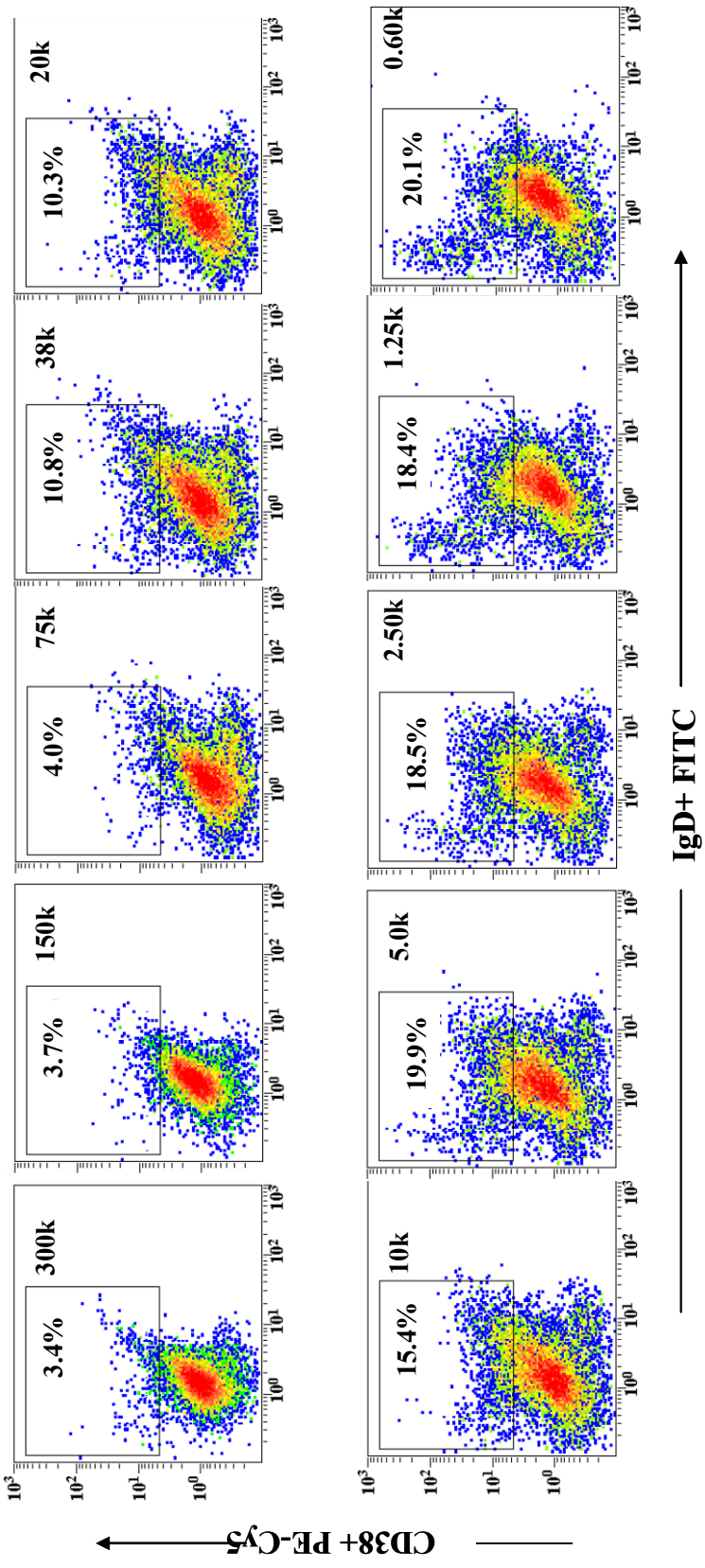
IL-21 Day 6
CD38+ PE-Cy5
IgD+ FITC
3.4%
300k
3.7%
150k
4.0%
75k
10.8%
38k
10.3%
20k
15.4%
10k
19.9%
5.0k
18.5%
2.50k
18.4%
1.25k
20.1%
0.60k

data the differentiation of the stimulated cells is also following this phenomenon. In the IL-4/antiCD40 stimulated cells the percentage of remaining IgD^+ cells is found to be the smallest in the higher cell populations, and that the percentage of naïve population is greater in the subsequent populations of reduced cell number. As can be seen there is ~ 7% and 20% of IgD^+ cells remaining at the two highest concentrations of 300k and 150k. As the concentrations decrease, however, the percentage of IgD^+ cells jumps and remains at around 40%.

When contrasted with the surface profile of the cells treated with the additional stimuli of IL-21, however, it is obvious that the inverse is true. The large trailing population of naïve IgD^+ cells at the lowest cell density is virtually gone, whereas in increasing cell density it is at a higher percentage. It is to be noted however, that there remain a percentage of IgD^+ cells in the IL-21 conditions, even though it remains significantly less than the remaining percentages of IgD^+ found in the IL-4/antiCD40 stimulated cells. What is striking, however, about the IL-21 treated cells is the emergence of the $CD38^+$ population is found in ever increasing percentages as the cell density decrease. This is to be expected as it is in the lower populations where the greatest IgE concentration is found. As can be seen, there is less than 5% $CD38^+$ cells in the 300k, 150k, and 75k wells. This jumps up to around 10-15% $CD38^+$ cells in the 38k, 20k and 10k cell populations. The number of $CD38^+$ cells continues to rise to around 20% and remains at this value in the remaining cell density wells, 5k, 2.5k, 1.25k, and 0.6k, respectively. However, while the four lowest density cell populations have a consistent ~20% $CD38^+$ population there is a significant population of IgD^-

/CD38hi cells that are emerging as seen around the 5k mark. It should also be noted that this population continues to grow as the initial plated densities decreases.

This trend continues and is further defined when looking at data from day 12. In the IL-4/antiCD40 conditions (**Figure 44**) the wells with the highest cells populations have the fewest remaining IgD^+ cells. The wells with the highest cell concentrations have ~0%, 3%, ~9%, and 10% remaining IgD^+ cell populations. The remaining wells with decreased cell densities have ~15%. When the IL-21 populations are examined it is clear that the IgD^+ populations are virtually gone (**Figure 45**). In addition, the earlier day 6 observations where there are higher populations of $CD38^+$ cells in the lower cell density wells are even more pronounced. As can be seen from the figure, the trend of increasing $CD38^+$ cell percentage is consistently increasing throughout the cell density range. The percentages of $IgD^-/CD38^{hi}$ are 0.9, 0.7, 0.5, 0.1, 0.2, 0.7, 0.9, 2.8, 4.8, and 8%. If the IgD^{int} $CD38^{int}$ are analyzed the percentages are 4, 2.7, 1.5, 2.5, 2.8, 2.8, 4, 4.5, 7.1, and 12.0%. When both $IgD^-/CD38^{hi}$ and IgD^{int} $CD38^{int}$ are combined they are 4.9, 3.4, 2.6, 3.0, 3.5, 4.9, 7.5, 11.9, and 20%, respectively. When both CD38hi and CD38int and combined, the wells that have the greatest significant percentages over the rest of the wells are the wells with the three least densities of 2.5k, 1.25k and 0.6k.

IgE Production Kinetics: IL-21 has been consistently shown to produce significantly higher IgE from IL-4/antiCD40 stimulated cells over that of IL-4/antiCD40 stimulated cells alone. IgE from IL-21 stimulated cells have also been shown to produce the greatest amount of IgE from wells that have been plated at relatively low cell numbers

of several hundred cells per well to up to ten thousand cells per well. As the IgE from IL-4/antiCD40 stimulated wells generally came from the higher initial cell density plated wells, and as the IgE from the IL-21 stimulated cells came from the lower wells, I sought to determine if the IgE production patters would be similar throughout the development of the IgE production time course. As can be seen from the

Figure 44: Day 12 IL-4/antiCD40 treated cells show the most loss of surface expression of IgD^+ in the highest cell density platings. Tonsilar B cells were purified using Milltenyi IgD^+ cell sorting and were then plated at decreasing cellular density titration starting from 300k per well to 0.6k cells per well. The cells were then treated with 10ng/mL IL-4 and 1000ng/mL antiCD40 and incubated for twelve days. After twelve days the cells were collected, washed, and stained with 5µl anti-IgD-FITC and 5µl anti-CD38- PE-CY5.

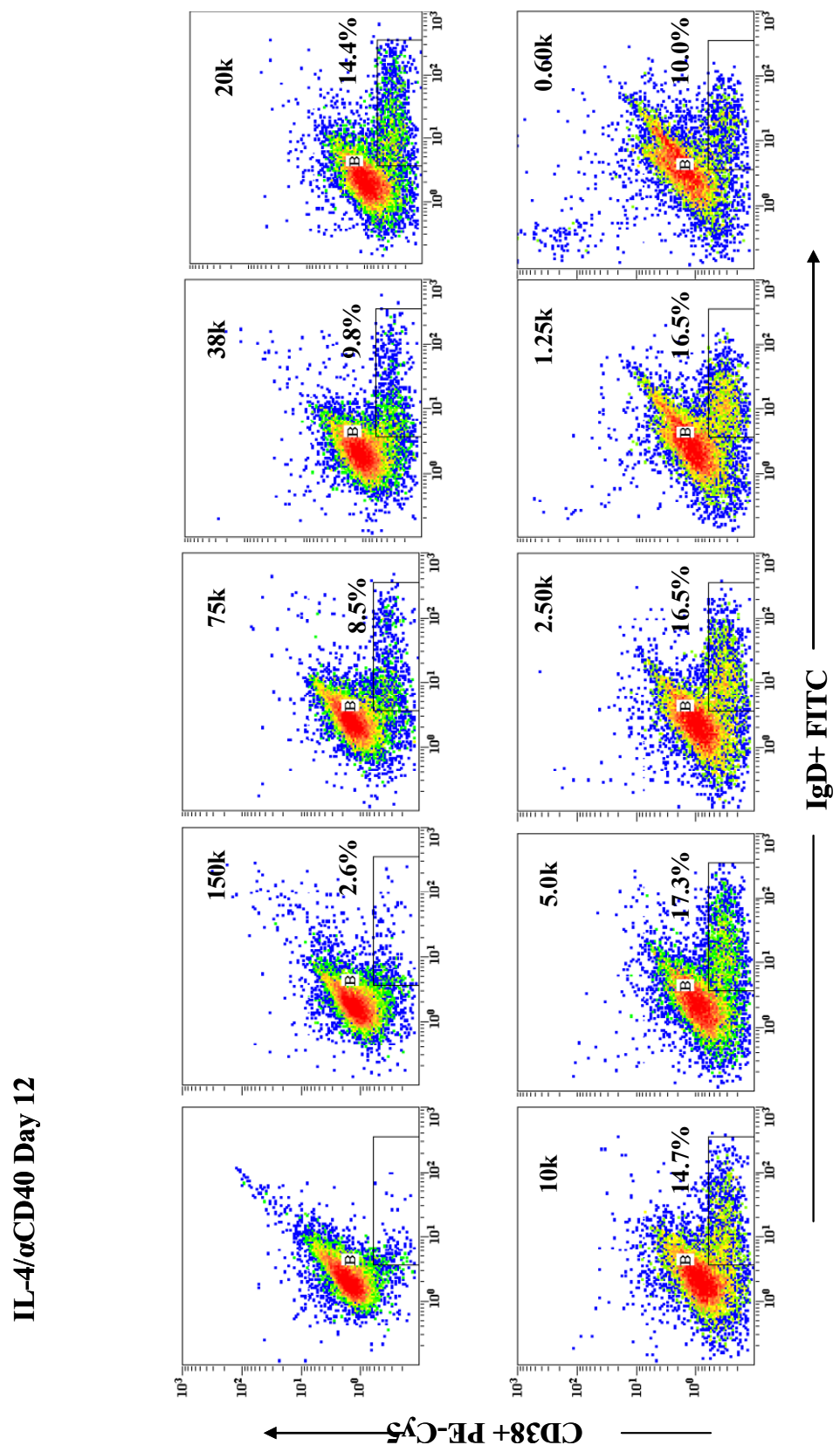
IL-4/αCD40 Day 12
CD38+ PE-Cy5
IgD+ FITC
10k
14.7%
5.0k
17.3%
2.50k
16.5%
1.25k
16.5%
0.60k
10.0%
150k
2.6%
75k
8.5%
38k
9.8%
20k
14.4%
B

Figure 45: Day 12 IL-21 treated IL-4/antiCD40 have strong expression of $CD38^{hi}IgD^{low}$ and $CD38^{int}IgD^{int}$ expression inversely proportional to cell density. Tonsilar B cells were purified using Milltenyi IgD^{+} cell sorting and were then plated at decreasing cellular density titration starting from 300k per well to 0.6k cells per well. The cells were then treated with 10ng/mL IL-4, 1000ng/mL antiCD40, and 25ng/ml IL-21 and incubated for twelve days. After twelve days the cells were collected, washed, and stained with 5µl anti-IgD-FITC and 5µl anti-CD38- PE-CY5.

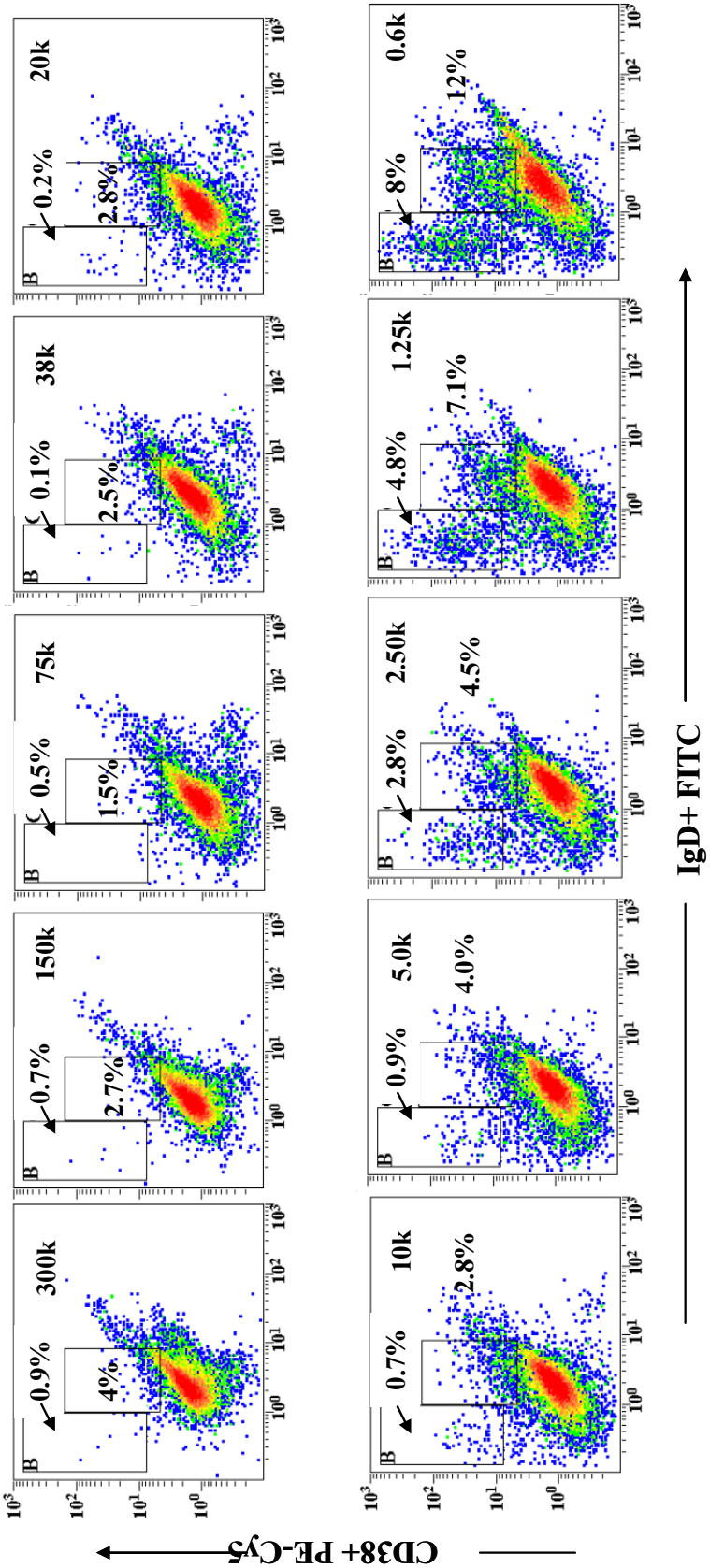
IL-21 Day 12
CD38+ PE-Cy5
IgD+ FITC
0.9%
4%
300k
0.7%
2.7%
150k
0.5%
1.5%
75k
0.1%
2.5%
38k
0.2%
2.8%
20k
0.7%
2.8%
10k
0.9%
4.0%
5.0k
2.8%
4.5%
2.50k
4.8%
7.1%
1.25k
8%
12%
0.6k

kinetics of the IL-4/antiCD40 stimulated cells seen in **Figure 46**, on day 4 there was only one data point that showed any IgE production, and that came from the wells that were plated with 20k cells per well. When supernatants from day 6 were analyzed, there are IgE found in all cell number conditions. It can also be seen that the 5ng/ml found in the supernatant has now quadrupled to ~20ng/ml. On day 8, the next time point the concentration has tripled again to ~60ng/ml IgE. When the supernatants were collected again in days 11 and 12 the concentration of IgE had risen further still, doubling again to ~120 ng/ml. There is no significant increases in IgE found in the supernatant between day 11 and 12 however, indicating that the production of IgE began to cease between days 8 and 11. The pattern of IgE production in the IL-4/antiCD40 stimulated cells indicates that IgE production can first be seen from wells that are plated at cell concentrations that are not in the lower ranges tested **(Figure 46A)**. It appears from the data that the wells that are in the tens of thousands produce earliest and greatest. However, it should be noted that although that IgE production from the lower plated cell densities is initially found wanting when compared to wells that are plated at a higher cell density, the IgE production quickly catches up and reaches nearly as high as maximal levels achieved. This indicates that there may be either a lag time in cells reaching capacity to produce IgE, or the number of IgE producing cells may initially be too low to be detected by ELISA. Another reason perhaps is that cells in the more favorable low density environment take longer to develop into better immunoglobin producing cells and it is only when that point is

Figure 46: IgE Production Kinetics from IL-4/antiCD40 IgD+ B cells. Cells from IgD+ tonsils were plated at increasing concentrations and treated with either IL-4/antiCD40 alone **(A)** or given additional stimulation of 25ng/ml IL-21 **(B)**. Supernatants were collected on days 4 (●), 6 (O), 8 (▼), 11 (▽), and 12 (■). By day 6 the IL-21 treated cells have reached the maximum IgE production that the IL-4/anti-CD40 treated cells attained. However, the low density plated cells in the IL-21 treated conditions continued to produce IgE until day 11 and reached IgE concentrations 30-fold higher than IL-4/anti-CD40 treated cells alone.

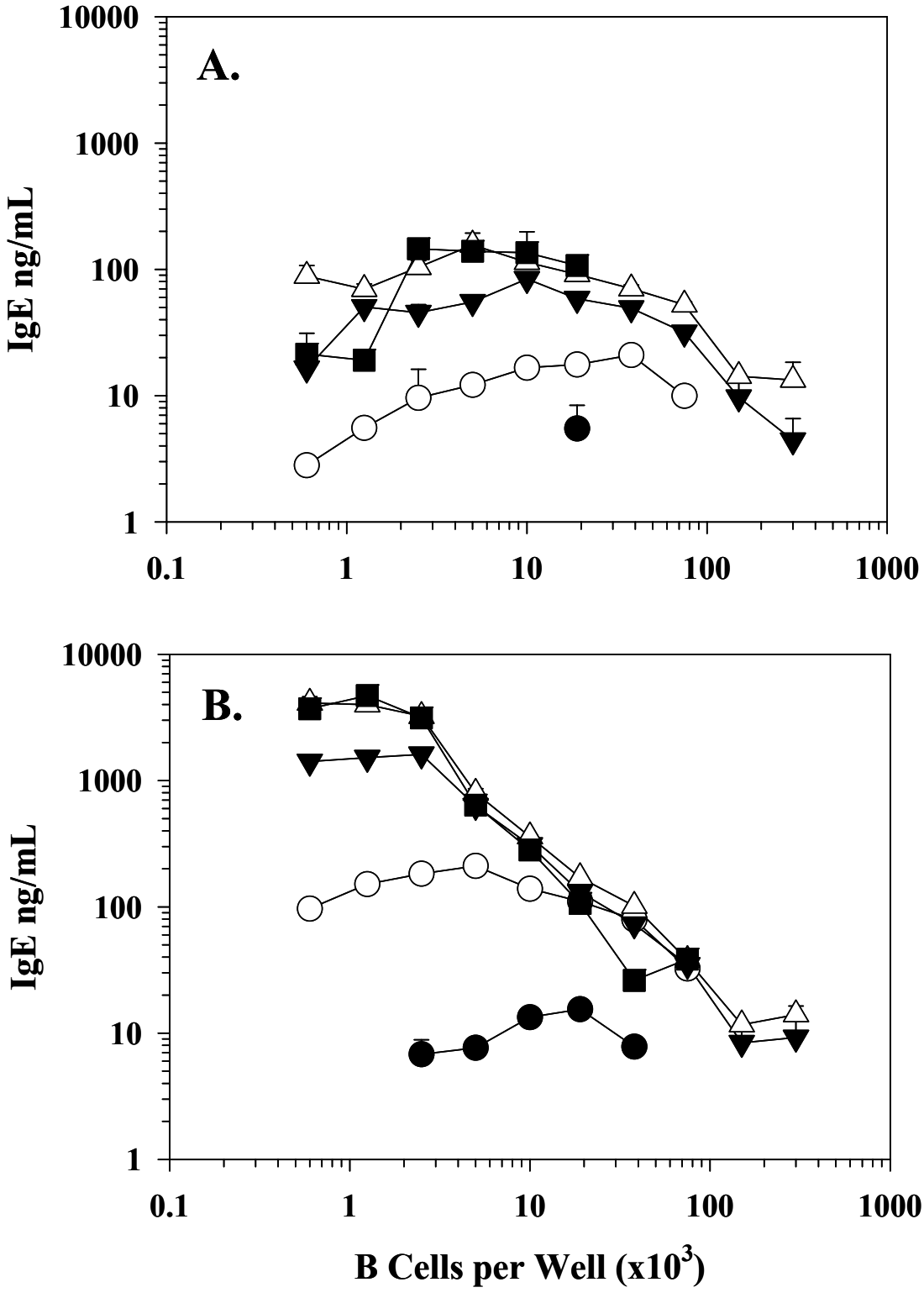
A.
B.
IgE ng/mL
IgE ng/mL
10000
1000
100
10
1
0.1
1
10
100
1000
B Cells per Well (x10^3)

reached, that their per cell IgE potential is realized and the total concentration of IgE is produced more rapidly.

Similar IgE production kinetics were also determined from cells that were additionally treated with 25ng/ml IL-21. As can be seen from **Figure 46B**, IgE could be quantified from the supernatant by day 4. Like the IgE concentrations found from the IL-4/antiCD40 data, the maximal IgE was found to be ~10ng/ml. However, 5 cell concentrations had values that could be determined as opposed to only one from the IL-4/antiCD40 conditions. It should be noted that again, like the IL-4/antiCD40 treated cells, the IL-21 stimulated cells had the greatest IgE found in the higher cell densities rather than the lower cell densities, (although not the highest). When supernatants from day 6 are analyzed, it is immediately obvious that the IgE production has logarithmically increased. If the day 4 20k cells/well IgE value of ~10ng/ml is compared to its day 6 value, the IgE concentration in the supernatant has risen 10-fold. If the day 4 5k cells/well IgE value of ~7ng/ml is compared to its day 6 value the fold increase is even greater at 30-fold. This 30-fold increase is also found at the 2.5k cells per well day 4-day 6 IgE concentration difference. This remarkable fold increase continues when day 6 IgE supernatant production is compared to day 8 IgE supernatant production. The most fold increase if found, however, from the wells at the lowest plated cell density, i.e. 0.6k, 1.25k, 2.5k. The IgE concentration from the day 6 wells was around 100-200ng/ml, and on day 8 around 1000-2000ng/ml. The values of IgE for the 5k, 10k, and 20k are all higher, but, as like the IL-4/antiCD40 conditions, their rates of increase are significantly lower than the rates of increase seen in the lower density.

On day 11 the IgE levels are still higher in the three lowest density wells, increasing another 2-fold. All other cell densities have no real significant increases, indicating that the IgE production, like that found in the production increase of the IL-4/antiCD40 stimulated cells has ceased sometime between day 8 and day 11. In the lower cell conditions, however, the production continued. From day 11 to day 12, there is no further increase in IgE concentrations found in the supernatants, indicating that these wells, too, have finally ceased to produce significant amounts of IgE.

When comparing the IgE production patterns of the IL-4/antiCD40 stimulated cells with those of the IL-21 stimulated cells, the higher cell densities reach their maximal first and then the lower cell densities' production catches up but at a significantly faster IgE production rate. In the case of the IL-4/antiCD40 cells, the lower cell density will eventually produce near similar IgE quantities as the quantities produced by the higher cell density well. In the case of the IL-21 stimulated cells, not only do the lower cell density cells produce at a faster rate than the higher cell density wells, they produced more IgE and at a significantly higher rate as well, 4000ng/ml vs. 100ng/ml and 30-fold vs. 3-fold. It therefore appears that the earliest production of IgE can be found in the higher cell densities in both the IL-4/antiCD40 stimulated cells as well as those that are additionally stimulated by IL-21. Also both stimulation conditions have the lower cell densities that produce significantly higher amounts of IgE relative to each respective higher cell density condition. With the IL-21 treated condition, however, the lower cell densities continue to produce at a significantly higher amount relative to it's higher cell density comparative.

Elispot determination of IgE production. One of the questions that remained to be answered was what was happening on the individual cell level in regards to IgE production. As evidenced previously, the maximal production of IgE depends on an optimal concentration of cells that are initially plated. This optimal amount was initially thought to be in the several hundred of thousand to up to half a million per well in a 96 well plate. The reasoning being that because so very few of the cells become IgE producers per total population, it is best to increase the population size, thus increasing the total number of cells that are producers of IgE. As it was discovered for Ig production this is not always true. The lower cell densities in fact were found to be better producers for total IgE. It was also discovered that those cells that were initially plated at lower cell densities also had more cells that had undergone significantly more divisions than cells that had been plated at higher cell densities. It remained to be seen if the cells that were plated at the differing cell densities also produced IgE at differing rates on a per cell basis. To determine this, ELISPOT was performed and the amount of IgE per cell was analyzed by CTL and the number of spots as well as the size of spots was calculated. To get a baseline for comparison, IL-4/antiCD40 cells were analyzed first, and as can be seen by the graph **Figure 47**, the size of the spots for cells at 150k (▲) and 20k (O) compared to background (+) is insignificantly different. Both conditions represented here are also representative as a whole for all other cell densities but only these two were shown for purposes of clarity. A higher cell density (150k), as well as a lower cell density (20k) were shown to cover the breadth of the ranges

involved. Background ranges of 5 spots were found in the very small side of the scale of $1*10^{-3}$ mm^2 (or -3 in terms of Square Log in millimeters) and virtually no spots that were ten times (-2 log sq. mm) larger. These spots size counts were virtually identical to the sizes found in the IL-4/antiCD40 conditions.

When the spot numbers as well as sizes are determined in the IL-21 stimulated cells it is clear that the number of spots are higher as well as spot size. Shown are background (+), 5k (■), 2.5k (□), 1.25k (♦), and 0.6k (Δ). Cells which came from higher plated cell densities (20k and higher) had similar spot sizes as those of background. Cells from 20k and 38k did have a number of spot sizes (~25) in the -2.5 to -3.0 log range but had similar spots sizes as background in the larger sizes as did background (data not shown). It should be noted, however, that the cells from the 10k well conditions produced similar spots as did background (data not shown). What is most striking is that as the cells reach the 5k cells/well the sizes of the spots begins to be found in the larger sizes (-2.4 to -1.2) and the numbers increase in the 2.5, 1.25, and 0.6 cells /well. The number of spots in the larger sizes, found in the lowest well's range, are roughly 3-fold, 6-fold,

Figure 47: A) IgE spots as determined by ELISPOT are not significantly greater in number or size as compared to background in day 8 IL-4/antiCD40 treated IgD^+ tonsilar B cells across all cell densities. Tonsilar B cells were purified using Milltenyi IgD^+ cell sorting and were then plated at decreasing cellular density titration starting from 300k per well to 0.6k cells per well. The cells were then treated with 10ng/mL IL-4, 1000ng/mL antiCD40 and incubated for days. After twelve days the cells were collected and washed to remove IgE already present in the supernatant. Cells were then plated in wells in a 96-well plate pre-coated with mouse anti-human-IgE, incubated overnight and washed. IgE content was determined by adding anti-human IgE-alkaline phosphatase followed by substrate. Shown are two conditions representative of all (▲300k/well, ○ 20k/well, + Background)

B) IgE spots as determined by ELISPOT are significantly greater in number and size as compared to background in day 8 IL-21/IL-4/antiCD40 treated IgD^+ tonsilar cells, especially in lower cell densities. Cells were purified and treated as in A) with the exception of the addition of 25ng/ml IL-21. 5k/well(■), 2.5k/well(□) 1.25k/well(♦), and 0.6k/well(▽) and background (+). Cells from wells with densities of 20k/well and 38k/well and greater, showed similar IgE spots in number (~25) but ~1 log smaller. Data not shown.

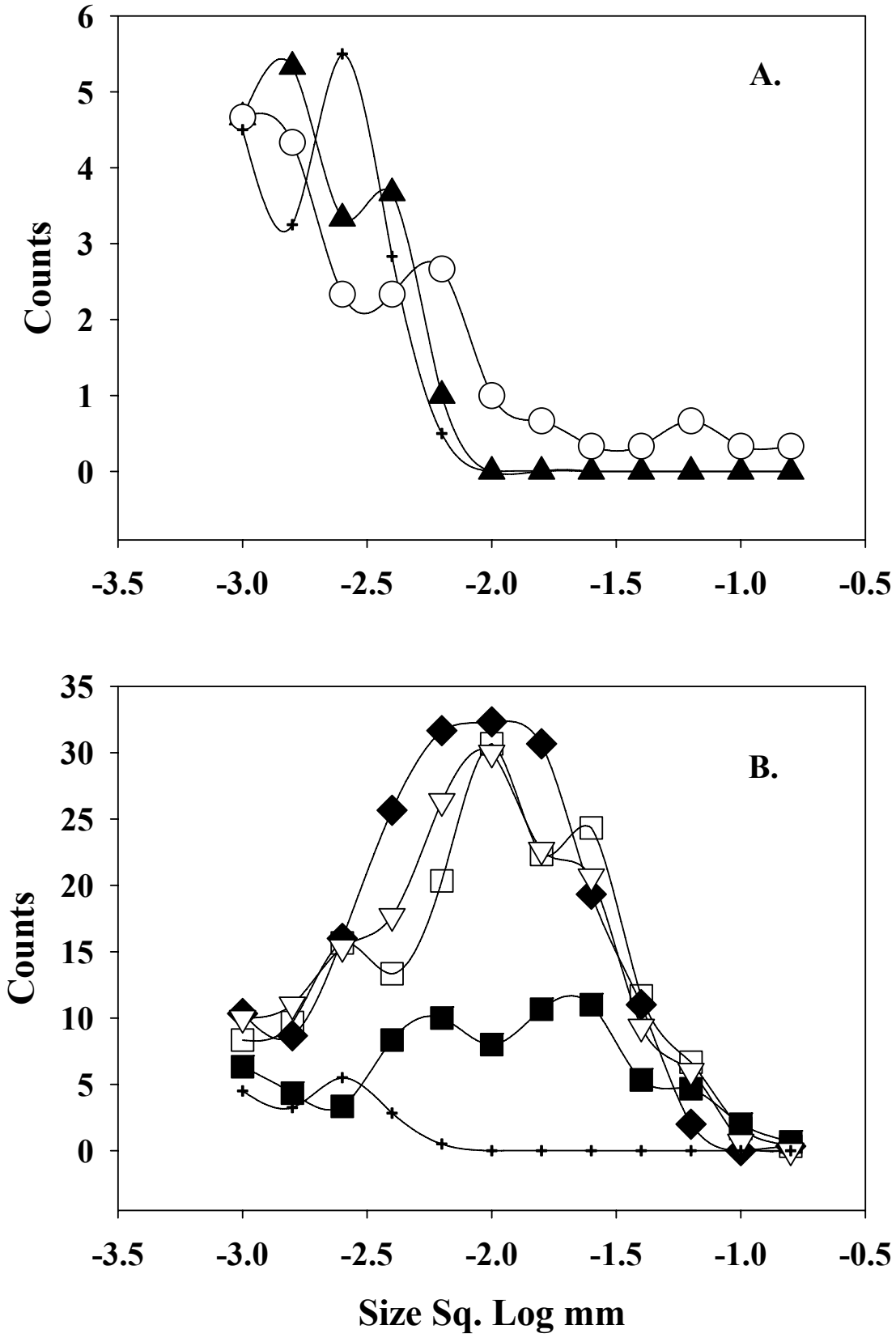
A.
B.
Counts
Counts
6
5
4
3
2
1
0
35
30
25
20
15
10
5
0
-3.5
-3.0
-2.5
-2.0
-1.5
-1.0
-0.5
Size Sq. Log mm

and 7-fold higher than the 5k cells per well for the 2.5k, 1.25k and 0.6k, respectively. The actual numbers of -2.4 to -1.2 spots are 19 spots for the 5k, and 58, 129, and 152 spots for the 2.5k, 1.25k, and 0.6k wells. These numbers are the average of three wells. This supports the possibility that a reason why the IgE production found in the lower cell wells at earlier time points can so quickly outperform the production found from wells that were plated with higher cell densities. The IgE producing cells are so much greater in number and more importantly in size at the lower cell densities that the amounts of IgE produced will quickly surpass the amounts of IgE from cells plated at higher cell densities.

As can be seen from the actual pictures of the ELISPOTS (**Figure 48**) the cells were plated in triplicate for each cell density. Both the IL-4/antiCD40 stimulated cells as well as the IL-21 stimulated cells had good spot generation as seen on day eight (**A**) but only the IL-21 stimulatory conditions were still producing IgE of any significant amounts by day eleven (**B**). By the 38k cell per well condition in the IL-21 stimulated cells there is significant IgE spot development seen. However it should be noted that the spot size is much smaller than the IgE spot size seen in the lower density wells. This was addressed previously regarding Fig.17 as data not shown in graphical representation, but upon visual inspection the IgE spots in the 38k/well and 20k/well is easily seen. It should also be noted that the spots in the IL-4/antiCD40 conditions on day eight in the 10k/well triplicate are significantly larger than any other spot size across any other density in the IL-4/antiCD40 conditions. This is interesting when compared to the graphical representation in **Figure 47**, where the values generated by

the analysis program washes out the spots in the calculations. It is unusual that only the one condition, seen in that one cell density, should have the larger spots seen, like those seen in the IL-21 low density conditions. There is one large spot seen in the 5k/well conditions in the IL-4/antiCD40 conditions and none in any of the triplicates in the 2.5k/well. However, there is the re-emergence of the presence of large spots seen in the 1.25k/well triplicates in the IL-4/antiCD40 conditions. The presence of the large spots in the lowest densities was unexpected when compared to the general phenomenon of IgE

Figure 48: IgE production as determined by ELISPOT is greatest in lower cell densities in IL-21 treated IgD$^+$ tonsilar cells, is produced in greater amounts than IL-4/antiCD40 only treated cells, and is produced for a longer time. IgD$^+$ cells were purified from tonsilar cells using positive selection anti-IgD$^+$ microbeads. Cells were then plated in triplicate at 300k cells per well and titrated to a low of 0.6k cells per well. Cells were then treated with IL-4/antiCD40 +/- IL-21 for either **A)** Eight days or **B)** Eleven days. Cells were then collected, pooled, and washed and plated again in fresh media containing original stimulating conditions of either IL-4/antiCD40 with or without IL-21 on Millipore ELISPOT 96-well plates overnight at 37˚C. Cells and unbound IgE was removed by washing after 16 hours and read on an ImmunoSpot CTL ELISPOT reader.

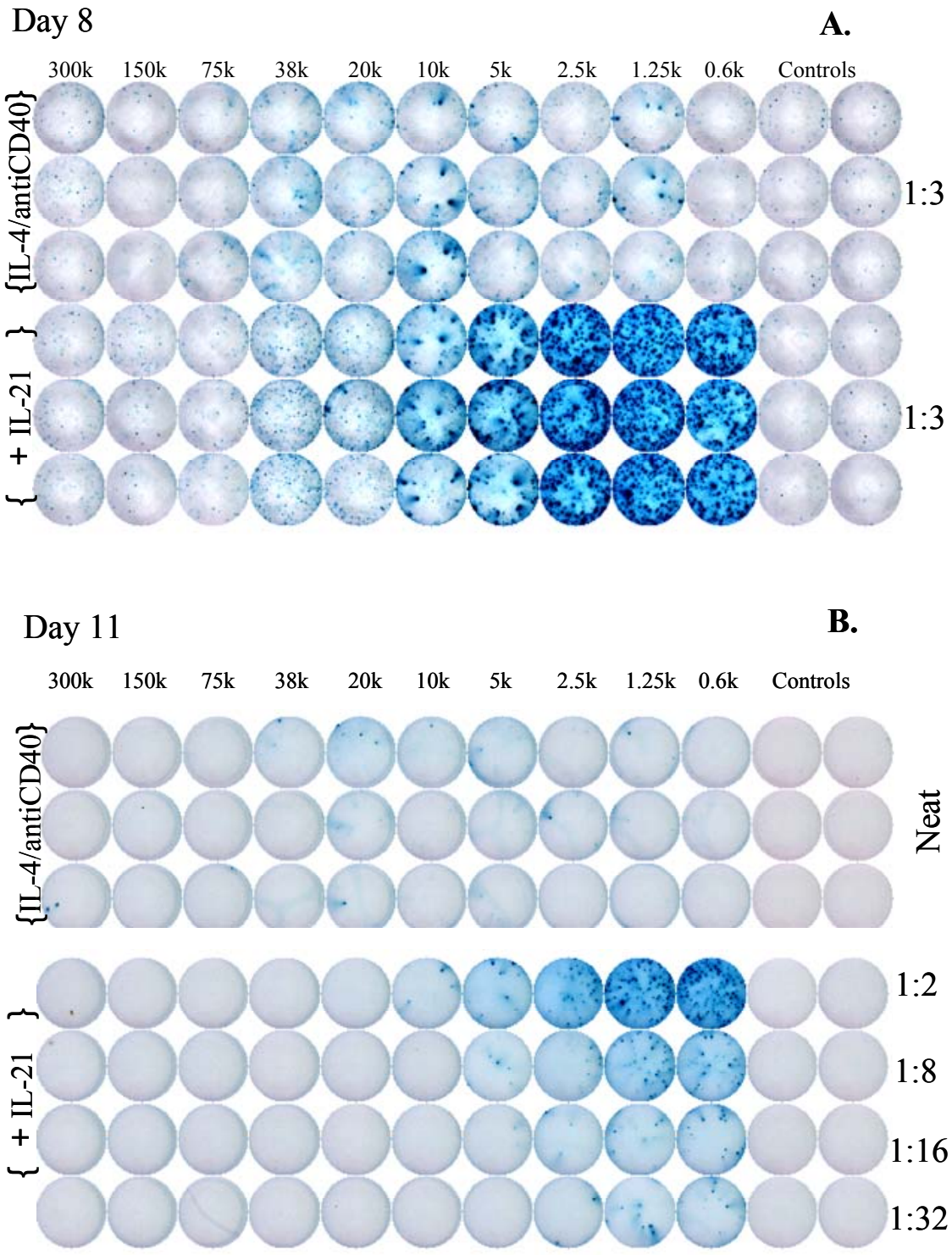
Day 8
A.
300k
150k
75k
38k
20k
10k
5k
2.5k
1.25k
0.6k
Controls
{IL-4/antiCD40}
{ + IL-21 }
1:3
1:3
Day 11
B.
300k
150k
75k
38k
20k
10k
5k
2.5k
1.25k
0.6k
Controls
{IL-4/antiCD40}
{ + IL-21 }
Neat
1:2
1:8
1:16
1:32

production in IL-4/antiCD40 stimulated cells. Generally the IgE production in IL-4/antiCD40 stimulated cells is greater in the higher cell densities.

In the IL-21 treated cells the presence of the number of spots increasing is dramatic as the original plated densities decrease. It is also striking how the number of spots is rapidly increasing as the cell densities decrease, becoming readily apparent by 38k/well. It is also noteworthy that not only are the numbers of the spots increasing but also the sizes are increasing as well. This indicates that the IgE producing B cell numbers are increasing in both absolute quantity as well as the absolute increase in IgE production per cell as well. Finally it can be seen that by day eleven the cells stimulated by IL-4/antiCD40 alone have stopped producing IgE in any significance as seen by the absence of spots of any great number. There are a few wells with single spots seen in the 38k/well to 5k/well. It should be noted that the cells that were plated on the Elispot plate were plated at original, or neat, concentrations, whereas the cells from the IL-21 stimulated conditions started at dilutions of 1:2 and were diluted down to 1:32. It is clearly seen that there remains a robust production of IgE producing cells even on day eleven in the IL-21 stimulated cells. Again, it the IgE seen is found at the highest concentrations in the lowest cell densities.

DISCUSSION

Allergy cases in the US continue to rise. There are many therapeutic approaches which alleviate the conditions brought on by IgE which is reactive to innocuous particles, such as pet dander, pollen, and dust mite antigens. One strategy to reduce allergic symptoms is to block the IgE from binding to the FcεRI by using anti-IgE antibodies [90;91]. This has been found to be clinically effective and is currently an available treatment. Since the anti-IgE therapy does not reduce IgE synthesis [91], there must be near total blockage of the IgE binding, since granule release requires cross linking of as few as ten basophil- or mast cell-bound IgE molecules. An approach aimed at removing IgE from the serum was employed. The role of CD23 in the regulation of IgE by limiting IgE synthesis and thus arriving at a good understanding of the mechanisms involved in the isotype switch to this antibody class.

One of the approaches that I used was to utilize a chimeric CD23 protein that had been coupled to a leucine zipper and analyzed the functionality of the stalk region for binding to IgE. As I discovered the stalk region is indeed required for effective binding to the IgE molecule. It was previously determined that the structure of the CD23 molecule which had been generated in this lab from data using a mouse model, and was hypothesized to exist in preformed trimeric form. My data using anti-stalk antibodies suggested that at the different temperatures the exposure of epitopes became more available to the antibodies at higher temperature at roughly 2-3 fold higher at 37ºC than at 4ºC. As evidenced in **Table 1**, the antibodies that had the greatest increase in binding were also those that had some of the greatest effects on IgE inhibition in IL-

4/antiCD40 stimulated cells, particularly the RAS1. But as was also shown this ability to bind and inhibit IgE binding to the CD23 when in the presence was not always consistently compatible with my observations that the effects of the anti-CD23stalk antibodies had on mitigating the IgE production. In some cases the addition of anti-CD23stalk antibodies caused an increase in IgE production and in others a decrease in IgE production.

Although my original intentions were to move away from the polyclonal antibodies from the rabbit (RASs), it was the rabbit antibodies that were more consistently inhibiting the production of IgE, as compared to the more variable results from the monoclonal antibodies. However, this greater and more consistent inhibition was determined to be largely due to the presence of the Fc portion of the antibody itself, for, as soon as it was removed by enzymatic degradation, and only the $F(ab')_2$ fragment was used, the inhibition of IgE production was lost. This implicates the role of the IgG inhibitory receptor CD32, FcγRIIb, in mediating the response of the B cell in the presence of the anti-CD23stalk antibodies. While the role of FcγRIIb seems to be strongly implicated in reducing IgE secretion, the addition of RAS1 and RAS2 also in increased sCD23 in the supernatants. This suggests that my original hypothesis that the exposure of the CD23 proteolytic cleavage sites to the CD23 sheddase may still play a role in controlling the IgE response. It is likely that the inhibition seen due to the RAS involves both the CD23 molecule as well as another (possibly the inhibitory FcγRIIb) as rabbit isotype controls did not inhibit the production at all. As the rabbit isotypes were not human absorbed against human antigens one can conclude that the IgG isotypes

would interact equally well with any surface antigen as the anti-CD23stalk rabbit antibodies would. This suggest that in the RAS system there is perhaps a capping of a FcγR (perhaps FcγRIIb) as well as the CD23 molecule that is responsible for the inhibition.

My work with the mouse monoclonal antibodies was very encouraging. It appeared that I had antibodies that would be theoretically targeting different portions of the stalk region and producing opposite results. However, I soon discovered that regardless of the source of the B cell, be it $CD19^+$ B cells from PBMC or naïve IgD^+ B cells purified from tonsils, the addition of the mouse monoclonal antibodies was yielding inconsistent results (**Table 2**). This suggested that the results were probably donor variable as the antibodies remained the same. Many experiments were repeatedly performed, yet the pattern of what was responsible remained out of reach when I started encountering difficulties in generating IgE from my normal methodologies. (However, after the successful results from the series of studies that I did after this, it would be interesting to revisit this area of monoclonal IgE modulation.)

As both rabbit and mouse IgG antibodies can interact with the human Fcγ receptors, and that the loss of the Fc fragment from pepsin digestion also resulted in the loss of rabbit anti-CD23stalk effect, I was surprised when an increase in IgE was shown. This indicates that the inhibitory effect seen with the polyclonal rabbit antibodies was present and dominant, and that for unknown reasons the mouse monoclonal antibodies did not have the same inhibition. As there were two effects seen regarding the presence of the RAS, that is both a Fcγ element as well as a sCD23

increase, it would appear that the IgE synthesis inhibition effect would be dominant over the sCD23 effect which has been reported to promote B cell differentiation to plasma cells [92] as well as promote IgE synthesis [38;44]. The isotype of the mice cannot be the determining reason to explain the differences between some IgE synthesis increases and some IgE synthesis inhibition as all mouse anti-CD23stalk antibodies are IgG1.

In addition, there have been Biacore binding analyses that have determined that although the binding of all antibodies but mouse anti-CD23stalk#23 share a common region of binding as mouse anti-CD23stalk#18, because both mouse#23 and mouse#18 cause consistent enhancement (see **Table 2**) and did not have within the same experiments both enhancement and inhibition. It is therefore a possibility that the binding of the mouse antibody to the gamma receptor for the mouse is not as strong as the binding of the rabbit Fc is to the gamma receptor. (This hypothesis is largely supported from conversations with Dr. Mark Hogarth Director of Research, University of Melbourne, Australia). This could make it likely that the strong negative signal of the FcγRIIb is not present in the mouse anti-CD23talk experiments, allowing only for the sCD23-CD21 binding to occur leading to an increase of IgE secretion. However, during the many experiments that were being performed, the levels of IgE being produced was consistently low and efforts were focused on increasing the IgE production from a baseline of IL-4/anti-CD40 stimulated cells. Therefore sCD23 levels from supernatants were not tested, so the hypothesis to explain the increase in IgE secretion from IL-4/anti-CD40 stimulated cells due to an increase in sCD23 levels, as well as performing

$F(ab')_2$ was not performed. I have put forth a model that may possibly explain that data that has been produced. As can be seen from **Figure 49**, there are two proposed mechanisms that have been observed to produce either a decrease in IgE synthesis (**Figure 49a**), or an increase in IgE synthesis (**Figure 49b**). From my data that has been produced using the rabbit antibodies both intact (**Figure 50a**) and enzyme digested $F(ab')_2$ fragments (**Figure 50b**), I propose that the greatest contribution is from the FcγRIIb inhibitory receptor, for any effects that were observed were lost once the Fc fragment was removed. My observations in mice would also suggest that the presence of the Fc fragment found on the intact mouse IgG1 ant-CD23stalk antibody has a lower affinity to the human FcγRIIb receptor than does the polyclonal RAS antibodies. Therefore it is possible that the strong negative signal that is seen in the rabbit antibody model is not present in the mouse antibody model. This make it possible for the soluble CD23 that I believe is produced in the mouse antibody model to bind to the CD21 and cause the increase in the IgE that is seen. Due to those difficulties in IgE production, however that I mentioned above, I switched gears somewhat and concentrated on optimizing human *in vitro* IgE production. Re-examination of the effects of the antibodies on optimized cultures has yet to be done. Based on an initial report that indicated IL-21 would enhance B cell proliferation, we decided to test this cytokine for enhancement of IgE production. While these studies were in progress, several reports appeared showing that IL-21 could enhance IgE production. Subsequent to these studies, I expanded my studies to examine the influence of cell proliferation and the

dual addition of IL-10 on human *in vitro* IgE production. As I was unable to obtain IL-21 commercially, I cloned via RT-PCR as discussed above.

Once I generated and collected the supernatants from the HEK293T cells, I established that cytokine was indeed IL-21 by functional assays and IL-21 neutralizing assays using an IL-21 chimera. As stated earlier, *in vitro* IgE studies in the human system had been hampered by the low production levels. In the mouse *in vitro* system IgE production is in the μg/ml, whereas in the human, IgE levels are usually in the upper picogram to nanogram levels per ml. Therefore I sought to determine a set of conditions that could be used to induce maximal IgE production in the human *in vitro* model. Cho et al [69] found that the level of mouse IgE produced *in vivo* was cell density dependent, and further examination of the cell density phenomenon indicated that the number of cell divisions was the most likely explanation for the increased IgE production [70]. A series of studies, primarily by the Hodgkin laboratory [71;72;75;76] demonstrated that increased murine cell division correlates with higher levels of IgE and to some extent, IgG production after appropriate *in vitro* stimulation. One of these studies examined the relationship between cell division number and IgG production using human B cells [75]. However, IgE was not examined, presumably due to the low amounts of IgE produced. One of the newest members of the hematopoietic cytokine family is IL-21 and indeed this is the most recent cytokine that uses the $gamma_c$ chain as part of its receptor. Although the initial report of IL-21 demonstrated its ability to co-stimulate human B cell proliferation [53], the major focus of research into IL-21 functions has revolved around NK and CTL activation, especially involving tumor

progression [93-95]. As mentioned in the introduction, recent reports have shown that IgE production is enhanced using the human *in vitro* culture model [32;48]. Several studies in mice, however, have indicated that IL-21 may be beneficial in inhibiting Type I allergic disease. IL-21Rα$^{-/-}$ mice exhibit normal lymphoid development, but have elevated serum IgE levels [55]. In addition, treatment of BALB/c mice with IL-21 inhibited antigen specific IgE production as well as eosinophil recruitment into airways [57]. In addition in this same study, IL-21 was shown to inhibit *in vitro* IgE production induced by LPS and IL-4, albeit at a single cell concentration. So as a parallel study I wished to examine the role of IL-21 in mice.

A cell density-dependent relationship to human IgE production is also seen when IL-21 is used in conjunction with IL-4 and anti-CD40 (**Figure 25**). Interestingly, IgG and IgM production levels are also cell density dependent when both IL-4 and IL-21 are added to anti-CD40 stimulated B cells (**Figure 26**). Confirmation that increased cell division is occurring is shown in **Figure 28** with CFSE labeled B cells, seen both with lower cell numbers compared to higher cell numbers, and with the addition of IL-21 to the IL-4/anti-CD40 cocktail providing even greater divisions. The increase in cell divisions of cells plated at lower cell densities seems to indicate that these cells continue to divide beyond day four when the proliferation studies were conducted (**Figure 22**), but is not simply due to nutrient depletion as seen in **Figure 27**, whereas

Figure 49: Proposed mechanisms that show increase and decreases in IgE production in B cells. Models that have been proposed to show increase and decreases in IgE production involving CD23 and IgE (**A**) and soluble CD23 and CD21 (**B**). The small carboxyl terminus that is intracellular on the CD23 has been proposed to contain an inhibitory tyrosine motif (ITIM) It is possible that a bound IgE-antigen complex is negatively signaling via the CD23 molecule, stopping further IgE synthesis. It has also been proposed that the absence of antigen-IgE complexes bound to the CD23 molecule allow the molecule to more freely move, enabling the protease to access the cleavage sites accomplishing a loss of inhibitory signaling that would occur via the CD23 molecule as well as provide a stimulatory signal that would occur with the interaction of CD23-CD21

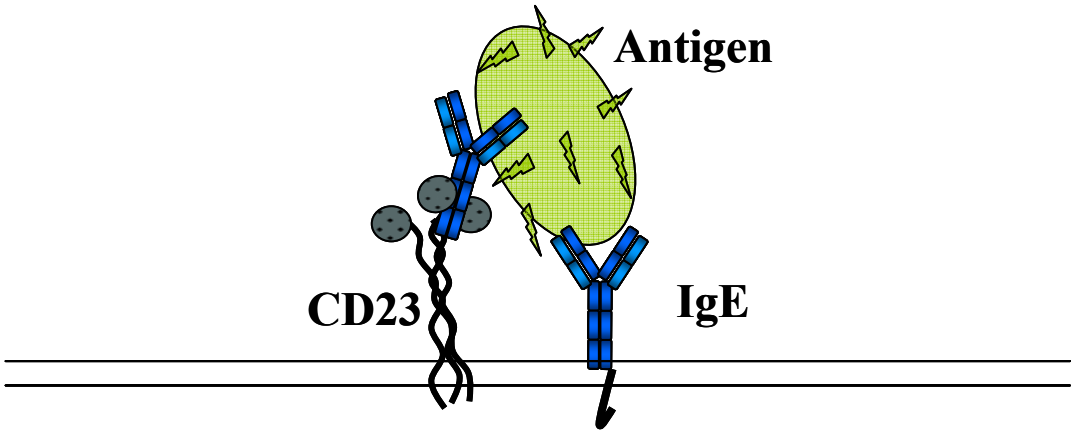

Decrease in IgE Synthesis

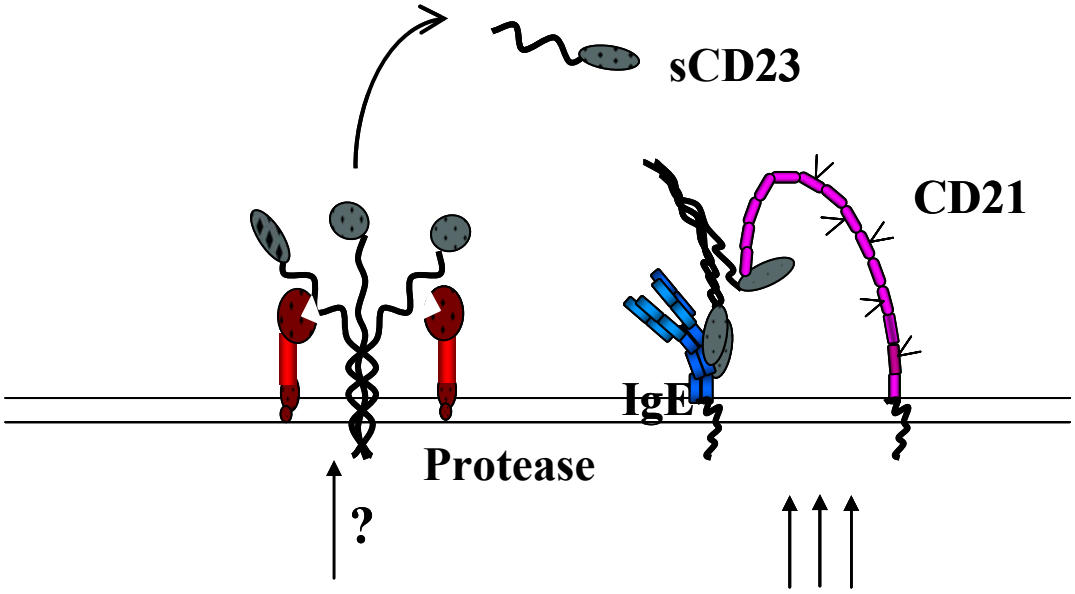

Increase in IgE Synthesis

Figure 50: Intact anti-CD23stalk IgG antibodies provide a dominant inhibitory signal via the FcγRIIb inhibitory receptor that is lost when the Fc portion of the antibody is removed. A proposed mechanism to explain the decrease in IgE production and increase in sCD23 using intact rabbit (RAS) anti-CD23stalk antibodies (**A**) and an increase in IgE production using $F(ab')_2$ RAS is the contribution of the FcγRIIB inhibitory receptor. In **A** the sCD23 is found to be increased possibly providing a stimulatory signal for IgE production. However, the net result is IgE inhibition, suggesting a dominant and overriding signal through the FcγRIIb using intact antibodies (**A**). The dominant signal is subsequently lost when the Fc is removed and interaction with the FcγRIIb is prevented and only the positive, enhancing signal of IgE remains (**B**)

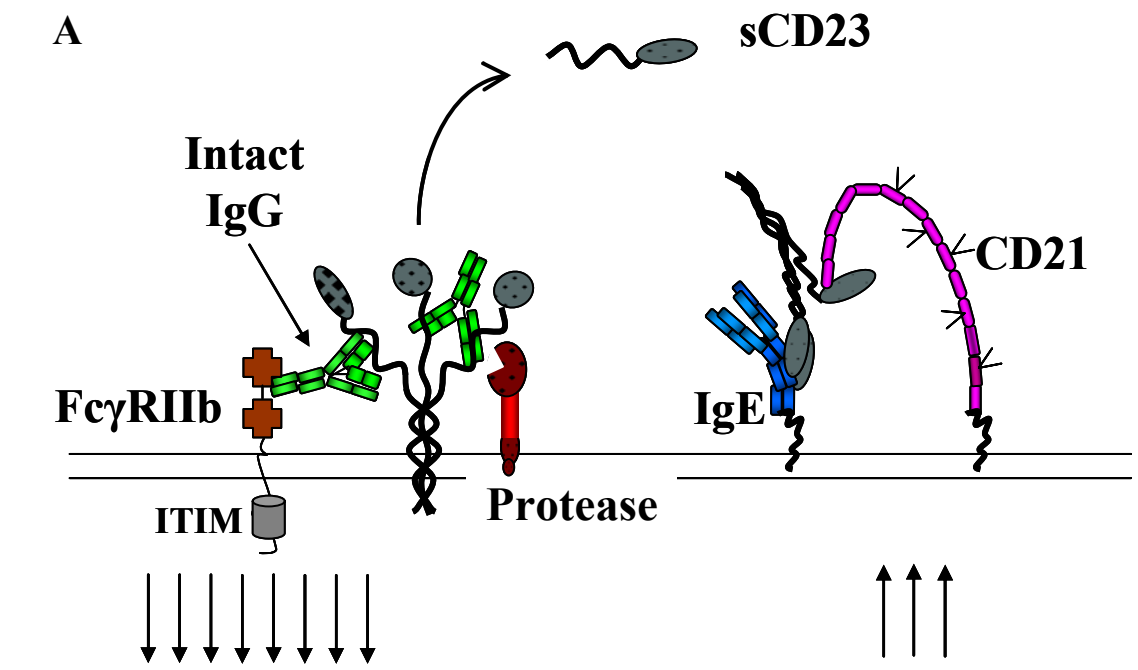

Decrease in IgE Synthesis

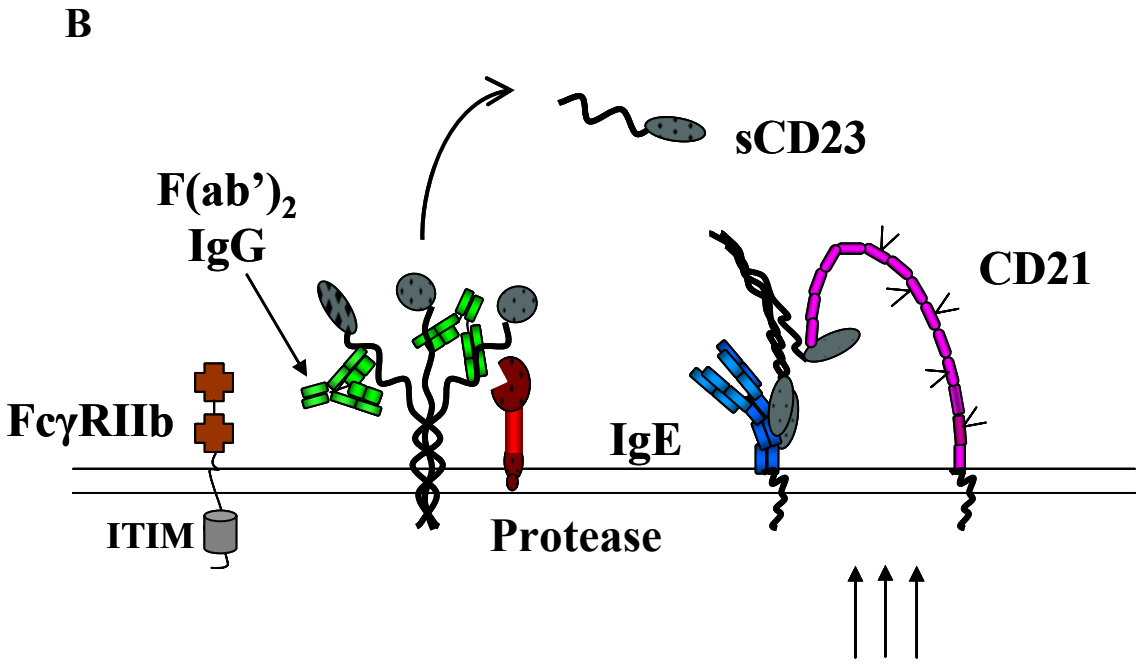

Increase in IgE Synthesis

the cells plated at higher cell densities stopped dividing and thus never reached and IgE division producing threshold number of divisions. Our lab has shown previously that the higher number cell divisions at the lower cell densities relative to higher cell densities cannot be explained due to depleted nutrients and is likely due to increased apoptosis [70]. The human IgM results were somewhat surprising, since in the murine system, IgM production is directly proportional to cell numbers; the more cells added the greater IgM yield [70]. This indicates that in the human *in vitro* system, increasing B cell densities beyond a relatively low ($5x10^3$ cells/well) cell concentrations, results in decreased antibody production per cell, compared to maximal antibody production seen at lower cell densities. This even holds true in the absence of isotype switching, as exemplified by IgM.

In the previous study correlating cell division with human IgG production [75], the highest level of IgG production was seen when IL-4 was used in conjunction with IL-10. IL-10 had not previously been tested in conjunction with IL-21, with regard to cell division. I observed that the addition of IL-10 to IL-4/anti-CD40 stimulated cells increased both IgE production (**Figure 30a**) and cellular division (**Figure 30b**). And as the addition of IL-10 to IL-21/4/anti-CD40 treated cells also increased IgE, I anticipated that there would be a corresponding increase in cellular division, when both cytokines were used. However, no further increase in cellular division was seen (**Figure 32**). This may be partially explained as it has been shown that IL-10 is involved in plasma cell differentiation [96;97]. Interestingly, cell division, as exemplified by reduced CFSE MFI, reaches the same limit seen after the addition of the highest dose of IL-21

(**Figure 32**). In the case of the two cytokines used, 50ng/mL IL-21 was able to reach this division limit while the highest dose of IL-10 (100ng/mL) was not. Additionally, the MFI at all IL-21 concentrations could not be further lowered even with the additional stimuli of IL-10 added. A logical explanation is that the increase in IgE is due to an increase of IgE per cell, induced by IL-10, without increased cell division. It has been shown that BLIMP-1 [98;99] is involved in plasma cell differentiation, and that AID is involved in CSR [100]. IL-21 has been shown to be able to induce differentiation in human naïve cells [101] and while this work was in progress IL-21 was shown to induce differentiation of B cells to a greater extent than IL-10.

Another possibility is there could be additional divisions and IgE production occurring after day 8 when the CFSE analysis occurred and day 14 when the supernatants were collected and analyzed for IgE. The reduced viability after day 8 made CFSE studies difficult and thus, I feel this is an unlikely explanation.

Since IL-10 has previously been used in the *in vitro* human IgE synthesis models, I wished to determine the relative efficacy of IL-10 *vs.* IL-21 and whether the combination was synergistic. As can be seen in **Figure 29** and **Figure 31**, synergy was seen with PBMC and with purified B cells. Note that the production of IgE due to IL-21 was consistently higher than IgE from IL-10. Correspondingly, IL-21 also caused a greater increase in cell division than was seen with IL-10 alone, both with PBMC and purified IgD^+ tonsilar B cells. When the two cytokines were combined and added to IL-4/anti-CD40 stimulated cells, a further increase in IgE was seen; the increase was synergistic rather than additive. As discussed above, this synergistic increase in IgE

occurs without additional cell division. It is possible that the increase in antibody synthesis is due to an increase in cellular differentiation of B cells to Ig producing non-dividing plasma cells.

Studies in the murine system have shown that IL-21 has an inhibitory effect on IgE production, both *in vivo* and *in vitro* [55;57]. Since the published studies *in vitro* used a single, relatively high, cell density, the effect of IL-21 on mouse B cells was re-examined as a function of cell concentration. Consistent with other reports [53], I confirmed that IL-21 enhanced the proliferation of mouse B cells stimulated with CD40LT and IL-4, and an optimal amount (based on proliferation) of IL-21 was added to increasing concentrations of mouse B cells. As shown in **Figure 33a**, addition of IL-21 shifted the peak of maximal mouse IgE production to lower cell densities. Mouse IgG_1 production was also marginally increased at lower cell densities (**Figure 33b**); IgM levels (**Figure 33c**) were minimally influenced by IL-21 addition, and remained proportional to cell density, as reported for IgM with CD40LT and IL-4 stimulated cells [70]. The lowest cell densities analyzed in the mouse model are of particular interest; as IgE levels were enhanced at these cell densities. Indeed, when IL-21-mediated influence on IgE production is plotted against their respective cell densities, both the human and mouse *in vitro* systems give a quite similar pattern (**Figure 35**). Thus, a primary difference in the two systems is that optimal IgE production is seen in the mouse at lower cell densities. Depending upon the cell density being examined, IL-21 can cause both enhancement and inhibition of IgE synthesis in both the human and mouse *in vitro* systems.

There have been recent reports that address the requirement of the transcription factor Pax-5 modulation required to maintain the differentiation of B cells. It was shown that B cells in Pax-$5^{-/-}$ mice were arrested at an early pro-B cell stage in the bone marrow [102], and are also multipotent and can generate T, NK, and myeloid cell types. It was also shown that in committed pro-B cells that had the conditional Pax-5 deletions, they could revert to the multipotent state from which T cells and macrophages could be generated [103]. Busslinger *et al.* demonstrated that Pax-5 required for B cell lineage maintenance [104]. Delogu *et al.* has recently shown that the Pax-5 gene repression is required for blood cell homeostasis. It is however, reversed in plasma cells [105] and its loss promotes plasma cell differentiation [106].

However, the results that have been shown throughout this work is that clearly considerable amounts of IgE are being produced when IL-21 is added to IL-4/atniCD40 stimulated cells; but according to Ettinger {87} while there was an increase in Blimp-1 expression to about 5-fold higher than with the addition of IL-21 to anti-CD40 stimulated cells, it actually decreased with the addition of IL-4 to only ~3-fold. In addition, when comparing the CD38 expression levels of IL-21/anti-CD40 and IL-21/IL-4/antiCD40 treated cells there is no change in CD38 expression. This is in contrast to my results where the $CD38^{+}$ expressions are clearly increased (**Figure 43 and Figure 45**) in day 6 and day 12 of IL-21 treated IL-4/anti-CD40 stimulated cells. However, this increase in expression is most readily seen in the lower cell densities of my results, and not readily seen in the higher cell densities. It has been argued that the results from the addition of IL-21 to anti-CD40/anti-IgM result in the terminal

differentiation of human B cells to non-dividing Ig secreting B cells [101]. However, this terminal differentiation is dependent and prevented, on the actions of IL-4 when the conditions are IL-21/IL-4 and antiCD40 as proposed by Ettinger {87}. I would propose that IL-21addition, especially under low cell density conditions, results in enhanced terminal plasma cell differentiation. This is especially striking when compared to the IL-4/antiCD40 cells of **Figure 44**. I anticipate that one would find a decrease in Pax-5, and an increase in Blimp-1 as well as XBP-1 and AID, again, especially in low cell density cultures. Also intriguing are the spots of IgE producing cells of **Figure 48**. When the IL-21 treated cells are compared to the IL-4/antiCD40 alone cells, it is clear that the IL-21 treated cells are still producing considerable amounts of IgE on day 11. It is equally obvious that the IL-4/antiCD40 treated cells are not, this is again supportive of plasma cell production.

There are three distinct stages of plasma cell development [63] involving short lived plasma cells living only 3-5 days [107] in the first week of exposure to antigen. Some plasma cells also enter a germinal center pathway where they are involved in somatic hypermutation, and production of memory cells and are generally long-lived [108]. The third distinct group of plasma cells are those that are considered to have left the germinal center and produce high affinity antibody and reside in the bone marrow [109].

It is likely that the addition of IL-21 to the IL-4/antiCD40 treated cells are both stimulating the cells and providing them with anti-apoptotic signals such as the Bcl2 anti-apoptotic member A1, which is important for the survival capacity of activated B

cells [110] as well as NF-κB activation-dependent expression of A1 to protect germinal center B cells from receptor-ligand induced apoptosis [111;112]. Although the NF-κB induced A1 expression was shown to go through the CD40/NF-κB pathway and has yet to definitively determined to be involved in the IL-21 pathway it remains an interesting avenue for discovery. In addition, it has been argued that there is a superabundance of immunoglobin heavy and light chain increases during the differentiation of plasmacytic cells, both due to increased transcription as well as mRNA stability [113].

As there can be both non-terminally differentiated Ig producing plasmablasts as well as fully terminated Ig producing plasma cells, a possible explanation for IgE level production differences, both in quantity in the numbers of IgE producing cells as well as total amount of IgE produced per cell, between the IL-4/antiCD40 stimulated cells, both high and low density, and the cells treated with the additional stimuli of IL-21, may lie in the fact that there is a greater number of fully differentiated terminally divided plasma cells in the low density IL-21 treated cells as compared to IL-4/antiCD40 treated cells alone. Further studies that could examine this hypothesis is the determination of c-Myc or cyclin E expression levels, whose presence prevents terminal differentiation and are required to be repressed [114] . In addition, one could also look at the cdk inhibitor $p18^{INK4c}$, as this had been shown to be required for cell cycle arrest in IL-6-dependent plasmacytic differentiation [115]. This could be potentially relevant as in addition to IL-21, IL-6 has previously been shown to play an obligatory role in IL-4 induced IgE synthesis [39;116].

X-box binding protein (XBP-1) has been shown to be essential for the differentiation of plasma cells [117]. Its discovery provided a link to the observation that the unfolded protein response (UPR) which was observed with the massive accumulation seen in the endoplasmic reticulum when plasma cells increased the Ig output. It has been shown that IL-4 alone can induce the expression of XBP-1. Interestingly when anti-CD40 and IL-4 stimulate the B cells the amounts of XBP-1 spliced protein is maximal for the required Ig secretion. This protein would be of interest in the study of the cell density effect due to the results that have shown increased Ig secretion at the lowest cell densities when stimulated with IL-4/IL-21 and anti-CD40 because others have observed that IL-4 can prevent the actions of IL-21 in IgE synthesis [57] and differentiation of cell differentiation [101]. It is to be noted, however, that the results presented here do support the data of others in regards to higher cell density but also demonstrate that the considerable increases in differentiation markers in B cells stimulated by the BCR, also seem to be found in cells that have been stimulated via the CD40 and IL-4 T cell-dependent manner when at low densities.

Overall, the data suggests that IL-21 may be acting as a survival stimulus depending on the stimulus received, especially at the lower cell concentrations, allowing the high level of cell division needed for IgE production to occur in addition to the signaling necessary for plasma cell differentiation (**Figure 51**). In the proposed model, IL-21 generates more cells that ultimately arrive at a fully terminally differentiated plasma state, that produce more IgE per cell, and do not have the IL-4 inhibitory effect when the cells are plated at such cell density. This provides greater

surface expression of plasma cell markers such as CD38 and modulation of transcription factors such as Bcl-6, Pax-5, Blimp-1, and A1.

Finally the synergy of IL-10 plus IL-21 on IL-4 and anti-CD40 stimulated human B cells provides an interesting avenue for examining the relationships between the two cytokines and the cell signaling pathways. This data provides an important and novel system in which to investigate the mechanism of IgE production and regulation in both model systems.

Figure 51: Addition of IL-21 to IL-4/antiCD40 stimulated cells induces greater proliferation and differentiation of the B cell. In this propsed model it is suggested that the massive increase in cell surface marker CD38 found at the lower cell densities in IL-21 stimulated cells demonstrates that the greatest differentiation is due to modulation of transcription factors responsible for terminally differentiated plasma cells. The cells are longer lived and produce more Ig per cell, the most differentiated cells are found at the lower cell densites.

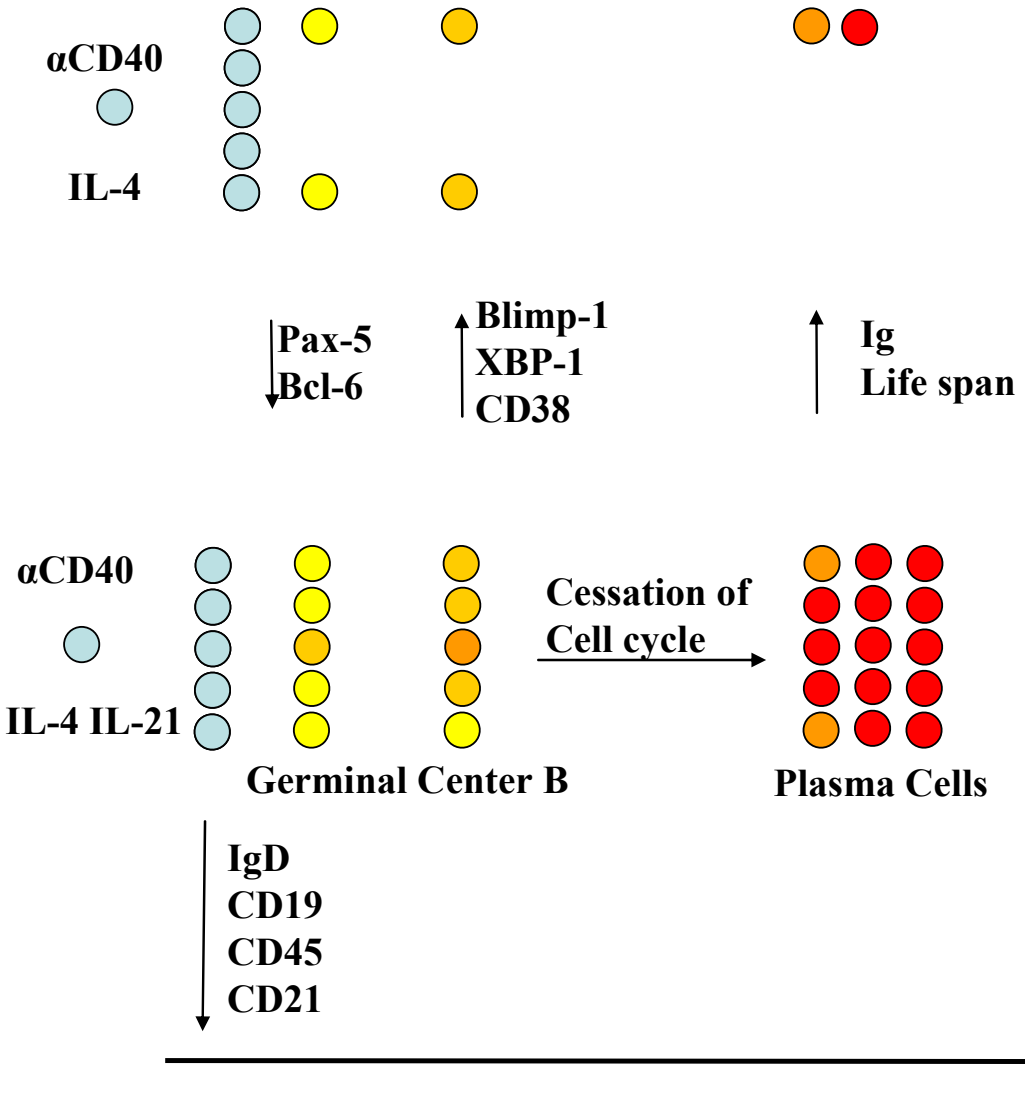
αCD40
IL-4
Pax-5
Bcl-6
Blimp-1
XBP-1
CD38
Ig
Life span
αCD40
IL-4 IL-21
Cessation of
Cell cycle
Germinal Center B
Plasma Cells
IgD
CD19
CD45
CD21
Differentiation to Plasmablasts and Terminal Plasma Cells
Naïve Mature B
Early Germinal Center B
Late Germinal Center B
Dividing Ig-Secreting Plasmablast
Non-Dividing Ig-Secreting Plasma Cell

Bibliography

Bibliography

1. I. Asher, C. Baena-Cagnani, A. Boner, Canonica GW, Chuchalin A, Custovic A, Dagli E, Haahtela T, Haus M, Hemmo-Loten M, Holgate S, Holloway J, Holt P, Host A, Iikura Y, Johansson SGO, Kaplan A, Kowalski ML, Lockey R, Naspitz C, Odhiambo J, Ring J, Sastre J, Schafer T, Venables K, Vichyanond P, Volovitz B, Wahn U, Warner J, Weiss K, and Zhong NS, World Allergy Organization Guidelines for Prevention of Allergy and Allergic Asthma, Allergy Clin Immunol Int-J World Allergy Org. 16 (2004) 176-185. Ref Type: Abstract

2. C. L. Kepley, F. T. Lauer, J. M. Oliver, and S. W. Burchiel, Environmental polycyclic aromatic hydrocarbons, benzo(a) pyrene (BaP) and BaP-quinones, enhance IgE-mediated histamine release and IL-4 production in human basophils, Clin Immunol 107 (2003) 10-19.

3. D. Prausnitz and H. Kustner, Studien uber die Ueberempfindlichkeit, Zentrabl.Bakteriol [A] 86 (1921) 160-175.

4. K. Ishizaka and T. Ishizaka, Identification of IgE-antibodies as a carrier of reaginic activity., J.Immunol. 99 (1967) 1187-1198.

5. S. G. Johansson and H. Bennich, Immunological studies of an atypical (myeloma) immunoglobulin, Immunology 13 (1967) 381-394.

6. M. Ogawa, O. R. McIntyre, K. Ishizaka, T. Ishizaka, W. D. Terry, and T. A. Waldmann, Biologic properties of E myeloma proteins, Am.J Med. 51 (1971) 193-199.

7. E. B. Reilly, R. M. Reilly, R. M. Breyer, R. T. Sauer, and H. N. Eisen, Amino acid and nucleotide sequences of variable regions of mouse immunoglobulin light chains of the lambda 3-subtype, J Immunol 133 (1984) 471-475.

8. Baezinger, J. U., "Immediate Hypersensitivity-Modern Concepts and Developments," Marcel Decker, Inc. NY, New York, 1978.

9. S. C. Garman, B. A. Wurzburg, S. S. Tarchevskaya, J. P. Kinet, and T. S. Jardetzky, Structure of the Fc fragment of human IgE bound to its high-affinity receptor Fc epsilonRI alpha, Nature 406 (2000) 259-266.

10. B. A. Wurzburg, S. C. Garman, and T. S. Jardetzky, Structure of the human IgE-Fc C epsilon 3-C epsilon 4 reveals conformational flexibility in the antibody effector domains, Immunity. 13 (2000) 375-385.

11. T. Wan, R. L. Beavil, S. M. Fabiane, A. J. Beavil, M. K. Sohi, M. Keown, R. J. Young, A. J. Henry, R. J. Owens, H. J. Gould, and B. J. Sutton, The crystal structure of IgE Fc reveals an asymmetrically bent conformation, Nat.Immunol 3 (2002) 681-686.

12. K. Ishizaka and H. Tomioka, Mechanisms of passive sensitization.I.Presence of IgE and IgG molecules on human leukocytes., J.Immunol. 105 (1970) 1459-67.

13. T. Ishizaka, A. M. Dvorak, D. H. Conrad, J. R. Niebyl, J. P. Marquette, and K. Ishizaka, Morphologic and immunologic characterization of human basophils developed in cultures of cord blood mononuclear cells, J Immunol 134 (1985) 532-540.

14. G. Rossi, S. A. Newman, and H. Metzger, Assay and partial characterization of the solubilized cell surface receptor for immunoglobulin., J.Biol.Chem. 252 (1977) 704-11.

15. D. Maurer, S. Fiebiger, C. Ebner, B. Reininger, G. F. Fischer, S. Wichlas, M. H. Jouvin, M. Schmitt-Egenolf, D. Kraft, J. P. Kinet, and G. Stingl, Peripheral blood dendritic cells express Fc epsilon RI as a complex composed of Fc epsilon RI alpha- and Fc epsilon RI gamma-chains and can use this receptor for IgE-mediated allergen presentation, J Immunol 157 (1996) 607-616.

16. D. Maurer, C. Ebner, B. Reininger, E. Fiebiger, D. Kraft, J. P. Kinet, and G. Stingl, The high affinity IgE receptor (Fc epsilon RI) mediates IgE-dependent allergen presentation, J Immunol 154 (1995) 6285-6290.

17. J. P. Kinet, The high-affinity IgE receptor (Fc epsilon RI): From physiology to pathology, Ann.Rev.Immunol. 17 (1999) 931-972.

18. D. Maurer, E. Fiebiger, B. Reininger, B. Wolff-Winiski, M. H. Jouvin, O. Kilgus, J. P. Kinet, and G. Stingl, Expression of functional high affinity immunoglobulin E receptors (Fc epsilon RI) on monocytes of atopic individuals, J Exp.Med. 179 (1994) 745-750.

19. A. S. Gounni, B. Lamkhioued, K. Ochiai, Y. Tanaka, E. Delaporte, A. Capron, J. P. Kinet, and M. Capron, High-affinity IgE receptor on eosinophils is involved in defence against parasites, Nature 367 (1994) 183-186.

20. B. Wang, A. Rieger, O. Kilgus, K. Ochiai, D. Maurer, D. Fodinger, J. P. Kinet, and G. Stingl, Epidermal Langerhans cells from normal human skin bind monomeric IgE via Fc epsilon RI, J Exp.Med. 175 (1992) 1353-1365.

21. D. A. Lawrence, W. O. Weigle, and H. L. Spiegelberg, Immunoglobulins cytophilic for human lymphocytes, monocytes, and neutrophils, J Clin Invest 55 (1975) 368-376.

22. M. Capron, J.-P. Kusnierz, L. Prin, H. L. Spiegelberg, G. Ovlaque, P. Gosset, A. B. Tonnel, and A. Capron, Cytophilic IgE on human blood and tissue eosinophils: detection by flow microfluorometry, J.Immunol. 134 (1985) 3013-3018.

23. M. Joseph, C. Auriault, A. Capron, H. Vorng, and P. Viens, A new function for platelets: IgE-dependent killing of schistosomes, Nature 303 (1983) 810-812.

24. Y. Tu, S. Salim, J. Bourgeois, L. Di, V, E. J. Irvine, J. K. Marshall, and M. H. Perdue, CD23-mediated IgE transport across human intestinal epithelium: inhibition by blocking sites of translation or binding, Gastroenterology 129 (2005) 928-940.

25. A. Yokota, K. Yukawa, A. Yamamoto, K. Sugiyama, M. Suemura, Y. Tashiro, T. Kishimoto, and H. Kikutani, Two forms of the low-affinity Fc receptor for IgE differentially mediate endocytosis and phagocytosis: Identification of the critical cytoplasmic domains., Proc.Natl.Acad.Sci.USA 89 (1992) 5030-5034.

26. S. Sukumar, D. H. Conrad, A. K. Szakal, and J. G. Tew, Differential T Cell-Mediated Regulation of CD23 (Fc{epsilon}RII) in B Cells and Follicular Dendritic Cells, J Immunol 176 (2006) 4811-4817.

27. H. J. Gould, B. J. Sutton, A. J. Beavil, R. L. Beavil, N. McCloskey, H. A. Coker, D. Fear, and L. Smurthwaite, The biology of IGE and the basis of allergic disease, Annu.Rev.Immunol. 21 (2003) 579-628.

28. D. A. Lebman and R. L. Coffman, Interleukin 4 causes isotype switching to IgE in T cell-stimulated clonal B cell cultures, J Exp.Med. 168 (1988) 853-862.

29. R. L. Coffman, J. Ohara, M. W. Bond, J. Carty, A. Zlotnik, and W. E. Paul, B cell stimulatory factor-1 enhances the IgE response of lipopolysaccharide-activated B cells, J Immunol 136 (1986) 4538-4541.

30. J. Punnonen, G. Aversa, B. G. Cocks, A. N. McKenzie, S. Menon, G. Zurawski, M. R. de Waal, and J. E. de Vries, Interleukin 13 induces interleukin 4-independent IgG4 and IgE synthesis and CD23 expression by human B cells, Proc.Natl.Acad.Sci.U.S.A 90 (1993) 3730-3734.

31. A. E. Kelly-Welch, E. M. Hanson, M. R. Boothby, and A. D. Keegan, Interleukin-4 and interleukin-13 signaling connections maps, Science 300 (2003) 1527-1528.

32. N. Wood, K. Bourque, D. D. Donaldson, M. Collins, D. Vercelli, S. J. Goldman, and M. T. Kasaian, IL-21 effects on human IgE production in response to IL-4 or IL-13, Cell Immunol. 231 (2004) 133-145.

33. R. J. Noelle, M. Roy, D. M. Shepherd, I. Stamenkovic, J. A. Ledbetter, and A. Aruffo, A 39-kDa protein on activated helper T cells binds CD40 and transduces the signal for cognate activation of B cells, Proc.Natl.Acad.Sci.U.S.A 89 (1992) 6550-6554.

34. J. F. Gauchat, G. Aversa, H. Gascan, and J. E. de Vries, Modulation of IL-4 induced germline epsilon RNA synthesis in human B cells by tumor necrosis factor-alpha, anti-CD40 monoclonal antibodies or transforming growth factor-beta correlates with levels of IgE production, Int Immunol 4 (1992) 397-406.

35. J. Punnonen and J. E. de Vries, IL-13 induces proliferation, Ig isotype switching, and Ig synthesis by immature human fetal B cells, J Immunol 152 (1994) 1094-1102.

36. J. Pene, F. Rousset, F. Briere, I. Chretien, J. Y. Bonnefoy, H. Spits, T. Yokota, N. Arai, K. Arai, J. Banchereau, and ., IgE production by normal human lymphocytes is induced by interleukin 4 and suppressed by interferons gamma and alpha and prostaglandin E2, Proc.Natl.Acad.Sci.U.S.A 85 (1988) 6880-6884.

37. E. Maggi, G. F. Del Prete, P. Parronchi, A. Tiri, D. Macchia, P. Biswas, C. Simonelli, M. Ricci, and S. Romagnani, Role for T cells, IL-2 and IL-6 in the IL-4-dependent in vitro human IgE synthesis, Immunology 68 (1989) 300-306.

38. J. Pene, F. Rousset, F. Briere, I. Chretien, J. Wideman, J. Y. Bonnefoy, and J. E. de Vries, Interleukin 5 enhances interleukin 4-induced IgE production by normal human B cells. The role of soluble CD23 antigen, Eur.J Immunol 18 (1988) 929-935.

39. D. Vercelli, H. H. Jabara, K. Arai, T. Yokota, and R. S. Geha, Endogenous interleukin 6 plays an obligatory role in interleukin 4-dependent human IgE synthesis, Eur.J Immunol 19 (1989) 1419-1424.

40. P. Jeannin, Y. Delneste, S. Lecoanet-Henchoz, D. Gretener, and J. Y. Bonnefoy, Interleukin-7 (IL-7) enhances class switching to IgE and IgG4 in the presence of T cells via IL-9 and sCD23, Blood 91 (1998) 1355-1361.

41. B. Dugas, J. C. Renauld, J. Pene, J. Y. Bonnefoy, C. Peti-Frere, P. Braquet, J. Bousquet, J. Van Snick, and J. M. Mencia-Huerta, Interleukin-9 potentiates the interleukin-4-induced immunoglobulin (IgG, IgM and IgE) production by normal human B lymphocytes, Eur.J Immunol 23 (1993) 1687-1692.

42. H. Kimata, M. Fujimoto, C. Ishioka, and A. Yoshida, Histamine selectively enhances human immunoglobulin E (IgE) and IgG4 production induced by anti-CD58 monoclonal antibody, J Exp.Med. 184 (1996) 357-364.

43. H. Kimata, A. Yoshida, C. Ishioka, M. Fujimoto, I. Lindley, and K. Furusho, RANTES and macrophage inflammatory protein 1 alpha selectively enhance immunoglobulin (IgE) and IgG4 production by human B cells, J Exp.Med. 183 (1996) 2397-2402.

44. J. P. Aubry, S. Pochon, P. Graber, K. U. Jansen, and J. Y. Bonnefoy, CD21 is a ligand for CD23 and regulates IgE production, Nature 358 (1992) 505-507.

45. D. Diaz-Sanchez, S. Chegini, K. Zhang, and A. Saxon, CD58 (LFA-3) stimulation provides a signal for human isotype switching and IgE production distinct from CD40, J Immunol 153 (1994) 10-20.

46. Y. Katada, T. Tanaka, H. Ochi, M. Aitani, A. Yokota, H. Kikutani, M. Suemura, and T. Kishimoto, B cell-B cell interaction through intercellular adhesion molecule-1 and lymphocyte functional antigen-1 regulates immunoglobulin E synthesis by B cells stimulated with interleukin-4 and anti-CD40 antibody, Eur.J Immunol 26 (1996) 192-200.

47. P. Jeannin, Y. Delneste, S. Lecoanet-Henchoz, J. F. Gauchat, J. Ellis, and J. Y. Bonnefoy, CD86 (B7-2) on human B cells. A functional role in proliferation and selective differentiation into IgE- and IgG4-producing cells, J Biol.Chem. 272 (1997) 15613-15619.

48. J. Pene, J. F. Gauchat, S. Lecart, E. Drouet, P. Guglielmi, V. Boulay, A. Delwail, D. Foster, J. C. Lecron, and H. Yssel, Cutting edge: IL-21 is a switch factor for the production of IgG1 and IgG3 by human B cells, J Immunol. 172 (2004) 5154-5157.

49. I. Kohler and E. P. Rieber, Allergy-associated I epsilon and Ec epsilon receptor II (CD23b) genes activated via binding of an interleukin-4-induced transcription factor to a novel responsive element, Eur.J Immunol 23 (1993) 3066-3071.

50. H. Asao, C. Okuyama, S. Kumaki, N. Ishii, S. Tsuchiya, D. Foster, and K. Sugamura, Cutting edge: the common gamma-chain is an indispensable subunit of the IL-21 receptor complex, J Immunol 167 (2001) 1-5.

51. T. Habib, S. Senadheera, K. Weinberg, and K. Kaushansky, The common gamma chain (gamma c) is a required signaling component of the IL-21 receptor and supports IL-21-induced cell proliferation via JAK3, Biochemistry 41 (2002) 8725-8731.

52. F. Bennett, D. Luxenberg, V. Ling, I. M. Wang, K. Marquette, D. Lowe, N. Khan, G. Veldman, K. A. Jacobs, V. E. Valge-Archer, M. Collins, and B. M. Carreno, Program death-1 engagement upon TCR activation has distinct effects on costimulation and cytokine-driven proliferation: attenuation of ICOS, IL-4, and IL-21, but not CD28, IL-7, and IL-15 responses, J Immunol 170 (2003) 711-718.

53. J. Parrish-Novak, S. R. Dillon, A. Nelson, A. Hammond, C. Sprecher, J. A. Gross, J. Johnston, K. Madden, W. Xu, J. West, S. Schrader, S. Burkhead, M. Heipel, C. Brandt, J. L. Kuijper, J. Kramer, D. Conklin, S. R. Presnell, J. Berry, F. Shiota, S. Bort, K. Hambly, S. Mudri, C. Clegg, M. Moore, F. J. Grant, C. Lofton-Day, T. Gilbert, F. Rayond, A. Ching, L. Yao, D. Smith, P. Webster, T. Whitmore, M. Maurer, K. Kaushansky, R. D. Holly, and D. Foster, Interleukin 21 and its receptor are involved in NK cell expansion and regulation of lymphocyte function, Nature 408 (2000) 57-63.

54. K. Ozaki, K. Kikly, D. Michalovich, P. R. Young, and W. J. Leonard, Cloning of a type I cytokine receptor most related to the IL-2 receptor beta chain, Proc.Natl.Acad.Sci.U.S.A 97 (2000) 11439-11444.

55. K. Ozaki, R. Spolski, C. G. Feng, C. F. Qi, J. Cheng, A. Sher, H. C. Morse, III, C. Liu, P. L. Schwartzberg, and W. J. Leonard, A critical role for IL-21 in regulating immunoglobulin production, Science 298 (2002) 1630-1634.

56. M. T. Kasaian, M. J. Whitters, L. L. Carter, L. D. Lowe, J. M. Jussif, B. Deng, K. A. Johnson, J. S. Witek, M. Senices, R. F. Konz, A. L. Wurster, D. D. Donaldson, M. Collins, D. A. Young, and M. J. Grusby, IL-21 limits NK cell responses and promotes antigen-specific T cell activation: a mediator of the transition from innate to adaptive immunity, Immunity. 16 (2002) 559-569.

57. A. Suto, H. Nakajima, K. Hirose, K. Suzuki, S. Kagami, Y. Seto, A. Hoshimoto, Y. Saito, D. C. Foster, and I. Iwamoto, Interleukin 21 prevents antigen-induced IgE production by inhibiting germ line C(epsilon) transcription of IL-4-stimulated B cells, Blood 100 (2002) 4565-4573.

58. M. Hecker, A. Bohnert, I. R. Konig, G. Bein, and H. Hackstein, Novel genetic variation of human interleukin-21 receptor is associated with elevated IgE levels in females, Genes Immun. 4 (2003) 228-233.

59. W. J. Leonard, Cytokines and immunodeficiency diseases, Nat.Rev.Immunol 1 (2001) 200-208.

60. M. Noguchi, H. Yi, H. M. Rosenblatt, A. H. Filipovich, S. Adelstein, W. S. Modi, O. W. McBride, and W. J. Leonard, Interleukin-2 receptor gamma chain mutation results in X-linked severe combined immunodeficiency in humans, Cell 73 (1993) 147-157.

61. P. Macchi, A. Villa, S. Giliani, M. G. Sacco, A. Frattini, F. Porta, A. G. Ugazio, J. A. Johnston, F. Candotti, J. J. O'Shea, and ., Mutations of Jak-3 gene in patients with autosomal severe combined immune deficiency (SCID), Nature 377 (1995) 65-68.

62. K. Ozaki, R. Spolski, R. Ettinger, H. P. Kim, G. Wang, C. F. Qi, P. Hwu, D. J. Shaffer, S. Akilesh, D. C. Roopenian, H. C. Morse, III, P. E. Lipsky, and W. J. Leonard, Regulation of B cell differentiation and plasma cell generation by IL-21, a novel inducer of Blimp-1 and Bcl-6, J Immunol 173 (2004) 5361-5371.

63. K. L. Calame, K. I. Lin, and C. Tunyaplin, Regulatory mechanisms that determine the development and function of plasma cells, Annu.Rev.Immunol 21 (2003) 205-230.

64. A. L. Shaffer, K. I. Lin, T. C. Kuo, X. Yu, E. M. Hurt, A. Rosenwald, J. M. Giltnane, L. Yang, H. Zhao, K. Calame, and L. M. Staudt, Blimp-1 orchestrates plasma cell differentiation by extinguishing the mature B cell gene expression program, Immunity. 17 (2002) 51-62.

65. P. Jeannin, S. Lecoanet, Y. Delneste, J. F. Gauchat, and J. Y. Bonnefoy, IgE versus IgG4 production can be differentially regulated by IL-10, J Immunol. 160 (1998) 3555-3561.

66. N. Kobayashi, H. Nagumo, and K. Agematsu, IL-10 enhances B-cell IgE synthesis by promoting differentiation into plasma cells, a process that is inhibited by CD27/CD70 interaction, Clin Exp.Immunol 129 (2002) 446-452.

67. J. Punnonen, M. R. de Waal, P. van Vlasselaer, J. F. Gauchat, and J. E. de Vries, IL-10 and viral IL-10 prevent IL-4-induced IgE synthesis by inhibiting the accessory cell function of monocytes, J Immunol 151 (1993) 1280-1289.

68. C. A. Akdis, T. Blesken, M. Akdis, B. Wuthrich, and K. Blaser, Role of interleukin 10 in specific immunotherapy, J Clin Invest 102 (1998) 98-106.

69. S. W. Cho, M. A. Kilmon, E. J. Studer, P. H. van der, and D. H. Conrad, B cell activation and Ig, especially IgE, production is inhibited by high CD23 levels in vivo and in vitro, Cell Immunol. 180 (1997) 36-46.

70. D. Rabah and D. H. Conrad, Effect of cell density on in vitro mouse immunoglobulin E production, Immunology 106 (2002) 503-510.

71. J. Hasbold, A. B. Lyons, M. R. Kehry, and P. D. Hodgkin, Cell division number regulates IgG1 and IgE switching of B cells following stimulation by CD40 ligand and IL-4, Eur.J.Immunol. 28 (1998) 1040-1051.

72. P. D. Hodgkin, J. H. Lee, and A. B. Lyons, B cell differentiation and isotype switching is related to division cycle number, J.Exp.Med. 184 (1996) 277-281.

73. D. A. Lebman and R. L. Coffman, Interleukin 4 causes isotype switching to IgE in T cell-stimulated clonal B cell cultures, J Exp.Med. 168 (1988) 853-862.

74. R. L. Coffman, D. A. Lebman, and P. Rothman, Mechanism and regulation of immunoglobulin isotype switching, Adv.Immunol. 54 (1993) 229-270.

75. S. G. Tangye, A. Ferguson, D. T. Avery, C. S. Ma, and P. D. Hodgkin, Isotype switching by human B cells is division-associated and regulated by cytokines, J.Immunol. 169 (2002) 4298-4306.

76. S. G. Tangye, D. T. Avery, and P. D. Hodgkin, A division-linked mechanism for the rapid generation of Ig-secreting cells from human memory B cells, J.Immunol. 170 (2003) 261-269.

77. M. Payet and D. H. Conrad, IgE regulation in CD23 knockout and transgenic mice, Allergy 54 (1999) 1125-1129.

78. M. E. Payet, E. C. Woodward, and D. H. Conrad, Humoral response suppression observed with CD23 transgenics, J Immunol 163 (1999) 217-223.

79. A. E. Kelly, B. H. Chen, E. C. Woodward, and D. H. Conrad, Production of a chimeric form of CD23 that is oligomeric and blocks IgE binding to the Fc epsilonRI, J Immunol 161 (1998) 6696-6704.

80. B. H. Chen, C. Ma, T. H. Caven, Y. Chan-Li, A. Beavil, R. Beavil, H. Gould, and D. H. Conrad, Necessity of the stalk region for immunoglobulin E interaction with CD23, Immunology 107 (2002) 373-381.

81. J. T. McGrew, D. Leiske, B. Dell, R. Klinke, D. Krasts, S. F. Wee, N. Abbott, R. Armitage, and K. Harrington, Expression of trimeric CD40 ligand in Pichia

pastoris: use of a rapid method to detect high-level expressing transformants, Gene 187 (1997) 193-200.

82. D. Bohmann and R. Tjian, Biochemical analysis of transcriptional activation by Jun: differential activity of c- and v-Jun, Cell 59 (1989) 709-717.

83. M. A. Taylor, K. A. Pratt, D. F. Revell, K. C. Baker, I. G. Sumner, and P. W. Goodenough, Active papain renatured and processed from insoluble recombinant propapain expressed in Escherichia coli, Protein Eng 5 (1992) 455-459.

84. B. Johnsson, S. Lofas, and G. Lindquist, Immobilization of proteins to a carboxymethyldextran-modified gold surface for biospecific interaction analysis in surface plasmon resonance sensors, Anal.Biochem. 198 (1991) 268-277.

85. L. M. Pecanha, H. Yamaguchi, A. Lees, R. J. Noelle, J. J. Mond, and C. M. Snapper, Dextran-conjugated anti-IgD antibodies inhibit T cell-mediated IgE production but augment the synthesis of IgM and IgG, J Immunol 150 (1993) 2160-2168.

86. E. Macy, M. Kemeny, and A. Saxon, Enhanced ELISA: how to measure less than 10 picograms of a specific protein (immunoglobulin) in less than 8 hours, FASEB J 2 (1988) 3003-3009.

87. A. D. Keegan, C. Fratazzi, B. Shopes, B. Baird, and D. H. Conrad, Characterization of new rat anti-mouse IgE monoclonals and their use along with chimeric IgE to further define the site that interacts with Fc epsilon RII and Fc epsilon RI, Mol.Immunol. 28 (1991) 1149-1154.

88. M. A. Kilmon, The Role Oligomerization of CD23 Plays in its Function, (2002).
Ref Type: Thesis/Dissertation

89. R. J. Armitage, B. M. Macduff, M. K. Spriggs, and W. C. Fanslow, Human B cell proliferation and Ig secretion induced by recombinant CD40 ligand are modulated by soluble cytokines, J Immunol. 150 (1993) 3671-3680.

90. P. Jardieu, Anti-IgE therapy, Curr.Opin.Immunol. 7 (1995) 779-782.

91. C. Heusser and P. Jardieu, Therapeutic potential of anti-IgE antibodies, Curr.Opin.Immunol. 9 (1997) 805-813.

92. Y. J. Liu, J. A. Cairns, M. J. Holder, S. D. Abbot, K. U. Jansen, J. Y. Bonnefoy, J. Gordon, and I. C. MacLennan, Recombinant 25-kDa CD23 and interleukin 1 alpha promote the survival of germinal center B cells: evidence for bifurcation

in the development of centrocytes rescued from apoptosis, Eur.J Immunol 21 (1991) 1107-1114.

93. T. Kishida, H. Asada, Y. Itokawa, F. D. Cui, M. Shin-Ya, S. Gojo, K. Yasutomi, Y. Ueda, H. Yamagishi, J. Imanishi, and O. Mazda, Interleukin (IL)-21 and IL-15 genetic transfer synergistically augments therapeutic antitumor immunity and promotes regression of metastatic lymphoma, Mol.Ther. 8 (2003) 552-558.

94. E. Di Carlo, A. Comes, A. M. Orengo, O. Rosso, R. Meazza, P. Musiani, M. P. Colombo, and S. Ferrini, IL-21 induces tumor rejection by specific CTL and IFN-gamma-dependent CXC chemokines in syngeneic mice, J Immunol. 172 (2004) 1540-1547.

95. G. Wang, M. Tschoi, R. Spolski, Y. Lou, K. Ozaki, C. Feng, G. Kim, W. J. Leonard, and P. Hwu, In vivo antitumor activity of interleukin 21 mediated by natural killer cells, Cancer Res. 63 (2003) 9016-9022.

96. V. Kindler and R. H. Zubler, Memory, but not naive, peripheral blood B lymphocytes differentiate into Ig-secreting cells after CD40 ligation and costimulation with IL-4 and the differentiation factors IL-2, IL-10, and IL-3, J Immunol 159 (1997) 2085-2090.

97. F. Briere, C. Servet-Delprat, J. M. Bridon, J. M. Saint-Remy, and J. Banchereau, Human interleukin 10 induces naive surface immunoglobulin D+ (sIgD+) B cells to secrete IgG1 and IgG3, J Exp.Med. 179 (1994) 757-762.

98. M. Shapiro-Shelef, K. I. Lin, L. J. McHeyzer-Williams, J. Liao, M. G. McHeyzer-Williams, and K. Calame, Blimp-1 is required for the formation of immunoglobulin secreting plasma cells and pre-plasma memory B cells, Immunity. 19 (2003) 607-620.

99. C. A. Turner, Jr., D. H. Mack, and M. M. Davis, Blimp-1, a novel zinc finger-containing protein that can drive the maturation of B lymphocytes into immunoglobulin-secreting cells, Cell 77 (1994) 297-306.

100. T. Honjo, M. Muramatsu, and S. Fagarasan, AID: how does it aid antibody diversity?, Immunity. 20 (2004) 659-668.

101. R. Ettinger, G. P. Sims, A. M. Fairhurst, R. Robbins, Y. S. da Silva, R. Spolski, W. J. Leonard, and P. E. Lipsky, IL-21 induces differentiation of human naive and memory B cells into antibody-secreting plasma cells, J Immunol 175 (2005) 7867-7879.

102. S. L. Nutt, C. Thevenin, and M. Busslinger, Essential functions of Pax-5 (BSAP) in pro-B cell development, Immunobiology 198 (1997) 227-235.

103. I. Mikkola, B. Heavey, M. Horcher, and M. Busslinger, Reversion of B cell commitment upon loss of Pax5 expression, Science 297 (2002) 110-113.

104. M. Busslinger, Transcriptional control of early B cell development, Annu.Rev.Immunol 22 (2004) 55-79.

105. A. Delogu, A. Schebesta, Q. Sun, K. Aschenbrenner, T. Perlot, and M. Busslinger, Gene repression by Pax5 in B cells is essential for blood cell homeostasis and is reversed in plasma cells, Immunity. 24 (2006) 269-281.

106. K. P. Nera, P. Kohonen, E. Narvi, A. Peippo, L. Mustonen, P. Terho, K. Koskela, J. M. Buerstedde, and O. Lassila, Loss of Pax5 promotes plasma cell differentiation, Immunity. 24 (2006) 283-293.

107. F. Ho, J. E. Lortan, I. C. MacLennan, and M. Khan, Distinct short-lived and long-lived antibody-producing cell populations, Eur.J Immunol 16 (1986) 1297-1301.

108. J. Jacob, R. Kassir, and G. Kelsoe, In situ studies of the primary immune response to (4-hydroxy-3-nitrophenyl)acetyl. I. The architecture and dynamics of responding cell populations, J Exp.Med. 173 (1991) 1165-1175.

109. R. Benner, W. Hijmans, and J. J. Haaijman, The bone marrow: the major source of serum immunoglobulins, but still a neglected site of antibody formation, Clin Exp.Immunol 46 (1981) 1-8.

110. M. M. Tomayko and M. P. Cancro, Long-lived B cells are distinguished by elevated expression of A1, J Immunol 160 (1998) 107-111.

111. C. Chen, L. C. Edelstein, and C. Gelinas, The Rel/NF-kappaB family directly activates expression of the apoptosis inhibitor Bcl-x(L), Mol.Cell Biol. 20 (2000) 2687-2695.

112. R. J. Grumont, I. J. Rourke, and S. Gerondakis, Rel-dependent induction of A1 transcription is required to protect B cells from antigen receptor ligation-induced apoptosis, Genes Dev. 13 (1999) 400-411.

113. U. Chen-Bettecken, E. Wecker, and A. Schimpl, Transcriptional control of mu- and kappa-gene expression in resting and bacterial lipopolysaccharide-activated normal B cells, Immunobiology 174 (1987) 162-176.

114. K. I. Lin, Y. Lin, and K. Calame, Repression of c-myc is necessary but not sufficient for terminal differentiation of B lymphocytes in vitro, Mol.Cell Biol. 20 (2000) 8684-8695.

115. L. Morse, D. Chen, D. Franklin, Y. Xiong, and S. Chen-Kiang, Induction of cell cycle arrest and B cell terminal differentiation by CDK inhibitor p18(INK4c) and IL-6, Immunity. 6 (1997) 47-56.

116. H. M. Jack and M. Wabl, Immunoglobulin mRNA stability varies during B lymphocyte differentiation, EMBO J 7 (1988) 1041-1046.

117. N. N. Iwakoshi, A. H. Lee, P. Vallabhajosyula, K. L. Otipoby, K. Rajewsky, and L. H. Glimcher, Plasma cell differentiation and the unfolded protein response intersect at the transcription factor XBP-1, Nat.Immunol 4 (2003) 321-329.

VITA

Timothy Hays Caven was born in Honolulu, Hawaii on a Wednesday. It was January 11th 1967. He was born of the Pacific and ever since he has had a life-long attraction to the sea. Being the number one son of six brothers and sisters to wonderful parents who had a bit of the wander lust, he was fortunate to have traveled to many climes and cultures. He received his Bachelor of Science in Biology Magna Cum Laude from the University of New England on the shores of the mighty Saco River, in the great State of Maine, where many a striped bass was had. He entered the Virginia Commonwealth of Virginia and received his Doctorate of Philosophy in Immunology in 2006.